

ABSTRACT

Title of Thesis: THE EFFECT OF SALINITY ON SPECIES SURVIVAL AND CARBON STORAGE ON THE LOWER EASTERN SHORE OF MARYLAND DUE TO SALTWATER INTRUSION

Elizabeth de la Reguera, Master of Science, 2019

Thesis Directed By: Dr. Kate Tully, Plant Science Department

As sea levels continue to rise, coastal ecosystems are vulnerable to saltwater intrusion (SWI), the landward movement of sea salts. Specifically, in coastal farmlands, we expect SWI to drive changes in plant species composition and carbon (C) storage. As soils salinize, standard crops (i.e. corn, soybean, and wheat) can no longer survive and farmers must consider alternatives. Further, transitioning agricultural fields may become C sinks as SWI advances inland and farmlands begin to resemble tidal wetlands. My objectives were to determine: (1) the effect of SWI on the germination of standard and alternative crop species, and (2) the C storage potential of salt-intruded farmlands. Most standard and alternative crops were intolerant to high levels of osmotic and ionic stress at the germination stage. However, sorghum and salt-tolerant soybean showed promise in field experiments. I show that agricultural fields exposed to SWI have a high potential to store C in soils.

THE EFFECT OF SALINITY ON SPECIES SURVIVAL AND CARBON
STORAGE ON THE LOWER EASTERN SHORE OF MARYLAND DUE TO
SALTWATER INTRUSION

by

Elizabeth de la Reguera

Thesis submitted to the Faculty of the Graduate School of the
University of Maryland, College Park, in partial fulfillment
of the requirements for the degree of
Master of Science
2019

Advisory Committee:
Professor Kate Tully, Chair
Dr. Margaret Palmer, Co-Chair
Dr. Keryn Gedan

© Copyright by
Elizabeth de la Reguera
2019

Dedication

To my better half, Kyle Fisk.

Acknowledgements

I am eternally grateful to my advisor, Kate Tully, for pushing me to think more deeply and become a better scientist and writer. My co-advisor, Margaret Palmer, has been supportive throughout the project. Margaret challenged me to think big-picture and how this work benefits both the scientific community and farmers. I am grateful for my committee member, Keryn Gedan, for her guidance on experimental design and data interpretation regarding my plant chapter.

I want to thank the many colleagues and friends that have supported me throughout my research. I am very grateful for those at the University of Maryland, including Dani Weissman, Cullen McAskill, Natalie Ceresnak, Zach Johnson, Dr. Christine Maietta, Alec Armstrong, Kelly Hondula, Anna Kottkamp, and Graham Stewart. I would also like to thank Man Qi, Jessica MacGregor, Justus Jobe, Jackie Veatch, Scott Dai, and Loukas Kang for their help both in the field and maintaining my experiment at George Washington University. I'm grateful for the help and conversations with the SWI team, especially Jarrod Miller and Shawn Tingle. I am very appreciative of the farmers and landowners of Somerset and Dorchester County, Maryland, who allowed me to conduct research on their salt-intruded farm fields.

Finally, my family has been tremendously supportive. Dad: Thank you for your unwavering support and love through all of my endeavors. I know my career path might not have been your first choice, but you always trusted me to make the right decision and one that would make me happy. To Kyle: There are no words to describe how much your love and support has meant to me. You've done field work on the Lower Eastern Shore, traveled to GWU to start experiments, counted radicles in the greenhouse, kept me company in the lab after a 10-hour experiment, and never once complained about my crazy hours. Thank you for believing in me and supporting me when I needed it the most. Without you, none of this would have been possible.

This research was supported by USDA-NIFA (Grant no. 12451226 project accession no. 1015143, a grant from the Harry R. Hughes Center for Agro-Ecology, SESYNC (Grant no. DBI-1639145), and Northeast SARE (Grant no. GNE 19-197-33243).

Table of Contents

Dedication	ii
Acknowledgements	iii
Table of Contents	iv
List of Tables	vi
List of Figures	ix
Chapter 1: Resist or adapt: farming in the face of sea level rise and saltwater intrusion ...	1
Abstract	1
Introduction	2
Methods	7
<i>Controlled environment experiment</i>	7
<i>Field experiment</i>	10
<i>Statistical analysis</i>	13
Results	16
<i>Controlled environment experiment: the effect of osmotic and ionic stress on seed germination</i>	16
<i>Field experiment: the effect of saltwater intrusion on field germination compared to lab germination</i>	17
Discussion	18
<i>Standard vs. alternative crop species</i>	19
<i>Field germination of salt-tolerant soybean and sorghum</i>	21
<i>Comparing controlled environment and field experiments</i>	23
Conclusion	25
Tables and Figures	27
Supplemental Material	37
Chapter 2: Farming carbon: the link between saltwater intrusion and carbon storage in coastal agricultural fields	41
Abstract	41
Introduction	42
Methods	46
<i>Study sites</i>	46
<i>Soil collections</i>	47
<i>Percent C</i>	48
<i>Bulk soil C metric</i>	48
<i>Aggregate size separation</i>	48
<i>Sand particle analysis</i>	49
<i>Aggregate soil C metrics</i>	50
<i>Statistical analysis</i>	51
Results	53
<i>Ditch bank soils have the largest soil C pool and highest C concentration</i>	53
<i>Soil C is stored in different aggregate size classes across a SWI transect</i>	54

Discussion	57
<i>Largest soil C pool in ditch bank</i>	57
<i>Aggregate soil C across a SWI transect</i>	61
<i>Farmland to wetland?</i>	64
Conclusion	65
Tables and Figures	66
Supplemental Material	73
References	89

List of Tables

Chapter 1: Resist or adapt: farming in the face of sea level rise and saltwater intrusion

Table 1.1. Salinity thresholds (dS m^{-1} and ppt) at mature plant stage of focal plant species. (Page 27)

Table 1.2. Water potentials (MPa) used in the study and their equivalent electrical conductivity (dS m^{-1})[†], salinity (ppt)[‡], and sodium chloride (NaCl) concentration (mM). (Page 28)

Table 1.3. Characteristics of Somerset farm and Dorchester farm on the Eastern Shore of Maryland where we conducted the field experiment. (Page 29)

Table 1.4. Percent germination of (A) sorghum at Somerset and Dorchester farm in 2018 and (B) sorghum and salt-tolerant soybean at Somerset and Dorchester farm in 2019 field water potential (MPa; mean \pm SE). (Page 30)

Table S1.1. Model parameter fit statistics for relationship between sorghum or salt-tolerant soybean percent germination and osmotic or ionic stress levels. (Page 37)

Chapter 2: Farming carbon: the link between saltwater intrusion and carbon storage in coastal agricultural fields

Table 2.1. Characteristics of the six no-till focal farms on the Eastern Shore of Maryland. (Page 66)

Table 2.2. Carbon calculations and metrics used in analysis. (Page 67)

Table S2.1. Summary statistics of global linear mixed-effect (LME) model for bulk soil C concentration. Summary statistics of reduced LME model (no interaction effect between location on the transect and depth category) for bulk soil C concentration. Fixed effects are location on the transect, depth category, and the interaction between location on the transect and depth category. (Page 73)

Table S2.2. Summary statistics of linear mixed-effect (LME) model to examine the effect of SWI on total bulk soil C concentration and pool (to 100 cm). Degrees of freedom numerator and denominator and P-value for each transect point and for model reported. (Page 74)

Table S2.3. Summary statistics of linear mixed-effect (LME) model to examine the size of the bulk C concentration and pool at the four depth categories. Degrees of freedom numerator and denominator and P-value for each depth category and for model reported. (Page 75)

Table S2.4. Total bulk soil C concentration (mg C g^{-1}) for each transect location (crop, crop edge, bare, field edge, and ditch bank) at four depth categories (0-20 cm, ~20-50 cm, ~50-80 cm, and ~80+ cm; mean \pm SE). Different uppercase letters signify statistically significant differences at $P < 0.05$ among transect location within depth category. Lower case letters signify statistically significant differences at $P < 0.05$ among depth category within transect location. (Page 76)

Table S2.5. Total bulk soil C pool (Mg C ha^{-1}) for each transect location (crop, crop edge, bare, field edge, and ditch bank) at four depth categories (0-20 cm, ~20-50 cm, ~50-80 cm, and ~80+ cm; mean \pm SE). Different uppercase letters signify statistically significant differences at $P < 0.05$ among transect location within depth category. Lower case letters signify statistically significant differences at $P < 0.05$ among depth category within transect location. (Page 77)

Table S2.6. Summary statistics of linear mixed-effect (LME) model of depth category 0-20 cm of (A) aggregate distribution (g aggregate per g bulk soil) and (B) total aggregate C (g C). (Page 78)

Table S2.7. (A) Aggregate distribution (g aggregate per g bulk soil) and (B) total aggregate C (g C) at depth category 0-20 cm for each transect location (crop, crop edge, bare, field edge, and ditch bank) at four aggregate size classes (large macroaggregate, small macroaggregate, microaggregate, silt+clay; mean \pm SE). Different uppercase letters signify statistically significant differences at $P < 0.05$ among aggregate size class within transect location. (Page 79)

Table S2.8. Summary statistics of linear mixed-effect (LME) model of depth category ~20-50 cm of (A) aggregate distribution (g aggregate per g bulk soil) and (B) total aggregate C (g C). (Page 80)

Table S2.9. (A) Aggregate distribution (g aggregate per g bulk soil) and (B) total aggregate C (g C) at depth category ~20-50 cm for each transect location (crop, crop edge, bare, field edge, and ditch bank) at four aggregate size classes (large macroaggregate, small macroaggregate, microaggregate, silt+clay; mean \pm SE). Different uppercase letters signify statistically significant differences at $P < 0.05$ among aggregate size class within transect location. (Page 81)

Table S2.10. Summary statistics of linear mixed-effect (LME) model of depth category ~50-80 cm of (A) aggregate distribution (g aggregate per g bulk soil) and (B) total aggregate C (g C). (Page 82)

Table S2.11. (A) Aggregate distribution (g aggregate per g bulk soil) and (B) total aggregate C (g C) at depth category ~50-80 cm for each transect location (crop, crop edge, bare, field edge, and ditch bank) at four aggregate size classes (large macroaggregate, small macroaggregate, microaggregate, silt+clay; mean \pm SE). Different uppercase letters signify statistically significant differences at $P < 0.05$ among aggregate size class within transect location. (Page 83)

Table S2.12. Summary statistics of linear mixed-effect (LME) model of depth category ~80+ cm of (A) aggregate distribution (g aggregate per g bulk soil) and (B) total aggregate C (g C). (Page 84)

Table S2.13. (A) Aggregate distribution (g aggregate per g bulk soil) and (B) total aggregate C (g C) at depth category ~80+ cm for each transect location (crop, crop edge, bare, field edge, and ditch bank) at four aggregate size classes (large macroaggregate, small macroaggregate, microaggregate, silt+clay; mean \pm SE). Different uppercase letters signify statistically significant differences at $P < 0.05$ among aggregate size class within transect location. (Page 85)

List of Figures

Chapter 1: Resist or adapt: farming in the face of sea level rise and saltwater intrusion

Figure 1.1. Percent germination of corn, soy, wheat, sorghum, salt-tolerant soy, barley, and quinoa along a water potential gradient of ionic stress (red circles) and osmotic stress (blue triangles). Error bars are standard error of the mean. (Page 31)

Figure 1.2. Percent germination of standard crop species – corn (blue), soy (gray), wheat (orange) – along a water potential gradient of ionic stress (circles) and osmotic stress (triangles). Error bars are standard error of the mean. (Page 32)

Figure 1.3. Percent germination of alternative crop species – barley (orange), quinoa (red), salt-tolerant soy (blue), sorghum (purple) – along a water potential gradient of ionic stress (circles) and osmotic stress (triangles). Error bars are standard error of the mean. (Page 33)

Figure 1.4. Time to 50% germination (hours) of all seven focal species – corn, soy, wheat, sorghum, salt-tolerant soy, barley, quinoa – along a water potential gradient (osmotic stress). Error bars are standard error of the mean. (Page 34)

Figure 1.5. Time to 50% germination (hours) of all seven focal species – corn, soy, wheat, sorghum, salt-tolerant soy, barley, quinoa – along a water potential gradient (ionic stress). Error bars are standard error of the mean. (Page 35)

Figure 1.6. Percent germination of field studies (both farms; purple squares) (A) sorghum in 2018 and 2019, and (B) salt-tolerant soybean in 2019 and controlled environment experiment. Osmotic stress indicated by blue triangles and ionic stress indicated by red circles and both in units of -MPa. Response to osmotic stress is indicated by solid black line fitted to logistic regression model and 95% confidence interval (dark grey shading). Response to ionic stress is indicated by the dashed black line fitted to logistic regression model and 95% confidence interval (light grey shading). The large confidence interval for salt-tolerant soybean response to ionic stress was driven by the standard error of the mean at water potential -0.2 MPa, which is why field germination of salt-tolerant soybean fell within the ionic stress confidence interval as well as the osmotic stress confidence interval. (Page 36)

Figure S1.1. Percent germination of rapeseed and switchgrass along a water potential gradient of ionic stress (circles) and osmotic stress (triangles). Error bars are standard error of the mean. (Page 38)

Figure S1.2. Time to 50% germination (hours) of rapeseed and switchgrass along a water potential gradient (osmotic stress). Error bars are standard error of the mean. (Page 39)

Figure S1.3. Time to 50% germination (hours) of rapeseed and switchgrass along a water potential gradient (ionic stress). Error bars are standard error of the mean. (Page 40)

Chapter 2: Farming carbon: the link between saltwater intrusion and carbon storage in coastal agricultural fields

Figure 2.1. Aerial view of SWI in Farm 1-6 and locations of transition zones along the transect. (Page 68)

Figure 2.2. Bulk soil C (A) concentration (mg C g^{-1}) and (B) pool (Mg C ha^{-1}) in bulk soils (not fractionated by size class) along the SWI transect at 0-20 cm, ~20-50 cm, ~50-80 cm, and ~80+ cm. Error bars are the standard error of the mean. Values above horizontal bars indicate the size of the total bulk soil C (A) concentration for each transect location and (B) C pool for each transect location. Different letters are statistically significant at $P < 0.05$ in Tukey *post hoc* pairwise comparisons. (Page 69)

Figure 2.3. Aggregate distribution ($\text{g sand-free aggregate g}^{-1}$ soil) in (A) 0-20 cm, (B) ~20-50 cm, (C) ~50-80 cm, and (D) ~80+ cm along the SWI transect. Error bars are the standard error of the mean. Transect location within depth categories are statistically significant at $P < 0.05$ in Tukey *post hoc* pairwise comparisons. Asterisk (*) indicates significance by class within a transect point at * $P < 0.05$, ** $P < 0.01$, *** $P < 0.005$ in Tukey *post hoc* pairwise comparisons. (Page 70)

Figure 2.4. Total aggregate C ($\text{g C sand-free aggregate}$) in (A) 0-20 cm, (B) ~20-50 cm, (C) ~50-80 cm, and (D) ~80+ cm along the SWI transect. Error bars are the standard error of the mean. Values above horizontal bars indicate the total aggregate C for each transect location. Different letters are statistically significant at $P < 0.05$ in Tukey *post hoc* pairwise comparisons. Asterisk (*) indicates significance by class within a transect point at * $P < 0.05$, ** $P < 0.01$, *** $P < 0.005$ in Tukey *post hoc* pairwise comparisons. (Page 71)

Figure 2.5. Drivers of soil C pools and physically protected soil C. Red text indicates drivers (wetting events, increased salinity, organo-metal complexation, changes in vegetation type, and soil management activities). Crop, crop edge, bare, field edge, and ditch bank are zones along the SWI transect. White circles in soil are silt+clays and light brown circles surrounding silt+clays are microaggregates. The orange circles surrounding microaggregates are small macroaggregates and dark brown circles surrounding small macroaggregates are large macroaggregates. (Page 72)

Figure S2.1. Normalized total aggregate C (g C g^{-1} C) in (A) 0-20 cm, (B) ~20-50 cm, (C) ~50-80 cm, and (D) ~80+ cm along the SWI transect. Error bars are the standard error of the mean. Transect locations within depth categories are statistically significant at $P < 0.05$ in Tukey *post-hoc* pairwise comparisons. (Page 86)

Figure S2.2. Sand proportion (g sand g⁻¹ aggregate) in (A) 0-20 cm, (B) ~20-50 cm, (C) ~50-80 cm, and (D) ~80+ cm along the SWI transect. Error bars are the standard error of the mean. Transect locations within depth categories are statistically significant at P<0.05 in Tukey post-hoc pairwise comparisons. (Page 87)

Figure S2.3. Soil C concentration (mg C g⁻¹) in the top 50 cm along the SWI transect and an average tidal wetland (Morris et al. 2016). (Page 88)

Chapter 1: Resist or adapt: farming in the face of sea level rise and saltwater intrusion

Abstract

Rising sea levels pose a threat to coastal agroecosystems as they become more vulnerable to saltwater intrusion (SWI). Saltwater intrusion is the landward movement of sea salts, which can salinize coastal farmlands and affect crop yields. Salt stress reduces a plant's ability to absorb water (osmotic stress) and causes an ion imbalance within the plant (ionic stress), ultimately resulting in decreased crop growth and even mortality. Two management strategies available to farmers wishing to continue farming in the face of sea level rise and SWI are to continue growing the standard crops as long as they can (*resist*) or grow salt-tolerant crops adapted to the Eastern Shore of Maryland (*adapt*). Our objectives were to (1) determine how osmotic and ionic stress levels affect seed germination in the standard crops and alternative salt-tolerant crops in a controlled environment experiment and (2) determine the germination success of alternative crops planted in salt-intruded farm fields on the Eastern Shore of Maryland. Standard crop species include corn (*Zea mays*), soybean (*Glycine max*), and wheat (*Triticum aestivum*); alternative salt-tolerant species include sorghum (*Sorghum bicolor*), salt-tolerant soybean, barley (*Hordeum vulgare*), and quinoa (*Chenopodium quinoa*). All of these species germinated in a controlled environment experiment under different levels of ionic and osmotic stress (measured in MPa of water potential) ranging from 0 to -4 MPa. Under controlled conditions, sorghum and corn successfully germinated at -0.8 MPa (22.2 dS m⁻¹) under osmotic stress; standard soybean and salt-tolerant soybean seeds had

an equal tolerance of ionic stress during germination. Overall, there was no significant difference in percent germination between the standard crop species and the alternative crop species under osmotic or ionic stress in controlled environmental conditions. We also established a trial on two salt-intruded farms on the Eastern Shore of Maryland to determine the success of sorghum and salt-tolerant soybeans under field conditions. Overall, germination percent was two times higher in salt-tolerant soybean than sorghum in the field ($P=0.001$). Sorghum field germination declined with increasing ionic stress levels, but salt-tolerant soybean declined with increasing osmotic stress levels. This research provides the groundwork for assessing the success of an alternative, salt-tolerant cropping rotation on farms experiencing SWI. Understanding the germination success of crop species experiencing SWI is critical to developing informed farm management strategies in coastal agricultural regions.

Introduction

Soil salinization is a global problem affecting at least 75 countries and more than 20% of global irrigated land (Ghassemi et al. 1995, Metternicht and Zinck 2003, Qadir et al. 2014). The extent of soil salinization is projected to increase due to climate change, specifically as a result of more variable weather conditions and rising sea levels (Zaman et al. 2018). For instance, salts may concentrate in soil as water evaporates during prolonged droughts (saltwater incursion; Ardón et al. 2013, Tully et al. 2019a). In arid regions, such as California and Colorado, fields can salinize following irrigation as groundwater is naturally high in salts (e.g. sulfate, sodium, and chloride) due to its flow through soils with easily weatherable minerals (Wichelns and Qadir 2015, Foster et al.

2018). These regions require large quantities of water to meet crop water demands, and soils salinize as water evaporates (Munns and Tester 2008). However, in our focal region of the Eastern Shore of Maryland, soils are salinizing via saltwater intrusion (SWI). Saltwater intrusion, the landward movement of sea salts, is driven by rising sea levels, water withdrawals from coastal aquifers, the frequency and duration of droughts, hydrological connectivity of agricultural ditches, and the frequency of storms and tides (Tully et al. 2019a). Although a great deal of research has focused on the effects of salinization on crop germination, yield, and plant performance (Zörb et al. 2019), SWI-induced salinization is a unique phenomenon comprised of high salinity levels and periods of saturation.

Salt tolerance in plants

Salt stress reduces a plant's ability to absorb water (osmotic stress) and causes an ion imbalance (e.g. ionic stress due to excess sodium [Na⁺] and chloride [Cl⁻]). These imbalances can suppress growth and limit productivity, ultimately resulting in plant death (Zhu 2001, Parida and Das 2005, Roy et al. 2014, Parihar et al. 2015). Osmotic stress occurs when there is a reduction in the absorption of water by plants (Parihar et al. 2015), which can suppress the rate of shoot growth, cell expansion, and causes stomatal closure (Munns and Tester 2008). Ionic stress, on the other hand, occurs when there is an accumulation of Na⁺ and Cl⁻ at toxic concentrations within plant tissues (Parida and Das 2005, Munns and Tester 2008, Roy et al. 2014). When concentrations of Na⁺ and Cl⁻ reach toxic levels, plants experience premature leaf death, reduced photosynthesis, and suppressed growth rates (Munns and Tester 2008). Further, these stressors are not

mutually exclusive as ionic stress is the combination of ion toxicity (both Na^+ and Cl^-) and lowered osmotic potential (Igartua et al. 1994, Shani and Dudley 2001).

Salt tolerance is the ability of a plant to complete its life cycle on a substrate with high concentrations of soluble salts (Parida and Das 2005, Zörb et al. 2019). Plants utilize biochemical strategies to manage salt exposure, including selective accumulation or exclusion of ions, control of ion uptake by roots and transport into leaves, and re-translocation of Na^+ and Cl^- from the leaves to the roots (Erdei and Taleisnik 1993, Koyro 1997, Netondo et al. 2004, Parida and Das 2005, Roy et al. 2014). Halophytes (e.g. *Salicornia*, *Taeniatherum*, *Chenopodium*) are plants adapted to growing in saline conditions and commonly exhibit salt tolerance through biophysical mechanisms. First, the plant compartmentalizes Na^+ in the vacuole in order to prevent toxicity in the cytosol (Zhu 2001, Flowers et al. 2010). Second, they suppress ion concentrations in the xylem through reducing movement of solution through the apoplast in order to reduce the amount of salt reaching the leaves (Flowers and Colmer 2008, 2015). However, halophytes may be sensitive to high levels of salinity ($\sim 25 \text{ dS m}^{-1}$; Colmer and Flowers 2008) during germination or seedling emergence stages, even if they can tolerate these levels as a mature plant (Malcolm et al. 2003, Debez et al. 2004, Adolf et al. 2013, Panuccio et al. 2014, Zörb et al. 2019). On the other hand, many mature glycophytes (salt-intolerant plants; e.g. *Triticum*, *Maize*, *Nicotiana*) are unable to regulate ions entering the xylem at salinity levels $>4 \text{ dS m}^{-1}$ in mature stages because they do not have the biochemical mechanisms to cope with salt stress (Munns and Tester 2008, Flowers and Colmer 2015). Most common agricultural crops are glycophytes and exhibit 50-80% declines in productivity when salinity reaches between 4-8 dS m^{-1} (2 ppt and 4 ppt,

respectively; Tanji and Kielen 2002, Munns and Tester 2008, Ventura et al. 2015, Zörb et al. 2019). Although a large body of research examines salt tolerance, it generally focuses on seedling or mature plant life stages when saline irrigation water is applied. However, in salt-intruded fields, farmers plant seeds that are frequently exposed to (and saturated by) saline water. Our work quantifies the germination success of agricultural crop species under osmotic and ionic stress in both a controlled environment experiment and in salt-intruded fields.

Successful seed germination requires the absorption of water through the seed wall via diffusion and capillary action as water moves from outside the seed wall (higher water potential) to inside the seed wall (lower water potential; Woodstock 1988). Salt may affect germination through osmotic, ionic, or a combination of the toxicities (Welbaum et al. 1990, Huang and Redmann 1995). Salinity lowers the water potential of the germination medium, giving the medium a lower water potential than inside the seed (Khan and Weber 2008, Parihar et al. 2015), slowing the absorption of water. As water prefers to move from higher to lower water potentials, seeds have difficulty imbibing when salt is present. In a controlled environment, we expect standard crop seeds (e.g. corn, soybean, wheat) to require more time to germinate than alternative crop seeds (e.g. sorghum, salt-tolerant soybean, barley). Furthermore, we expect alternative crop seeds to have a higher germination threshold at higher ionic and osmotic stress levels than standard crop seeds.

Plant breeders have been working for decades to develop salt-tolerant crop varieties, especially those adapted to the arid and semi-arid regions experiencing salinization due to irrigation demands (Ashraf and Akram 2009). However, breeding for

salt-tolerance is difficult because it is a multigenetic trait (Flowers 2004, Flowers et al. 2010), and while the genes used for ion exclusion (e.g. Cl⁻) are well-established and manipulated, the mechanisms of osmotic tolerance remain unknown (Roy et al. 2014, Munns and Tester 2008). Thus, crops bred for salt-tolerance may remain vigorous when experiencing ionic stress, but not osmotic stress. Other crops, such as barley (*Hordeum vulgare* L.), sorghum (*Sorghum bicolor* L.), and rapeseed (*Brassica napus* L.; Table 1.1), are naturally salt-tolerant due to the activation of salt-induced genes of the Lea gene family, which are responsible for the efficient transport of ions across vacuole and cell membranes (Chandra Babu et al. 2004, Roychoudhury and Chakraborty 2013, Li et al. 2013, Gürel et al. 2016, Chen et al. 2019). Our research examines the germination success of crops with natural and bred salt-tolerance in fields experiencing SWI. We expect crops bred for salt-tolerance (e.g. salt-tolerant soybean) will have higher laboratory and in-field germination than natural salt-tolerant crops (e.g. sorghum).

Standard vs. alternative crop species

The low-lying topography of the Eastern Shore of Maryland (2.7 m above sea level) allows saline water to move into ground- and surface water. The rates of sea level rise in the region are three times the global average (Sallenger et al. 2012), pushing saltwater further inland each year. Unsurprisingly, we have observed dramatic declines in the productivity of crops on salt-intruded agricultural fields (Jarrod Miller and Larry Fykes, *personal communication*). Two management strategies available to farmers battling SWI are (1) to resist change, and continue growing the standard crop rotation (corn [*Zea mays* L.], soy [*Glycine max* (L.) Merr.], and wheat [*Triticum aestivum* L.]) as long as they can or (2) to adapt to change, and grow salt-tolerant crops economically-

appropriate for the region (sorghum, salt-tolerant soybean, and barley). Our objectives were: (1) to determine how osmotic and ionic stress levels affect seed germination in the standard crops and alternative salt-tolerant crops; and (2) to determine the germination success of alternative crop species planted on salt-intruded farm fields. We hypothesized that: (H1) in the controlled environment experiment, alternative crop species (sorghum, salt-tolerant soy, and barley) will have a higher germination threshold at elevated ionic and osmotic stress levels than the standard crop species (corn, soybean, and wheat); (H2) in the field experiment, soybean bred for salt-tolerance will have higher in-field germination success than sorghum.

Methods

Controlled environment experiment

Effect of osmotic and ionic stress on crop germination

We grouped crop species by their utility into two farmer management scenarios: *resist* and *adapt*. In the Mid-Atlantic US, standard (*resist*) crops like corn (*Zea mays* L.), soy (*Glycine max* (L.) Merr.), and wheat (*Triticum aestivum* L.), all have salinity thresholds of 2, 5, and 6 dS m⁻¹, respectively (Tanji and Kielen 2002; Table 1.1), and are typically grown in rotation. These thresholds are far below salinity levels observed in the fields on the Eastern Shore of Maryland where this research was conducted (12 dS m⁻¹; Tully et al. 2019b). Alternative (*adapt*) crop species include: sorghum (*Sorghum bicolor*), salt-tolerant soybean (*Glycine max*), barley (*Hordeum vulgare*), and quinoa (*Chenopodium quinoa*), which have salinity thresholds of 7, 11, 8, 30 dS m⁻¹, respectively (Table 1.1). We designed a 10 x 7 factorial experiment at George Washington University

(Washington, D.C.) to test the effect of osmotic and ionic stress on seed germination (Table 1.2). We created ten osmotic potentials using mixtures of Polyethylene Glycol 8000 (PEG) and distilled water and ten ionic potentials using mixtures of sodium chloride (NaCl) and distilled water. The ten potentials were the same for osmotic and ionic stress: 0, -0.2, -0.5, -0.8, -1.1, -1.4, -1.8, -2, -3, -4 MPa.

When PEG has a molecular weight greater than or equal to 6000, it cannot penetrate the cell wall of seeds (Carpita et al. 1979, Verslues et al. 1998), thus mimicking osmotic stress. The concentration of PEG used to create each solution was calculated using Eq. 1 (Hardegree and Emmerich 1990).

$$\psi = 0.130[PEG]^2T - 13.7[PEG]^2 \quad \text{Eq. 1}$$

Where, Ψ is the water potential in MPa, PEG is grams of PEG per gram of water, and T is temperature in degrees Celsius. In this study, $T=25^\circ\text{C}$ because seeds in solution were kept in an incubator set to 30°C and 20°C for equal amounts of time. The concentration of NaCl was calculated using Eq. 2 (Lang 1967).

$$[NaCl] = \frac{\psi}{2RT} \quad \text{Eq. 2}$$

Where, Ψ is the water potential in atm, T is temperature in Kelvin, and R is the ideal gas constant $\left(0.8206 * \frac{L*atm}{mol*K}\right)$. In our case, $T=25^\circ\text{C}$ as the solutions were in an incubator for equal amounts of time at both 30°C and 20°C .

To mimic field conditions where seeds are regularly saturated with saltwater, we placed 25 seeds per species on one 85 mm Grade 1 Whatman filter paper, 11 μm pore size, in 100 x 20 mm glass petri dishes and moistened with 3.2 mL of deionized water, PEG solution, or NaCl solution. Each species x solution combination was replicated four times (total of 100 seeds per species x solution combination). The petri dishes were

tightly covered and wrapped with parafilm to prevent evaporation and were incubated in a Percival Incubator (Percival Scientific, Perry, IA) on a diurnal cycle of 30°C for 12 hours light and 20°C for 12 hours dark. If the filter paper appeared to be drying or there visibly was no solution in the petri dish, we replaced the filter paper and added 3.2 mL of solution to the petri dish. Due to the large seed size of corn, larger petri dishes and filter paper were used (150 and 125 mm diameter, respectively), and 7.8 mL of solution was added to fill the larger volume. Germination counts were made in ~6 hour intervals in the first 48 hours of experiment initiation and then in ~2-4 hour intervals for the following two days. After four days, a daily single count was made until there was no new germination observed for 14 consecutive days. A seed was considered germinated, if a radical was present.

We used germination data to calculate the time to 50% germination (Eq. 3).

$$t_{50} = T_i + \frac{\left(\frac{N}{2} - N_i\right)(T_j - T_i)}{N_j - N_i} \quad \text{Eq. 3}$$

Where, t_{50} is the median germination time, N is the final number of germinated seeds, N_i and N_j are the total number of seeds germinated in adjacent counts at time T_i and T_j , respectively (Farooq et al. 2005). The time to 50% germination standardizes germination rates so that they are comparable among studies (Scott et al. 1984, Ranal and Santana 2006). Within a species seed lot or across different species, seeds can germinate at varying rates, and data is not normally distributed, making it challenging to draw comparisons. Time to 50% germination is a measurement that provides a central tendency to the data, which is comparable to the mean of normal distribution (Scott et al. 1984, Ranal and Santana 2006).

Field experiment

Study location

Our study sites are near Crisfield, Maryland in Somerset Co. (37.983436° N, -75.854527° W) and Cambridge, Maryland in Dorchester Co. (38.5632° N, 76.0785° W); farm fields in the region have been no-till for at least 40 years (Huggins and Reganold 2008). The majority of soils in Somerset Co. are Quindocqua silt loams with little to no slope (USDA NRCS 2019). The focal farm located in Somerset Co. sits on predominantly Othello-Fallsington complex sandy loam soils and has a mean elevation of 1 m above sea level. In 2018, Somerset Co. received 1110 mm of rainfall and the mean temperature was 21.8°C over the growing season (April to October; NOAA 2018; Table 1.3). A second farm is located in Dorchester Co., received 1022 mm of rainfall, and the mean temperature was 21.4°C during the 2018 growing season (NOAA 2018). The majority of soils in Dorchester are very frequently flooded Honga peat soils (USDA NRCS 2019). The Dorchester Co. farm sits on predominantly Elkton silt loam soils and has a mean elevation of 1 m above sea level (Table 1.3). Saltwater moves onto agricultural fields via hydrologically connected ditch networks and the groundwater table (Tully et al. 2019a). The extensive agricultural ditch network designed to drain excess water from farms often serves the reverse purpose by acting as a conduit for saltwater to reach the fields during high tides and storms (Bhattachan et al. 2018, Tully et al. 2019a).

Experimental design

To determine the effect of SWI on germination *in situ*, experimental plots were established in a randomized complete block design with four replicates per treatment at farms in Somerset Co. and Dorchester Co. (herein referred to as “Somerset farm” and

“Dorchester farm”). Treatments consisted of: (1) a natural recruitment control (colonized by species in the seed bank, predominantly agricultural weeds and locally sourced species); and (2-4) a sorghum-salt tolerant soybean-barley rotation with each entry point present each year (total of three plots per block). Each plot was 3 m wide by 20 m long and established within 2 m of the field edge with evidence of SWI. Plots were made intentionally long so as to span a natural salinity gradient, from high salinity near the field edge (0-5 m) to low salinity towards the center of the field (15-20 m). There were 0.5-1 m buffers between each plot and four replicates of each treatment for a total of 24 plots per farm.

Porous cup lysimeters (22 mm diameter; Soil Solution Access Tubes, Irrrometer Riverside, California, USA) were installed to 60 cm depth at 5 m (near salt source) and 15 m from the edge of the plot (far from salt source). Lysimeters were installed using a soil probe and a slurry made with the deepest soil was poured into the hole before inserting the lysimeter to ensure good soil contact. Finally, lysimeters were sealed at the soil surface with a bentonite/clay mixture to avoid preferential flow of water down the side of the tube. Pilot studies confirmed that soil solution collection was only possible following rain events that were greater than or equal to 6 mm, thus soil solution was only collected following rain events of this level. For this study, we used soil solution collected on August 8, 2018 and June 21, 2019. The day before sampling, lysimeters were purged of any water, and an internal pressure of -60 to -70 kPa was applied. Soil solutions were collected, filtered (Whatman No. 42; 2.5 μ m), and stored in a freezer at -20°C until further analysis for electrical conductivity. Electrical conductivity (EC) was

measured on a Thermo Scientific Orion Versa Star Advanced Electrochemistry Meter probe (Waltham, MA).

Prior to planting, plots were sprayed with glyphosate [N-(phosphonomethyl) glycine] (~0.91 kg active ingredient per acre) in early-May 2018. Sorghum (var. *Dekalb* DKS 2805) and salt-tolerant soybean seeds (Pioneer P42a52x; Cl⁻-excluder) were sown once in mid-May 2018 using a 1.52-m Tye drill and again in mid-June 2018 due to poor germination as a result of heavy rainfall (328 mm) between May 16 and June 16, 2018. Sorghum and salt-tolerant soybean were planted in 38.1 cm rows at a rate of 197,600 seeds ha⁻¹ and 481,650 seeds ha⁻¹, respectively. Salt-tolerant soybean plots received 39 kg ha⁻¹ of K⁺ in the form of potash (K₂SO₄) and sorghum received 84 kg ha⁻¹ as urea in late-June 2018. In early August 2018, salt-tolerant soybean was sprayed with glyphosate (~0.45 kg active ingredient per acre) and fomesafen sodium salt [5-[2-chloro-4-(trifluoromethyl)phenoxy]-N-methylsulfonyl-2-nitrobenzamide (~0.32 kg active ingredient per acre). All plots were sprayed with glyphosate [N-(phosphonomethyl) glycine] (~0.91 kg active ingredient per acre) in early-May 2019. Sorghum and salt-tolerant soybean were sown in early-June 2019 using a 1.52-m Tye drill. Sorghum was planted with the same row width and seeding rate as in 2018. In 2019, salt-tolerant soybean was planted in 19 cm rows at a rate of 481,650 seeds ha⁻¹. Sorghum received 84 kg ha⁻¹ as urea and salt-tolerant soybean received 67 kg ha⁻¹ of K in the form of potash in early-June 2019. Due to poor germination, sorghum and salt-tolerant soybean were re-sown, with the same seeding practice, in late-June 2019.

Field germination surveys

In late July 2018 and 2019, plots were surveyed in order to determine the percent germination in each field. On July 24, 2018, every sorghum plant was counted in each 0-5 m, 5-15 m, and 15-20 m segment of each plot. We also recorded the percent cover of salt-tolerant soybean in each plot as the stands were too dense to easily identify individuals without damaging plants. We conducted germination studies slightly differently in 2019. On July 18, 2019, three out of six rows were randomly selected from each plot and every sorghum and salt-tolerant soybean plant was counted along the row in each 0-5 m, 5-15 m, and 15-20 m plot segment. For each plot segment, we summed counts of the 3 rows and multiplied by two because we assumed that three rows were a representative sample of the six rows. Seedling emergence of sorghum and salt-tolerant soybean was used as a proxy for field germination as they were planted as seeds. Percent germination for each plot was calculated based on the known seeding rate and the number of plants surveyed (Eq. 4).

$$\text{field germination rate (\%)} = \frac{\# \text{ of plants in plot after } \sim 30 \text{ days}}{\text{seeding rate (seeds per plot)}} \quad \text{Eq. 4}$$

Statistical analysis

Controlled environment experiment

First, we tested the effect of osmotic and ionic stress on percent germination using a linear mixed-effects (LME) model (*lme4* package for R; Bates et al. 2013) where water potential and species were fixed effects and replicate was a random effect (total of two LME models: osmotic stress and ionic stress). There was a significant interaction between water potential and species for both osmotic stress and ionic stress, but the

model did not provide us the level of detail needed to compare percent germination of species at every water potential. Therefore, to test the effects of salinity (as a function of osmotic vs. ionic stress) on species germination, we used a non-parametric test (Mann-Whitney) to determine differences in percent germination in planned comparisons between standard and alternative crop species, which represent parallel points in a rotation at each salinity stress (osmotic or ionic) and water potential (*stats* package in R; R Development Core Team 2019). Specifically, we compared the percent germination of barley to wheat, salt-tolerant soybean to standard soybean, sorghum to corn, and quinoa to every species. Given a large number of comparisons generated, a Bonferroni-corrected α was used to reduce Type I error (Sedgwick 2012). Significance was determined at $P < 0.0002$. We tested for effects of each osmotic stress and ionic stress on the time for each species to reach 50% germination (Eq. 3) using an unpaired Mann-Whitney test. Significance was determined at $P < 0.0002$ in all cases.

To test the effects of salinity stress at the same water potential on the percent germination of crop categories (standard vs. alternative), we ran one Mann-Whitney test without quinoa and a second with quinoa included as a species of the alternative crop category. Initially, we excluded quinoa because we wanted to compare the standard crops in rotation to the alternative crops farmers would grow in the region. We then included quinoa as a species of the alternative crop category because we wanted to assess how it compared to the standard crops. Given a large number of comparisons generated, a Bonferroni-corrected α was used to reduce Type I error. Significance was determined at $P < 0.003$ in all cases.

Field experiment

At Somerset farm and Dorchester farm, we did not manipulate ionic or osmotic stress. In order to evaluate the levels of osmotic and ionic stress in the field, we used EC (measured in dS m^{-1}) of soil porewater collected from lysimeters located 5 m and 15 m from the plot edge in the SWI fields (installed 60 cm below ground surface) on August 8, 2018 and June 21, 2019. To test if there was a difference in porewater EC between the two locations on the SWI transect, we used a LME model with distance (5 m vs. 15 m from plot edge) as the main effect and block as the random effect. We conducted separate LME models for each farm and each year (total of four LME models: Somerset farm in 2018, Dorchester farm in 2018, Somerset farm in 2019, Dorchester farm in 2019).

To determine if sorghum germination differed with distance from the saltwater source (5 m vs. 15 m) in 2018, we conducted LME models with distance as the main effect and block as the random effect (total of two LME models: Somerset farm and Dorchester farm). To determine if sorghum germination differed between 2018 and 2019, we conducted LME models with year and distance from plot edge (5 m vs. 15 m) as main effects and block as the random effect.

To evaluate if in-field germination was better explained by ionic or osmotic stress, we used a generalized linear model (GLM) with ionic or osmotic stress levels as a fixed effect and controlled environment sorghum or salt-tolerant soybean germination as the response variable (total of 4 GLMs: sorghum germination by ionic stress; sorghum germination by osmotic stress; salt-tolerant soybean germination by ionic stress; salt-tolerant soybean germination by osmotic stress; *lme4* package for R; Bates et al. 2013). Upon inspection, patterns appeared to be non-linear, suggesting threshold responses.

Thus, we tested non-linear models (e.g. quadratic and logistic regression). We conducted an AIC model comparison to determine which model better fit the data (*MASS* package for R; Venables and Ripley 2002; Table S1.1). The germination responses in-field in relation to the 95% confidence intervals of the model (on controlled environment germination response) were used to evaluate if in-field germination was better explained by ionic or osmotic stress.

We used Box-Cox transformations (Box and Cox 1964) prior to analysis when necessary to satisfy the assumptions of the statistical model. All analyses were conducted in the R environment for Macintosh (v1.2.1335).

Results

Controlled environment experiment: the effect of osmotic and ionic stress on seed germination

Across all seven species, we observed variable tolerance to osmotic stress (reduced ability to absorb water; Fig 1.1). Barley and wheat were the only species to germinate at osmotic stress levels below -1.1 MPa. However, there was no significant difference between wheat and barley percent germination at every osmotic stress levels. Surprisingly, standard soybean and salt-tolerant soybean had very similar germination responses to osmotic stress (Fig 1.1). Quinoa was able to germinate to -0.8 MPa (osmotic stress) but did not have higher percent germination at -0.8 MPa than corn, sorghum, and barley. When grouped, we found no difference in percent germination between the standard crops and alternative crops at any osmotic stress level (Fig 1.2 & 1.3). In addition, there was no difference in time to 50% germination between the standard crops and the alternative crops at any osmotic stress levels (Fig 1.4).

Salt-tolerant soybean, soybean, and quinoa were the only species able to germinate under ionic stress levels. Salt-tolerant soybean was able to germinate at high ionic stress levels (-2 MPa; 36.9 ppt), which is equivalent to levels found in seawater (Fig 1.1). Standard soybean was also surprisingly tolerant of ionic stress; it was able to germinate at -1.8 MPa (32.9 ppt). There was no difference in percent germination between standard soybean and quinoa or salt-tolerant soybean and quinoa at any ionic stress level. We found no difference in percent germination between salt-tolerant soybean and standard soybean at any ionic stress level. When grouped, we found no difference in percent germination between the standard crops (corn, soybean, and wheat) and alternative crops (sorghum, salt-tolerant soybean, barley, quinoa) at any ionic stress level (Fig 1.2 & 1.3). We also found no difference in time to 50% germination between standard crops and alternative crops experiencing ionic stress (Fig 1.5).

Field experiment: the effect of saltwater intrusion on field germination compared to lab germination

Salt-tolerant soybean and sorghum were grown on Somerset farm and Dorchester farm in 2018 and 2019 however, due to a change in survey protocol (see *field germination surveys* in Methods), we only have in-field germination percent for salt-tolerant soybean in 2019 but germination percent for sorghum in both 2018 and 2019.

At Somerset farm, there was no significant difference in EC of soil solutions (60 cm below ground surface) with distance from saltwater source (5 m vs. 15 m from the plot edge). As there was no effect of year on EC (2018 vs. 2019), the mean EC of soil solutions at 60 cm at Somerset farm was 5.44 ± 0.61 dS m⁻¹ (-0.2 MPa) across 2018 and 2019. At Dorchester farm, there was no effect of year on the EC of soil solutions.

However, in both years, the EC of soil solutions was significantly higher 5 m from the plot edge ($6.49 \pm 0.35 \text{ dS m}^{-1}$; -0.23 MPa) than at 15 m from the plot edge in Dorchester farm ($4.92 \pm 0.42 \text{ dS m}^{-1}$; -0.18 MPa ; $P=0.02$ for both years).

In 2018, we observed no significant effect of distance from the plot edge (SWI effect) on sorghum germination at either Somerset or Dorchester farm (Table 1.4A). In 2019, percent germination did not differ between sorghum and salt-tolerant soybean at Somerset farm (Table 1.4B). Further, there was no difference in salt-tolerant soybean and sorghum percent germination with distance from the plot edge (SWI effect). In 2019 at Dorchester farm, salt-tolerant soybean percent germination was two times higher than sorghum ($P=0.001$).

We observed no significant effect of year (2018 vs. 2019) on sorghum germination at Somerset farm. However, at Dorchester farm, sorghum germination in 2018 was two times higher than in 2019 ($P=0.001$; Table 1.4A & 1.4B).

We combined in-field germination of sorghum in 2018 and 2019 to evaluate if in-field germination was better explained by ionic or osmotic stress. As we only had salt-tolerant soybean in-field germination for 2019, we paired that data with the controlled environment salt-tolerant soybean germination data. The decline in sorghum germination was best explained by increasing ionic stress levels (Fig 1.6A), but declines in salt-tolerant soybean were better explained by increasing osmotic stress levels (Fig 1.6B).

Discussion

This is the first study to determine the effect of SWI on crop seed germination by (1) determining how osmotic and ionic stress levels affect seed germination in standard

and alternative salt-tolerant crops in a controlled environment experiment and (2) determining the germination success of alternative crop species planted on salt-intruded farm fields. We focused on the germination phase of crop species because it is the initial determinant of plant success and because farmers plant seeds, thus relying on successful germination to have productive yields.

Standard vs. alternative crop species

In our controlled environment experiment, we observed lower percent germination under ionic stress compared to osmotic stress, which is in contrast to many studies that report higher percent germination under ionic than osmotic stress (Francois et al. 1984a, Prado et al. 2000, Radic et al. 2007, Carpıcı et al. 2009, Khayatnezhad et al. 2010, Zhang et al. 2010, Ruiz-Carrasco et al. 2011, El Naim et al. 2012, Kırmızı and Bell 2012, Panuccio et al. 2014, Faijunnahar et al. 2017). We propose that the difference is due to the way we assessed the effect of ionic and osmotic stress, which was meant to closely resemble the salt-intruded field conditions where farmers are planting seeds. Farmers seed fields that are regularly inundated with saltwater and experience saline soil conditions, resulting in seeds germinating under high salinity stress, at the soil surface, and under saturated conditions. Therefore, we germinated seeds on saturated filter paper (Radic et al. 2007, Carpıcı et al. 2009, Khayatnezhad et al. 2010, Kırmızı and Bell 2012) because seeds drilled into the soil at a shallow depth often float to the surface following an influx of saltwater via a storm or high tide (*personal observation*). Most studies use sand or soil as a germination medium because they report salt-tolerance at several life stages and/or they report the effect of saline irrigation water on plant survival, which

provides an episodic input of salt, that drains rapidly through the soil matrix (Zhao et al. 2010, Maas et al. 1983, Peterson and Murphy 2015, Maas et al. 1986, Ghassemi-Golezani and Taifeh-Noori 2011, Zheng et al. 2008). Of note is that we did not include the most salt-tolerant crop varieties available to growers, but instead used alternative crop varieties farmers of the Mid-Atlantic region would purchase and plant (as determined after extensive stakeholder meetings). It was important that our research was designed to answer questions relevant and applicable to the farmers in the region and under the current market and environmental conditions.

Nevertheless, we were curious to document how quinoa would germinate under the same salinity conditions imposed on the standard and alternative crop species because quinoa is a halophyte and tolerant of salinity levels approaching those of seawater (Adolf et al. 2013, Adolf et al. 2012, Shabala et al. 2012). Furthermore, quinoa can grow in drought-prone and marginal soils (Jacobsen et al. 2003, 2005, 2007, Sun et al. 2014) such as those found on the Eastern Shore, MD. Quinoa germination was similar to other studies (Maas et al. 1983, Almansouri 2001, Panuccio et al. 2014), and germinated at high levels of ionic stress (-0.2 to -0.5 MPa), outperforming barley, wheat, corn, and sorghum. However, we did not include quinoa in the field experiment because our farmer partners stated they would not plant quinoa due to the cost of new equipment (e.g. new seed plates) and the non-existent market. Further research is needed to assess if there could be a market for quinoa in the region and if it would be advantageous for farmers to plant quinoa on their salt-intruded farm fields.

Markets on the Eastern Shore, MD support the cultivation of sorghum, salt-tolerant soybean, and barley, all of which past research indicated should have a higher

salt tolerance than corn, soybean, and wheat (Rani et al. 2012, Munns et al. 2006, Munns and Tester 2008; Table 1.1). For example, barley seeds are capable of absorbing Na^+ , which facilitates imbibition and germination under salt stress as water is able to pass through the cell wall (Zhang et al. 2010). Although we hypothesized the alternative crop species (e.g. sorghum, salt-tolerant soybean, and barley) would have higher ionic and osmotic stress levels than the standard crops (e.g. corn, soybean, and wheat), our data does not support the hypothesis. Instead, we observed no difference in germination (Fig 1.2 & 1.3) or time to 50% germination (Fig 1.4 & 1.5) between the alternative and standard crop species in the controlled environment experiment. Based on the controlled environment data alone, one might assume there would be no reason for a farmer to switch from the standard crops to alternative crops. However, farmers on the Eastern Shore, MD are already switching to sorghum on salt-intruded farm fields instead of corn because corn cannot produce profitable yields (Jarrod Miller, *personal communication*), further highlighting the importance of pairing controlled environment experiments with field trials.

Field germination of salt-tolerant soybean and sorghum

Overall, we observed reduced percent germination in areas near the field edge, where salinity was highest. Although the plot edge soil solution salinity levels were within the threshold range of sorghum and salt-tolerant soybean (Table 1.1), the soil surface (0-10 cm) salt concentrations were higher (-0.4 MPa; 6.4 ppt; unpublished data) likely as a result of capillary rise, drawing water up the profile where it evaporates and leaves salts behind (van Hoorn 1991; Barica 1972). In addition, it can be difficult for

roots to establish in salt-encrusted soils because the seed radicle cannot penetrate the soil (Hanks and Thorp 1957). Therefore, the reduced germination on salt-intruded farm fields is likely due to the fact that seeds germinate on the soil surface where the salinity level is above the threshold of sorghum and salt-tolerant soybean.

Germination success at Dorchester farm in 2019 supported our hypothesis that salt-tolerant soybean would have higher germination than sorghum, which is likely due to the greater sensitivity of sorghum to salinity at the seedling phase compared to soybean (Maas et al. 1986, Igartua et al. 1995, Hosseini et al. 2002). Lower sorghum germination at Dorchester farm in 2019 compared to 2018 may be a result of fluctuations in weather (e.g. rainfall and drought; Table 1.3). Following sorghum planting, Dorchester farm received ~220 mm of rainfall in July 2018 (more than double the rainfall in June; SERCC 2018). Freshwater inputs from heavy rainfall could dilute soil salinity, allowing seeds to germinate in freshwater conditions. However, in July 2019, Dorchester farm received less rainfall (~60 mm) than June (160 mm) when sorghum was planted. Increased evaporative demand could have elevated soil salinity and thus suppressed in-field germination. Annual variability in the frequency of storms and droughts with climate change will drive saltwater further inland and keep it there for longer (Tully et al. 2019a) with clear implications for crop germination and survival. For instance, both Somerset and Dorchester farm required reseeding in 2018 and 2019 because of poor germination as a result of heavy rainfall. Both Somerset and Dorchester farm, in 2018 and 2019, received between 100 and 200 mm at the time of initial seeding. Over the growing season in 2018 (April to October), Somerset farm received 1110 mm of rainfall, 518 mm higher than the historical average of 592 mm of rain; Dorchester farm received 1022 mm of rainfall, 330

mm more rain than the historical average of 692 mm (Table 1.3). Over the growing season in 2019, Somerset farm received 655 mm of rain, only 63 mm higher than the historical average and Dorchester farm received 626 mm of rain, which was 66 mm less than the historical average (Table 1.3). As reseeding fields is an additional expense to farmers, finding the window of time in which weather and soil conditions are favorable to germination success is key.

Comparing controlled environment and field experiments

Saltwater intrusion causes ionic and osmotic stress in crop plants. Saltwater can transport Na^+ and Cl^- ions, initially in the form of flooding, high groundwater tables, or high tides. These salts can also concentrate as water recedes and evaporates from the soil surface (e.g. during droughts). We did not manipulate for ionic or osmotic stress in the field but did so in the controlled environment experiment. We compared field and lab germination to determine whether field germination of sorghum and salt-tolerant soybean was driven by osmotic stress or ionic stress.

The decline in salt-tolerant soybean germination in-field was better explained by increasing osmotic stress rather than ionic stress (Fig 1.6B), suggesting that germinating salt-tolerant soybeans were more sensitive to reduced water availability than Na^+ and Cl^- toxicity. This is likely due to the fact that the cultivar we planted was bred to exclude Cl^- (Pioneer Co®), making it more resistant to changes in ionic strength. Additionally, soybean germination tends to decline sharply in response to reduced water availability (e.g. under drought conditions), which osmotic stress imitates (Dornbos et al. 1989). In addition, studies show that soybean has poor performance following flooding events

(Wuebker et al. 2001). Thus, it follows that field observations on farms across the Eastern Shore of MD indicate no difference in overall performance of standard vs. salt-tolerant soybean (Jarrod Miller, *personal communication*), possibly due to the fact that neither cultivar tolerates fluctuating inundation-drought conditions, a feature of SWI (Tully et al. 2019a). Therefore, we suggest that there is little reason for farmers facing SWI to switch to salt-tolerant soybean because, although the salt-tolerant cultivar shows resistance to ionic stress, it cannot tolerate inundation and drought.

In contrast to soybeans, the decline in sorghum germination (in-field) was better explained by increasing ionic stress than osmotic stress (Fig 1.6A), suggesting that sorghum germination was more sensitive to Na^+ and Cl^- toxicity than water availability (e.g. inundation and drought). This pattern is supported by research that shows sorghum is sensitive to ionic stress at the seedling life stage (Geressu and Gezaghegne 2008, Francois et al. 1984b). In addition, sorghum is a well-known drought-tolerant crop as it was first domesticated in arid regions of Africa (Bibi et al. 2012, Patanè et al. 2013, Tari et al. 2013). Sorghum's response to inundation is less clear with some studies indicating flood tolerance (Ejeta and Knoll 2007, Tari et al. 2013) and others flood-intolerance (Orchard and Jessop 1984, Promkhambut et al. 2011). However, all of these studies report sorghum survival and/or productivity and no studies to date have reported sorghum seed germination (or seedling emergence) in response to flooding. Our data suggest that sorghum germination in-field was a response to changes in ionic stress (Na^+ and Cl^- toxicity) rather than osmotic stress. Coastal farmers facing SWI have already started planting sorghum (Jarrod Miller and Larry Fykes *personal communication*), which we show may be tolerant to osmotic stressors induced by SWI. Therefore, we see no reason

to advise farmers to stop planting sorghum, as it is successfully germinating on salt-intruded fields and outperforming its competitor, corn (Jarrod Miller and Larry Fykes *personal communication*).

The fact that sorghum and salt-tolerant soybean show sensitivity to different stressors associated with SWI highlights the complexity and challenges of identifying crop species capable of germinating on salt-intruded farm fields. Of note, is that this study focused only on germination and not crop yield (of greater importance to farmers). Therefore, more research is needed to understand if sorghum and salt-tolerant soybean are productive and provide profitable yields to farmers. Additionally, as weather conditions become variable (e.g. frequency in storms and droughts) and sea level continues to rise due to climate change, SWI will only move further inland. Emphasis should be placed on the potential of halophytic crops (e.g. quinoa) or restoration species (e.g. *Spartina patens* and *Panicum virgatum*) to be planted on salt-intruded farm fields as a means of ameliorating salt damage or promoting coastal wetland restoration.

Conclusion

The purpose of this study was to (1) determine how osmotic and ionic stress levels affect seed germination in standard crops and alternative salt-tolerant crops in a controlled environment experiment and (2) determine the germination success of alternative crops planted in salt-intruded farm fields on the Eastern Shore of Maryland. Overall, there was no significant difference in percent germination between the standard and the alternative crop species under osmotic or ionic stress in controlled environmental conditions. Under field conditions, germination percent was two times higher in salt-

tolerant soybean than sorghum. The in-field germination patterns of sorghum and salt-tolerant soybean were explained by increasing ionic stress and osmotic stress, respectively. The fact that sorghum and salt-tolerant soybean show sensitivity to different stressors associated with saltwater highlights the complexity and challenges of identifying crop species capable of germinating on salt-intruded farm fields. Farmers facing SWI have to decide whether to resist change and continue growing the standard crops or adapt and begin planting alternative crop species. Understanding the germination success of crop species experiencing SWI is critical to developing informed farm management strategies in coastal agricultural regions. This research provides the groundwork for assessing the success of an alternative salt-tolerant cropping rotation on farms experiencing SWI.

Tables and Figures

Table 1.1. Salinity thresholds (dS m⁻¹ and ppt) at mature plant stage of focal plant species.

Common name	Botanical name	Crop group	Threshold (EC) dS m ⁻¹	Threshold (salinity) ppt	References
Corn	<i>Zea mays</i> L.	Standard	1.8	0.9	Tanji and Kielen 2002
Soybean	<i>Glycine max</i> (L.) Merrill	Standard	5.0	2.7	Tanji and Kielen 2002
Wheat	<i>Triticum aestivum</i> L.	Standard	6.0	3.3	Tanji and Kielen 2002
Sorghum	<i>Sorghum bicolor</i> (L.) Moench	Alternative	6.8	3.7	Tanji and Kielen 2002
Salt-tolerant soybean cultivar	Salt-tolerant <i>Glycine max</i> (L.) Merrill	Alternative	10.6	6.0	Tanji and Kielen 2002
Barley	<i>Hordeum vulgare</i> L.	Alternative	8.0	4.4	Tanji and Kielen 2002
Quinoa	<i>Chenopodium quinoa</i>	Alternative	30	18.9	Adolf et al 2013

Table 1.2. Water potentials (MPa) used in the study and their equivalent electrical conductivity (dS m⁻¹)[†], salinity (ppt)[‡], and sodium chloride (NaCl) concentration (mM).

Water potentials (MPa)	Electrical conductivity (dS m⁻¹)	Salinity (ppt)	NaCl (mM)
0	0	0.0	0
-0.2	5.6	3.0	40.3
-0.5	13.9	8.2	100.9
-0.8	22.2	13.6	161.4
-1.1	30.6	19.3	222.0
-1.4	38.9	25.0	282.5
-1.8	50.0	32.9	363.3
-2	55.6	36.9	403.6
-3	83.3	57.3	605.4
-4	111.1	78.4	807.2

[†] To convert from water potentials (MPa) to electrical conductivity (dS m⁻¹), we used the following equation, EC (dS m⁻¹) = MPa ÷ -0.036 (U.S. Salinity Laboratory Staff).

[‡] The conversion from electrical conductivity (dS m⁻¹) to salinity (ppt) was based on the following equation, ppt = (dS m⁻¹)^{1.0878} * 0.4665, assuming the temperature was 25°C (William 1986).

Table 1.3. Characteristics of Somerset farm and Dorchester farm on the Eastern Shore of Maryland where we conducted the field experiment.

	Somerset farm	Dorchester farm
County	Somerset	Dorchester
Historical growing season rainfall (mm) ^{†‡}	592	692
2018 growing season rainfall (mm)	1110	1022
2019 growing season rainfall (mm)	655	626
Historical growing season mean temperature (°C) [‡]	20.6	20.2
2018 growing season mean temperature (°C)	21.8	21.4
2019 growing season mean temperature (°C)	22.0	22.0
Texture class	sandy loam	silt loam
Soil type	mesic Typic Endoaquults	mesic Typic Endoaquults
Soil series	Othello-Fallsington complex	Elkton

[†] Growing season in Maryland is April to October

[‡] Data from 1971-2000 (SRCC 2018)

Table 1.4. Percent germination of (A) sorghum at Somerset and Dorchester farm in 2018 and (B) sorghum and salt-tolerant soybean at Somerset and Dorchester farm in 2019 field water potential (MPa; mean \pm SE).

(A)	Somerset farm		Dorchester farm	
	Sorghum			
Water potential (MPa)				
-0.18				61 \pm 2.7
-0.20	20 \pm 2.4			
-0.23				45 \pm 6.7

(B)	Somerset farm		Dorchester farm	
	Sorghum	Salt-tolerant soybean	Sorghum	Salt-tolerant soybean
Water potential (MPa)				
-0.18			24 \pm 4.4	54 \pm 4.2
-0.20	12 \pm 3.7	14 \pm 1.7		
-0.23			26 \pm 0.5	43 \pm 5.0

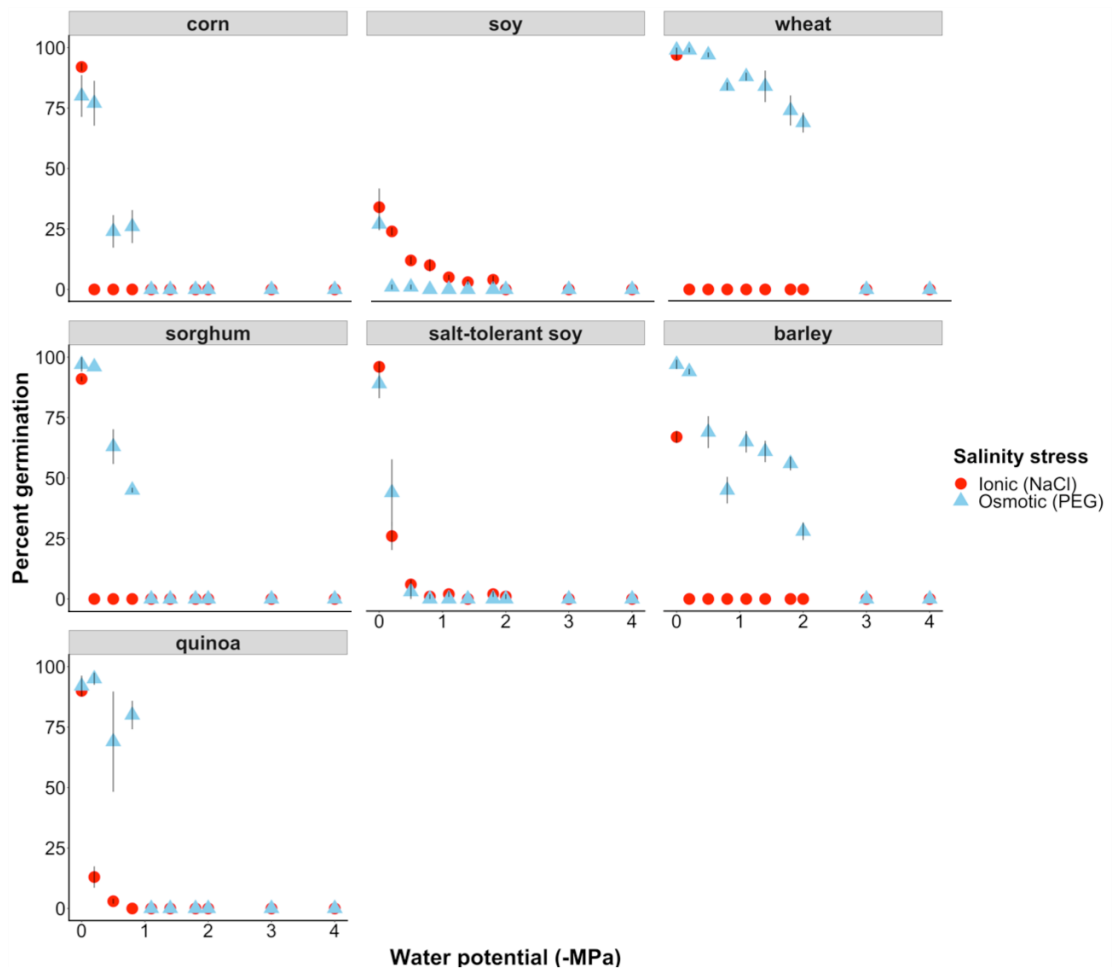


Figure 1.1. Percent germination of corn, soy, wheat, sorghum, salt-tolerant soy, barley, and quinoa along a water potential gradient of ionic stress (red circles) and osmotic stress (blue triangles). Error bars are standard error of the mean.

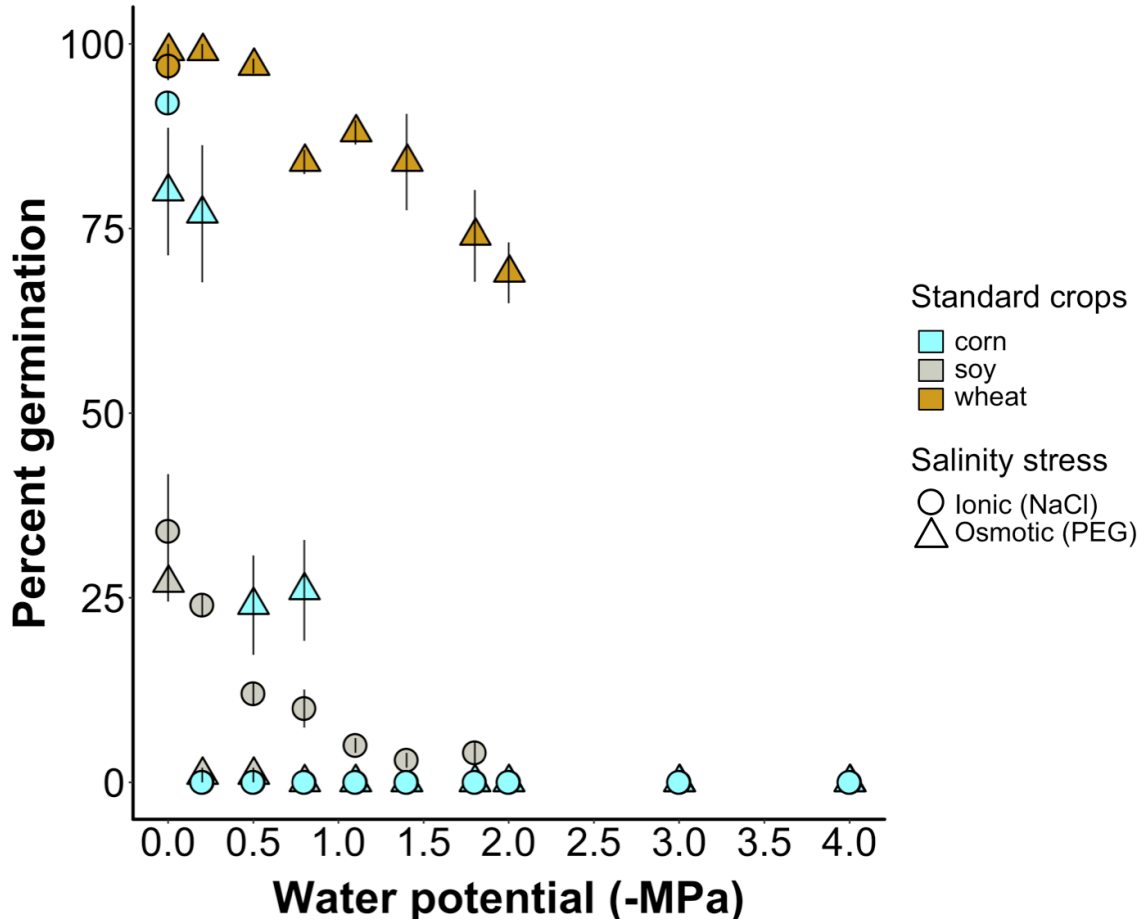


Figure 1.2. Percent germination of standard crop species – corn (blue), soy (gray), wheat (orange) – along a water potential gradient of ionic stress (circles) and osmotic stress (triangles). Error bars are standard error of the mean.

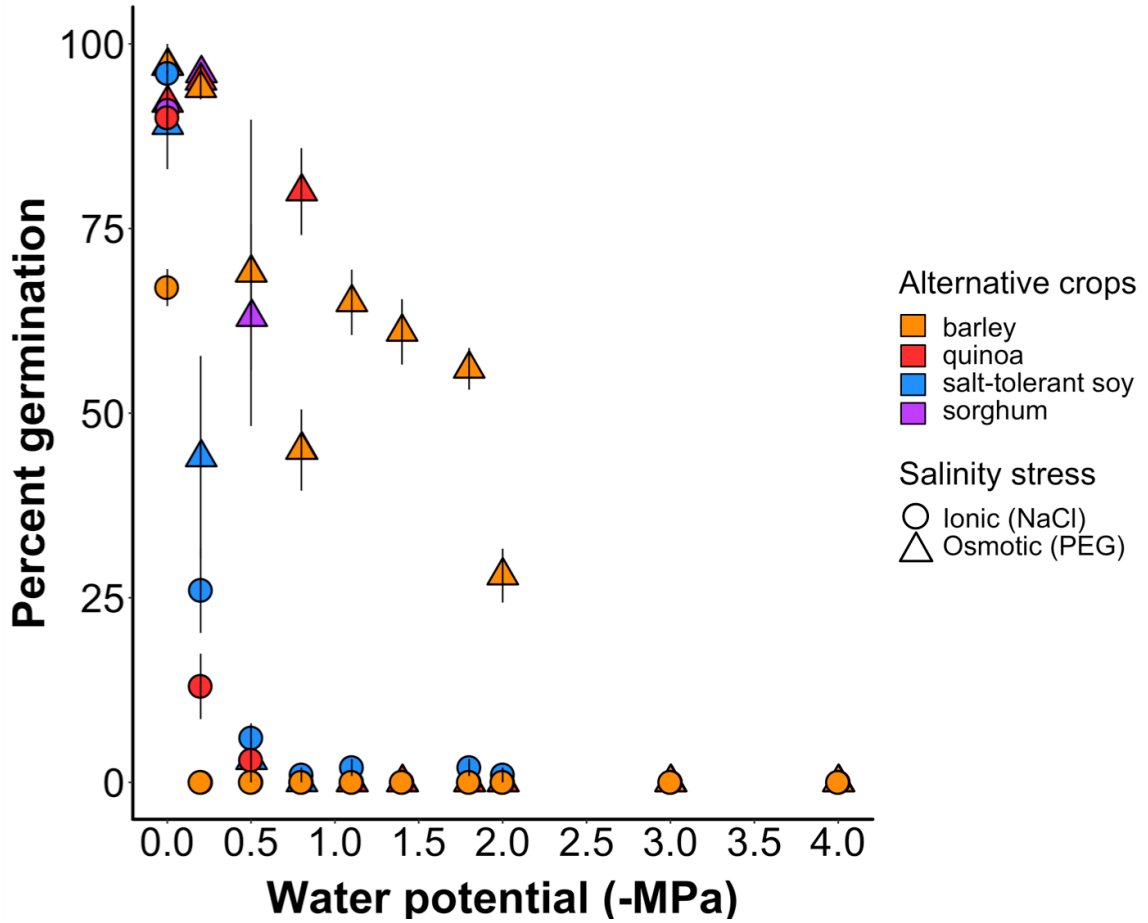


Figure 1.3. Percent germination of alternative crop species – barley (orange), quinoa (red), salt-tolerant soy (blue), sorghum (purple) – along a water potential gradient of ionic stress (circles) and osmotic stress (triangles). Error bars are standard error of the mean.

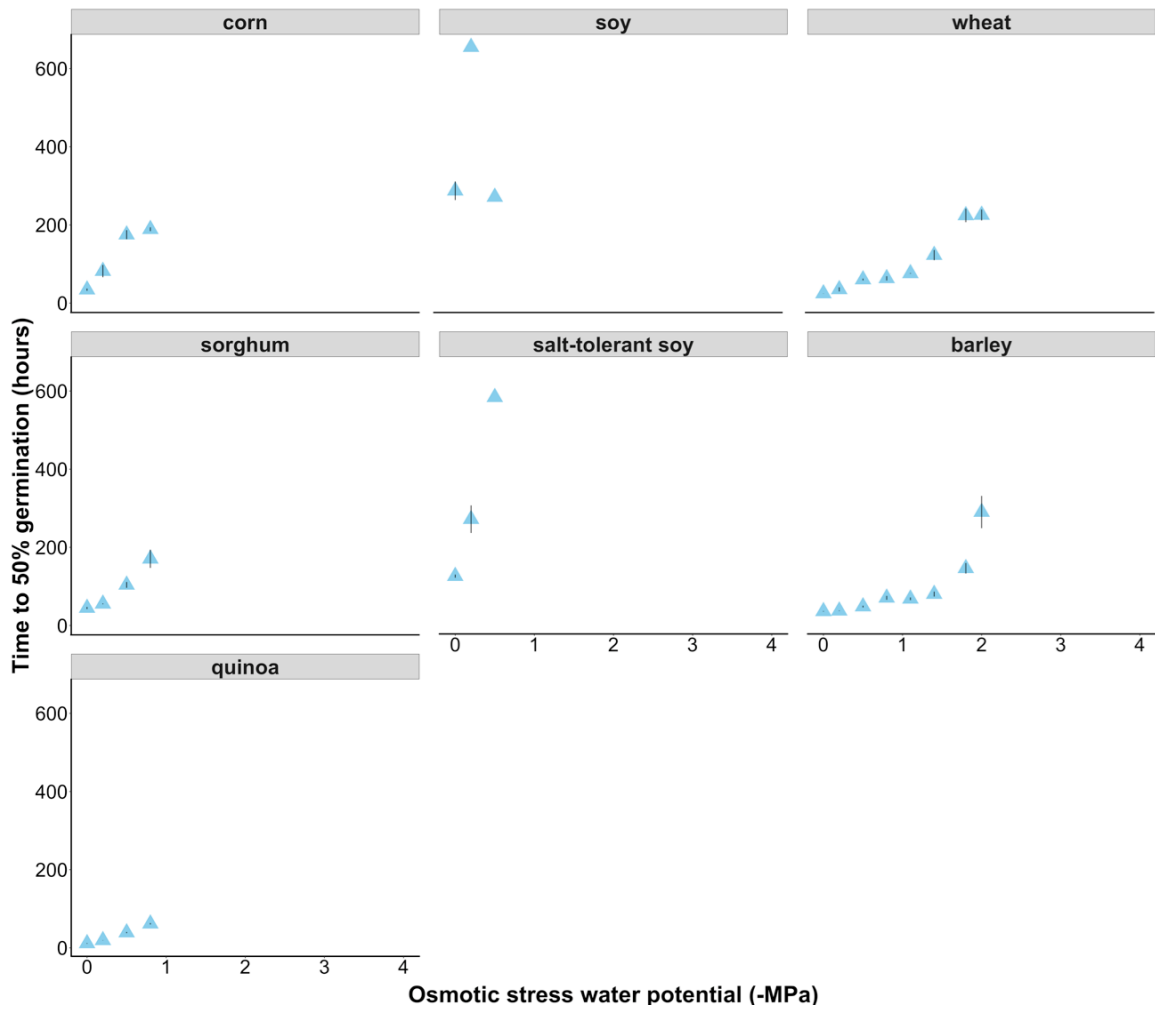


Figure 1.4. Time to 50% germination (hours) of all seven focal species – corn, soy, wheat, sorghum, salt-tolerant soy, barley, quinoa – along a water potential gradient (osmotic stress). Error bars are standard error of the mean.

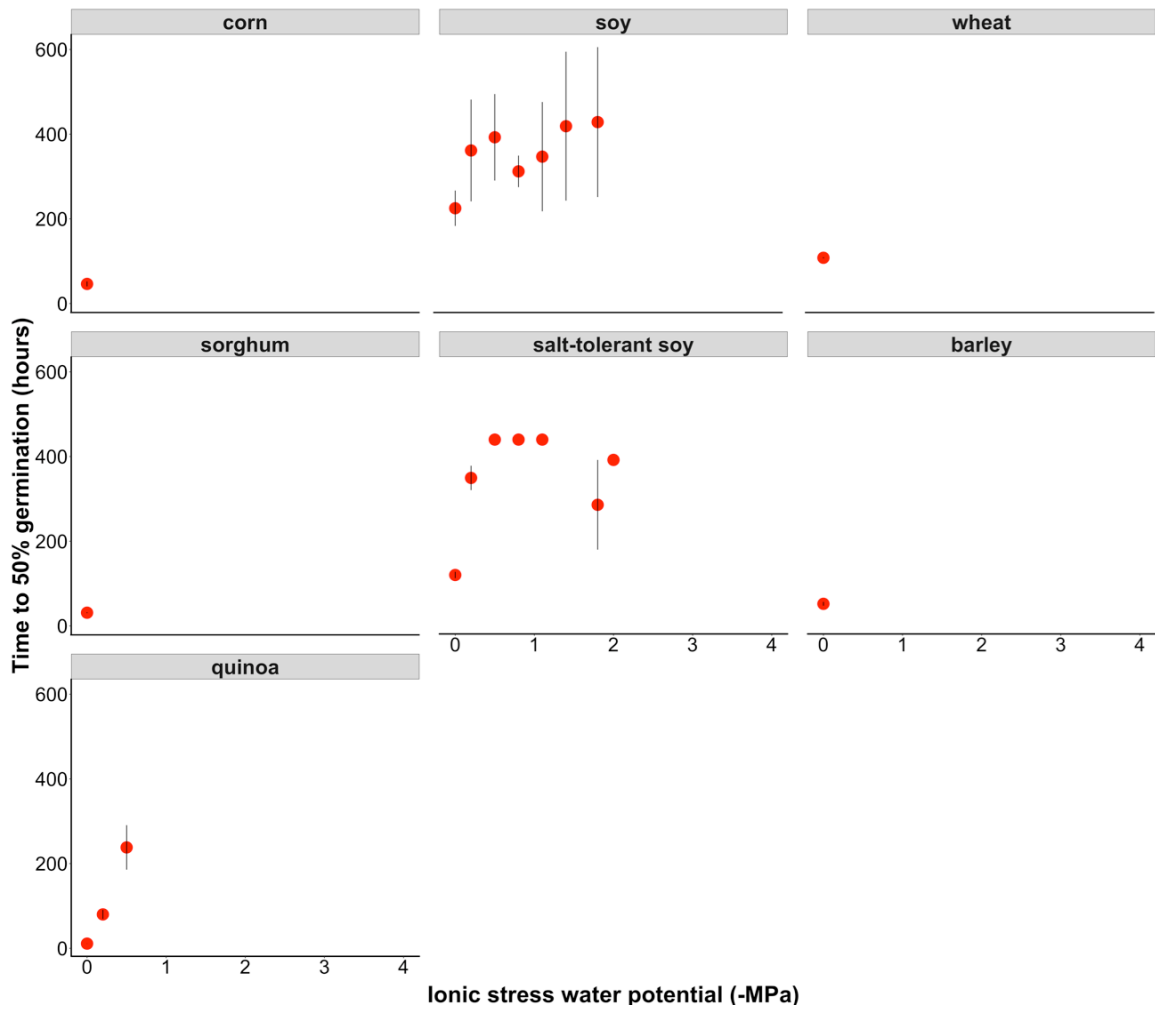
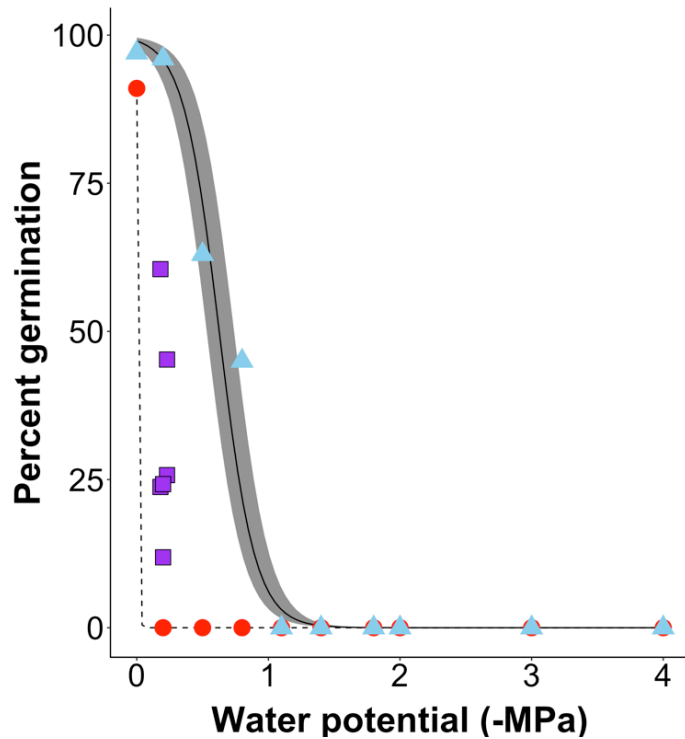


Figure 1.5. Time to 50% germination (hours) of all seven focal species – corn, soy, wheat, sorghum, salt-tolerant soy, barley, quinoa – along a water potential gradient (ionic stress). Error bars are standard error of the mean.

(A) Sorghum 2018 and 2019



(B) Salt-tolerant soybean 2019

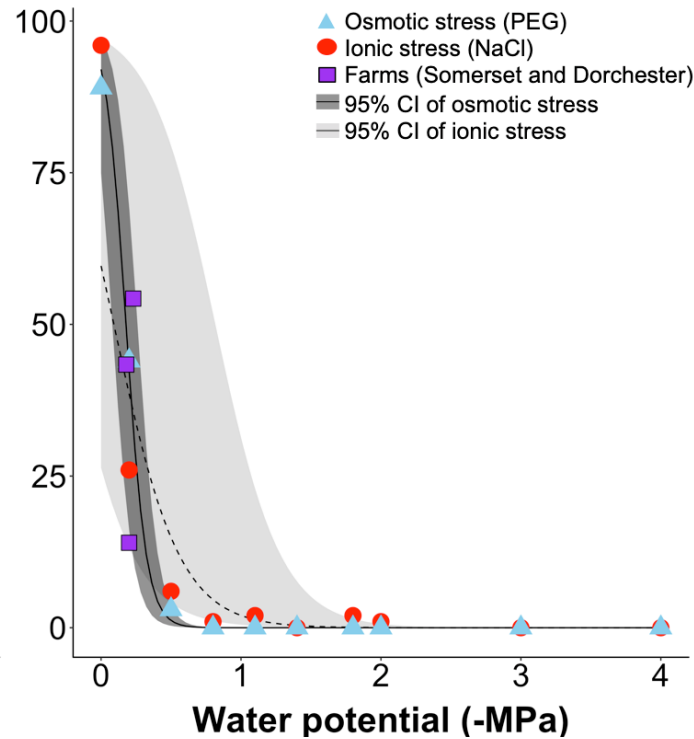


Figure 1.6. Percent germination of field studies (both farms; purple squares) (A) sorghum in 2018 and 2019, and (B) salt-tolerant soybean in 2019 and controlled environment experiment. Osmotic stress indicated by blue triangles and ionic stress indicated by red circles and both in units of -MPa. Response to osmotic stress is indicated by solid black line fitted to logistic regression model and 95% confidence interval (dark grey shading). Response to ionic stress is indicated by the dashed black line fitted to logistic regression model and 95% confidence interval (light grey shading). The large confidence interval for salt-tolerant soybean response to ionic stress was driven by the standard error of the mean at water potential -0.2 MPa, which is why field germination of salt-tolerant soybean feel within the ionic stress confidence interval as well as the osmotic stress confidence interval.

Supplemental Material

Supplemental figures S1.1, S1.2, and S1.3 are controlled environment germination data for rapeseed (*Brassica napus*) and switchgrass (*Panicum virgatum*).

Table S1.1. Model parameter fit statistics for relationship between sorghum or salt-tolerant soybean percent germination and osmotic or ionic stress levels.

	AIC	Adjusted r²
<i>Sorghum germination by osmotic stress (Fig 1.6A; dark grey shading)</i>		
Quadratic	54.8	0.89
Logistic	357.7	0.96
<i>Sorghum germination by ionic stress (Fig 1.6A; light grey shading)</i>		
Quadratic	67.2	0.22
Logistic	66.5	0.99
<i>Salt-tolerant soy germination by osmotic stress (Fig 1.6B; dark grey shading)</i>		
Quadratic	62.0	0.57
Logistic	219.7	0.99
<i>Salt-tolerant soy germination by ionic stress (Fig 1.6B; light grey shading)</i>		
Quadratic	64.35	0.46
Logistic	302.1	0.90

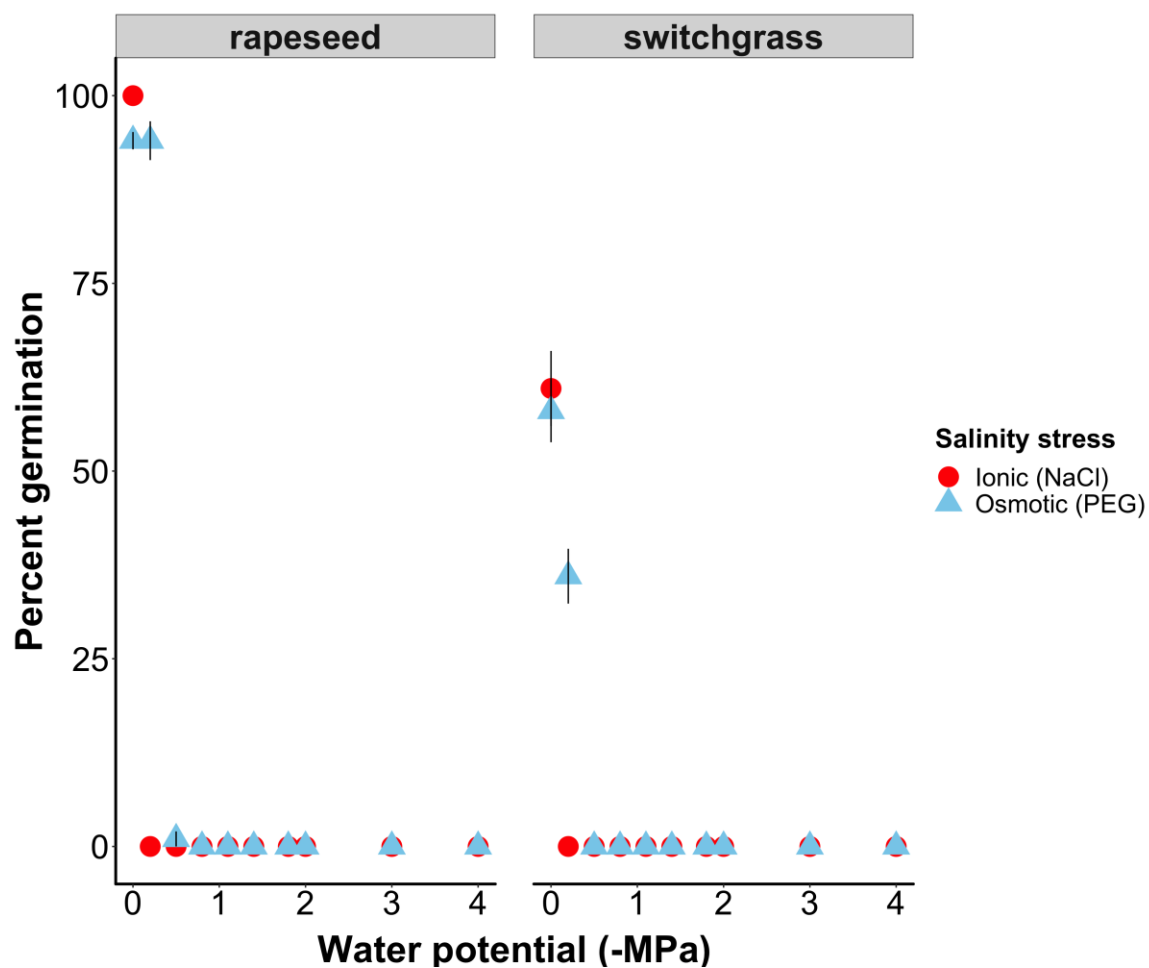


Figure S1.1. Percent germination of rapeseed and switchgrass along a water potential gradient of ionic stress (circles) and osmotic stress (triangles). Error bars are standard error of the mean.

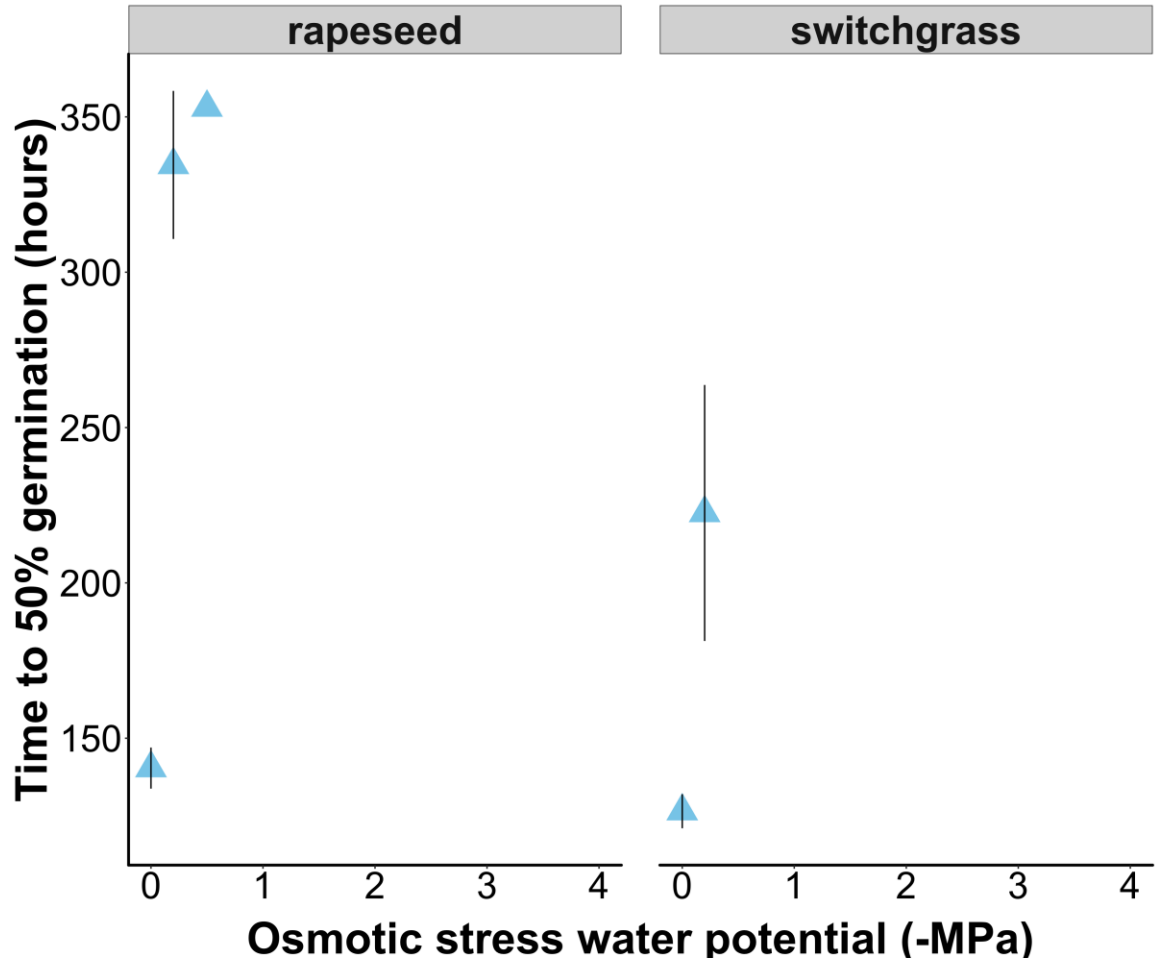


Figure S1.2. Time to 50% germination (hours) of rapeseed and switchgrass along a water potential gradient (osmotic stress). Error bars are standard error of the mean.

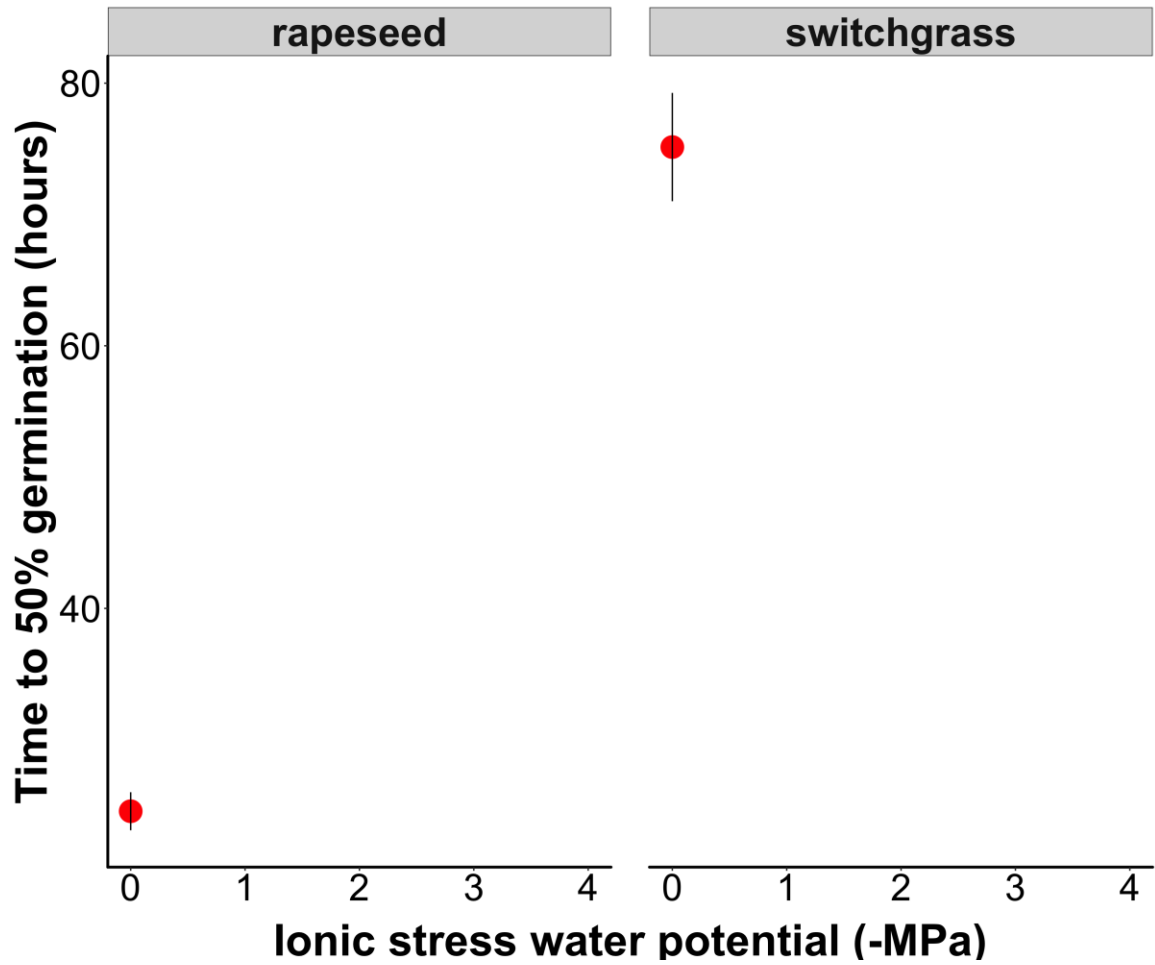


Figure S1.3. Time to 50% germination (hours) of rapeseed and switchgrass along a water potential gradient (ionic stress). Error bars are standard error of the mean.

Chapter 2: Farming carbon: the link between saltwater intrusion and carbon storage in coastal agricultural fields

Abstract

As sea levels continue to rise, coastal agroecosystems have become more vulnerable to saltwater intrusion. Saltwater intrusion (SWI) is the landward movement of sea salts, which can force ecosystem shifts. Among other changes to coastal farmlands, SWI can alter carbon (C) storage. Transitioning agricultural fields have the potential to become C sinks as SWI advances inland and turns farms to marshes. The objectives of our study were to (1) quantify changes in the size of C pools along a salinity transect and (2) understand the degree to which soil C along the salinity transect was physically protected from microbial degradation (via soil aggregates). To determine the effect of SWI on soil C, we collected soils (to a depth of ~140 cm) along a transect from the edge of a salt-damaged field (high salinity) to the center (low salinity). We measured bulk soil C pools and the amount of C stored in large macroaggregates, small macroaggregates, microaggregates, and silt+clay size classes. Soil C pools were largest in the edge of field and ditch bank soils (high salinity) compared to the center of the field ($P=0.01$). Over 70% of soil C was stored in the top 50 cm. In high saline soils (near field edges), most of the C was stored in large macroaggregates (physically protected); however, in the center of the field, most C was stored in silt+clays (not physically protected). We propose five main drivers for the patterns seen in the saline soils: wetting events; organo-metal complexation; increased salinity; vegetation type, structure, and management; and soil management activities. This research is the first to identify the C storage potential of

agricultural soils transitioning into marshes as a result of SWI. Understanding the mechanisms of C stabilization is critical to develop informed conservation strategies that support farm and environmental wellbeing.

Introduction

Soil organic matter (SOM) is the largest global reservoir of terrestrial organic carbon (C) and plays an integral role in ecosystem function, soil fertility, and climate regulation (Paul et al. 2015). Agricultural practices have contributed ~124 Pg of C to the atmosphere between 1850 and 1990 through forest clearing and tillage (Houghton and Hackler 2008, Syswerda et al. 2011). In the United States, agricultural soils are very low in C (~16 mg C g⁻¹ soil from 0-40 cm; Martens et al. 2004) as compared to high-C soils in tidal wetlands (~150 mg C g⁻¹ soil from 0-50 cm; Morris et al. 2016). As sea levels rise along the North American Coastal Plain, both tidal wetlands and agricultural fields are at the leading edge of climate change. A major consequence of sea level rise is saltwater intrusion (SWI), the landward movement of sea salts, which may greatly alter the balance of C additions and losses to soil. The movement of saltwater onto agricultural landscapes occurs via hydrologically connected ditch networks and the groundwater table (Tully et al. 2019a). In the Mid-Atlantic (USA), the extensive agricultural ditch network was designed to drain excess water from farm fields, but is often serving the reverse purpose by acting as a conduit for saltwater to reach farm fields during high tides and storms (Bhattachan et al. 2018, Tully et al. 2019a). As saltwater moves onto agricultural fields, soils closest to agricultural ditches experience repeated wetting with high salinity water while soils further inland, away from ditches, do not experience wetting due to saltwater.

Repeated soil wetting leads to anaerobic soils, which experience slower decomposition compared to aerobic soils, which results in increased C storage (Bridgham et al. 2006, Mitsch and Gosselink 2015). This research investigates the potential for salt-intruded agricultural fields to become a C sink as SWI advances inland.

To date, the effect of SWI on C storage in active agricultural fields has not been investigated. However, there is a large body of research focused on the impacts of SWI on C in tidal freshwater wetlands. In freshwater wetlands, SWI can lead to increased organic C mineralization and accelerated soil organic C loss (Chambers et al. 2013, Weston et al. 2006, 2011), decreased transport of dissolved organic C to coastal estuaries (Ardón et al. 2016), and suppressed carbon dioxide (CO₂) emissions (suggesting C storage; Ardón et al. 2018, Herbert et al. 2018). We expect soils closest to the saltwater source (e.g. ditch bank) to store more C than soils in the center of agricultural fields because of slower decomposition and suppressed CO₂ emissions due to SWI. Our work is the first study to investigate the potential of agricultural soils to store C as they undergo SWI and, more specifically, the degree to which that C is protected and stabilized.

Until the late 20th century, the paradigm of soil organic C stabilization, maintaining C sequestration and storage in a given area, focused on the importance of chemical recalcitrance (Schmidt et al. 2011, Dungait et al. 2012, Lehmann and Kleber 2015). The theory proposed that recalcitrant compounds would decompose more slowly and thus were more stable compared to simple C compounds (Ågren and Bosatta 2002, Dungait et al. 2012). However, subsequent systematic reviews have shown that C stabilization is also mediated by adsorption of C to clay minerals through cation bridging, the interaction of metal ions with organic matter, and the spatial inaccessibility of C

inside soil aggregates (Sollins et al. 1996, von Lützow et al. 2006, Jastrow et al. 2007, von Lützow et al. 2007, Sarkar et al. 2018). These stabilization mechanisms are likely affected by SWI and the salinization and inundation of soils. First, alkaline saltwater introduces both multivalent and monovalent cations (e.g. calcium, sodium, potassium) into solution, which can induce cation bridging (Tully et al. 2019a) and enhance soil C stabilization. For instance, calcium (Ca^{2+}) and magnesium (Mg^{2+}) are polyvalent cations able to neutralize negatively charged soil surfaces (e.g. clay minerals) and organic matter, acting as a bridge between the two (von Lützow et al. 2006). Second, the wetting and drying of intruded soils can change the structure of metals present in the system with implications for increased C storage (Wahid and Kamalam 1993, Sollins et al. 1996, Deneff et al. 2001, Sodano et al. 2017). For instance, frequent SWI can cause iron (Fe) to shift from crystalline to poorly-crystalline forms and thus increase SOM pools through organo-metal complexation (Tully et al. 2019b). Finally, SWI may affect soil aggregation through sodium (Na)-induced clay dispersion or repeated wetting and drying of soil, which can impact the spatial inaccessibility of soil C (Oades 1984, Deneff et al. 2001, Ben-Hur et al. 2009). Soil C may be inaccessible to microbes and enzymes due to occlusion within aggregates at multiple levels of physical protection. The levels of physical protection are considered hierarchical (Tisdall and Oades 1982, Six et al. 2000b), suggesting that microaggregates (250-53 μm) are formed when silt+clay particles (<53 μm) are bound by fungi, bacteria, and plant debris. Microaggregates are then bound together by plant-derived polysaccharides, roots, and fungal hyphae to form macroaggregates of varying size classes (>250 μm ; Six et al. 2000b). The C associated with each aggregate size class becomes progressively more protected as smaller size

classes are encapsulated inside larger aggregate size classes. As SWI advances inland, plant community composition changes annual crops to more perennial wetland vegetation, which has a high density of roots (Gedan and Fernández-Pascual 2019, USDA NRCS 2017). As roots enmesh particles and hold microaggregates together, thus forming macroaggregates, we expect higher abundance of and C associated with large macroaggregates closest to the saltwater source where the vegetation is predominantly perennial wetland species (e.g. ditch bank).

Past research has focused on macroaggregate turnover time in agroecosystems (Six et al. 2000a, Plante and McGill 2002), seasonal dynamics of macroaggregation (Coote et al. 1988, Angers and Mehuys 1988, Perfect et al. 1990a, 1990b), and the effect of land use on soil aggregation (Six et al. 1998, 2000b, Grandy and Robertson 2007). However, there has been no research to date on the potential of agricultural fields undergoing SWI to accumulate and stabilize C. The main objectives of this study were to: (1) quantify the size of C pools along a SWI transect; and (2) to understand how C is occluded through levels of physical protection in coastal farms. We established transects on six no-till farm fields on the Lower Eastern Shore of Maryland that spanned a SWI gradient from the ditch bank (saline) to the center of the agricultural field (fresh). We expect to see larger soil C pools in soils closest to the saltwater source (e.g. ditch bank). Further, we expect a higher proportion of large macroaggregates and more C associated with large macroaggregates in ditch bank soils, due to change in vegetation type.

Methods

Study sites

Study sites were located near Princess Anne, Maryland in Somerset Co. (38.2029°N, 75.6924°W) and Cambridge, Maryland in Dorchester Co. (38.5632°N, 76.0785°W); all sites have an approximate elevation of 1 m above sea level. Somerset Co. is the southernmost county in Maryland, bounded by the Chesapeake Bay to the west, Virginia to the south, and Worcester Co., MD to the east. Both counties are major producers of poultry, grains, and soybean (USDA 2017). Somerset Co. has 1,780 km of coastline and about 64% of the land area is in cropland (Hennessee et al. 2003, USDA 2017). The majority of soils in Somerset Co. are Quindocqua silt loams with little to no slope (USDA NRCS 2019). Dorchester Co. lies 82 km north of Somerset Co., has 1,476 km of coastline, and has about 73% of the land area in cropland (Hennessee et al. 2003, USDA 2017). The majority of soils in Dorchester Co. are very frequently flooded Honga peat (USDA NRCS 2019).

We selected five salt-intruded farm fields in Somerset Co. and one in Dorchester Co. on which to conduct this study, all of which have been no-till for at least 40 years (Huggins and Reganold 2008). The effects of SWI on soil chemical changes were described in detail for three of these farms by Tully et al. (2019b). Farms 1, 2, 4, 5, and 6 are predominantly silt loam soils, while Farm 3 is predominantly a sandy loam soil (Table 2.1; USDA NRCS 2019). All six farms show evidence of SWI, with saltier soil near the agricultural ditch (little to no crop growth). Towards the center of the fields, each field has a relatively healthy crop stand. Due to poor field germination of crops, fields often require reseeding (de la Reguera et al. *in prep*). The intrusion area is characterized

by five distinct zones: ditch bank, field edge, bare, crop edge, and crop (Tully et al. 2019b; Fig 2.1). At each farm, we established a transect along the intrusion zone, which ranged from 26 to 78 m long (Table 2.1). All five zones were sampled from Farms 3, 4, and 5. In Farms 1, 2, and 6, only four zones were sampled due to impenetrable vegetation along the ditch banks.

Soil collections

On 19 and 20 March 2018, soils were collected (to ~140 cm) with a 7-cm diameter bucket auger in each field at each zone along the intrusion transect. We randomly selected four locations within each zone, collected soils from 0-10 cm, 10-20 cm, and 20-30 cm in those zones, and composited the four soil core samples at each depth. Then, we randomly selected one of the four holes and augered down to ~140 cm. As we cored, soil horizons were described in the field and compared to the series mapped by Web Soil Survey (USDA NRCS 2019). Because soil horizons varied along the transect (even within a farm), the number of soils collected per core varied at each zone and each farm with a range of four to nine depths per 140 cm core (Table 2.1). Soil samples were homogenized by soil horizon, and horizon depth was recorded. A subsample (~200 g) of the homogenized soil was placed into a bag for aggregate size separation. The remaining soil (herein referred to as “bulk soil”) was stored on ice and brought to the University of Maryland College Park laboratory for additional soil analyses, including soil %C.

Bulk density was determined in Farms 1, 2, and 3 in May 2018 using a 15-cm core and an AMS compact slide hammer (Core Sampler Complete, AMS, American Falls, ID, USA). Soil bulk density cores were collected from the crop, crop edge, bare,

field edge, and ditch bank zones every 15 cm in the top 60 cm. We collected soil samples for bulk density on Farms 4, 5, and 6 in July of 2019 by digging pits to 55 cm at the crop, crop edge, bare, field edge, and ditch bank zones. A 5-cm aluminum core was pushed horizontally into the side of the pit at 0-10 cm, 10-20 cm, 20-30 cm, and 30-50 cm. In both cases, soils were returned to the University of Maryland College Park and dried at 105°C for 7 days. Core volume was used to calculate bulk density (g cm^{-3}).

Percent C

Following collection, soils cores were immediately returned to the lab and air-dried for 5 days. A sub-sample of approximately 0.25 g was ground, oven-dried at 60°C for 2 days, and analyzed for %C using dry combustion (LECO TruMac N, St. Joseph, MI).

Bulk soil C metric

Because cores varied in depth along the transect and among farms, we used a consistent soil depth of 100 cm to calculate bulk total soil C pool (Mg C ha^{-1}), which was calculated by multiplying the C concentration of bulk soil (mg C g^{-1}) by the bulk density (g cm^{-3}), and the soil depth segment (cm). These values were summed for all segments up to 100 cm (Table 2.2; Eq. 1).

$$\text{Bulk C pool} = \Sigma(\text{C concentration} * \text{bulk density} * \text{depth segment} * 100) \quad \text{Eq. 1}$$

Aggregate size separation

The 200 g subsample of soil was fractionated into five size classes using the slaking method developed by (Six et al. 2000b). Briefly, 200 g of fresh soil was air-dried for at least 7 days and passed through a 4.75 mm sieve. A 100 g sub-sample was placed

on a 2000 μm sieve and submerged in ultrapure water for 5 min. Soil was slaked at 25 repetitions over 2 min by moving the sieve up and down at an angle through the ultrapure water. Soil remaining on top of the 2000 μm sieve (large macroaggregates) was transferred to a pre-weighed tin. Floating particulate organic matter was skimmed from the water surface. Soil that passed through 2000 μm was sequentially passed through 250 μm , and 53 μm sieves and the soil that remained on the sieve was identified as small macroaggregates and microaggregates, respectively. Floating particulate organic matter was also skimmed from the water surface of the small macroaggregate size class. Soil that passed through 53 μm was identified as silt+clay. All aggregate sizes were force air-dried in an oven at $\sim 65^\circ\text{C}$ for at least 4 days. Oven-dried size classes were weighed and scraped from the tins into coin envelopes to store for later analysis. Large macroaggregates and small macroaggregates were passed through a 250 μm sieve to remove rocks, which were weighed separately. Soils (without rocks) were ground with a mortar and pestle to ensure they easily passed through a 250 μm sieve for C analysis. Approximately 0.25 g of ground, oven-dried soils were analyzed for %C using dry combustion (LECO TruMac N, St. Joseph, MI).

Sand particle analysis

Large macroaggregates, small macroaggregates, and microaggregates were measured for sand content using the pipette method to avoid overestimating C pools, as sand is not defined as an aggregate (Six et al. 2000b). Briefly, 5 g of oven-dried large macroaggregates, small macroaggregates, and microaggregates were placed in a pre-weighed beaker followed by 10 mL of distilled water and 5 mL of 30% hydrogen peroxide. Beakers rested for 1 hour and then were placed on a hot plate, set to 80°C , for

an additional 1 hour. Then, beakers received an additional 5 mL of 30% hydrogen peroxide and placed back on the hot plate for another hour. After the second hour of boiling, the hot plate was reduced to ~30°C, and samples rested overnight. The following day, the solution was transferred to a 50 mL centrifuge tube to which 5 mL of Calgon (sodium hexametaphosphate [(NaPO₃)₆] and sodium carbonate [Na₂CO₃]) was added. Tubes were topped with deionized water to 50 mL and centrifuged at 270 RPM for 40 min. The samples were then sieved through a 53 µm sieve. Remaining sand was returned to its original beaker, oven-dried at 105°C for 24 hours, and weighed.

Initial tests determined that samples could not be composited for sand particle analysis across transect points or across depths. Thus, sand particle analysis was determined for every sample that contained at least 5 g of oven-dried large macroaggregates, small macroaggregates, or microaggregates. We assumed that size classes containing less than 5 g out of 100 g of soil had negligible sand content.

Aggregate soil C metrics

Total aggregate mass (aggregate fraction mass) was calculated based on the air-dried weight of aggregates after removing rocks but still containing sand (Table 2.2; Eq. 2).

$$\text{Total aggregate mass} = \text{oven dried aggregate mass} - \text{tin mass} - \text{rock mass} \quad \text{Eq. 2}$$

After we conducted the sand particle analysis on large macroaggregates, small macroaggregates, and microaggregates, we calculated the proportion of sand within each aggregate size (Fig S2.2). We then calculated the mass of sand (g) from each of those

samples was calculated by multiplying the proportion of sand by the total aggregate mass (g) (Eq. 3).

$$\text{Sand mass} = \text{proportion of sand} * \text{total aggregate mass} \quad \text{Eq. 3}$$

To determine the sand-free aggregate mass (g), the sand mass (g) was subtracted from the total aggregate mass (g) (Eq. 4).

$$\text{Sand free aggregate mass} = \text{total aggregate mass} - \text{sand mass} \quad \text{Eq. 4}$$

In order to understand the proportion of each aggregate size class within a soil sample, we calculated the aggregate distribution as the g aggregate per g of soil (Eq. 5).

$$\text{Agg distribution} = \frac{\text{sand free aggregate mass}}{\Sigma(\text{sand free aggregate mass of soil sample})} \quad \text{Eq. 5}$$

We calculated total aggregate C of sand-free aggregates (g C) by multiplying C concentration (mg C g⁻¹) by sand-free aggregate mass (g) and then dividing by 1000 (conversion factor; Eq. 6).

$$\text{Total aggregate C} = \frac{\text{C concentration} * \text{sand free aggregate mass}}{1000} \quad \text{Eq. 6}$$

Statistical analysis

First, we tested the effect of soil depth on soil C concentration (mg C g⁻¹) in bulk soils because bulk soil C pools and aggregate C are subsets of (or calculated from) the bulk soil C concentration. Ultimately, we grouped soil horizons into four categories of increasing depth: 0-20 cm, ~20-50 cm, ~50-80 cm, and ~80+ cm based on preliminary tests of C changes with depth.

To test the effect of SWI and soil depth on bulk soil C concentration, we used a linear mixed-effects (LME) model (*lme4* package for R; Bates et al. 2013) where location on the transect and soil depth category were fixed effects and farm was a random effect.

We used Tukey *post hoc* tests (*multcomp* package for R; Hothorn et al. 2008) to examine the differences of bulk soil C concentration with either transect location or depth. Full model results are presented in Supplemental Material (Table S2.1).

To examine the effect of SWI on total bulk soil C pools (to 100 cm), we ran LME models with transect point (i.e. crop, crop edge, bare, field edge, and ditch bank) as the main effect and farm as a random effect (Table S2.2). In addition, we examined the size of the bulk C pools at the four depth categories to determine if different soil depths were more sensitive to the effects of SWI. Therefore, we used a similar LME model with transect as the main effect and farm as a random effect to look at changes in soil C pools across the transect for each depth category separately (total of four LME models: 0-20, ~20-50, ~50-80, ~80+ cm; Table S2.3). We used Tukey *post hoc* tests to examine the effect of transect location on soil C pool size.

To determine the aggregate distribution (g aggregate g bulk soil⁻¹) within each depth segment, we used four LME models (one for each depth category) with transect and aggregate size class as main effects and farm field as a random effect. To determine if total aggregate C (g C) is stored in different size classes (a measure of physical protection) along a SWI transect, we used four LME models (one for each depth category) with transect point and aggregate size class as main effects and farm as a random effect. In each case, we used Tukey *post hoc* tests to examine differences in aggregate size class or location on the SWI transect.

When necessary, we used Box-Cox transformations (Box and Cox 1964) prior to analysis to satisfy the assumptions of the statistical models. Significance was determined

at $P < 0.05$ in all cases. Statistical analyses were conducted in the R environment for Macintosh (v1.2.1335).

Results

Ditch bank soils have the largest soil C pool and highest C concentration

There was no significant interaction between location on the SWI transect and depth category on bulk soil C concentration (mg C g^{-1}), so we discuss these effects separately (Table S2.1A). In general, soil C concentrations in ditch bank soils were 4.5 times higher than in crop, crop edge, and bare soils ($P = 0.003$; Fig 2.2A; Table S2.4). Soil C concentrations were ~ 2 times higher in field edge soils than in the crop, crop edge, and bare soils, but still 2 times lower than in ditch bank soils. Soil C concentrations were significantly higher in top soils (0-20 cm) than deep soils ($\sim 80+$ cm; $P < 0.0001$).

As C pool size would differ by the size of the depth segment (e.g. 10 cm vs. 30 cm), we looked at depth categories separately. We found significantly larger soil C pools in the ditch bank soils than all other locations on the transect in the 0-20 cm and ~ 20 -50 cm depth categories ($P = 0.04$ in both cases; Fig 2.2B; Table S2.5). Soil C pools in field edge soils were 1.5 times larger than the crop, crop edge, and bare soils at 0-20 cm and two times larger at ~ 20 -50 cm depth categories, but still smaller than the ditch bank soil C pools. In deep soils (~ 50 -80 and 80+ cm), we observed no effect of transect location on bulk total C pools.

Total bulk soil C pools (0-100 cm) varied significantly across the SWI transect ($P = 0.009$; Table S2.1B), and trends were driven by the patterns observed in the upper two depth categories (0-20 cm and ~ 20 -50 cm). Overall, soil C pools were highest in ditch

bank soils (85.9 Mg C ha⁻¹) and lowest in crop soils (36.5 Mg C ha⁻¹). Total bulk C pools in field edge soils (48.1 Mg C ha⁻¹) were 1.5 times larger in the crop, crop edge, and bare soils (36.2 Mg C ha⁻¹ on average), but still ~2 times smaller than the ditch bank soil C pools (Fig 2.2B).

Soil C is stored in different aggregate size classes across a SWI transect

Because soil C concentrations varied significantly across the transect with depth category (0-20 cm, ~20-50 cm, ~50-80 cm, ~80+ cm), we examined the effect of transect location and aggregate size class at each depth category separately. In the 0-20 cm depth category, there was a significant interaction between location on the transect and aggregate size class on aggregate distribution (g aggregate per g bulk soil; P=0.002; Table S2.6A). The significant interaction was driven by a change in the large macroaggregate mass, which comprised the smallest proportion of the aggregate distribution in crop, crop edge, and bare soils, but was equal to all the other size classes in the field edge and ditch bank soils (Fig 2.3A; Table S2.7A). There was also a significant interaction between location on the transect and aggregate size class on total aggregate C (g C) at the 0-20 cm depth category (P=0.006; Table S2.6B). Similar to aggregate distribution, this pattern was driven by changes in the large macroaggregate size class. Large macroaggregates contained the lowest aggregate C at the crop, crop edge, and bare locations, but the highest total aggregate C at the field edge and ditch bank locations (compared to microaggregates and silt+clays; Fig 2.4A; Table S2.7B). At 0-20 cm, aggregate C in the large and small macroaggregate size classes comprised 75% of the

total aggregate C in the field edge soils and 80% of the total aggregate C in ditch bank soils (Fig S2.1A).

In the ~20-50 cm depth category, there was no significant interaction between location on the transect and aggregate size and no effect of transect location alone on class on aggregate distribution (Table S2.9). However, there was a significant effect of size class ($P < 0.0001$; Table S2.8A), whereby the aggregate distribution of microaggregates and silt+clays were significantly greater compared to the large macroaggregates at all five transect locations ($P = 0.001$) and larger than small macroaggregates at crop, crop edge, and bare zones ($P = 0.01$; Fig 2.3B; Table S2.9A). There was a significant interaction between location on the transect and aggregate size class on total aggregate C at the ~20-50 cm soil depth ($P = 0.04$; Table S2.8B). This pattern was driven by changes in the large macroaggregate size class alone, whereby large macroaggregates had the lowest total aggregate C at the crop, crop edge, and bare locations, but an equal amount of total aggregate C to all other size classes in the field edge and ditch bank soils (Fig 2.4B; Table S2.9B). Aggregate C of large and small macroaggregates comprised ~78% of the total aggregate C found in the field edge soils and ~60% in the ditch bank soils at ~20-50 cm (Fig S2.1B).

In soils from ~50-80 cm, there was no significant interaction between the location on the transect and aggregate size class and no effect of transect location alone on aggregate distribution (Table S2.10A). There was a significant effect of size class ($P < 0.0001$), whereby the aggregate distribution of small macroaggregates, microaggregates, and silt+clays were significantly greater compared to the large macroaggregates at all five transect locations ($P = 0.001$; Fig 2.3C; Table S2.11A).

Additionally, the aggregate distribution of microaggregates and silt+clays were significantly greater compared to the small macroaggregates at all five transect locations, except the field edge ($P=0.004$). There was also no significant interaction between the location on the transect and aggregate size class and no effect of transect location alone on total aggregate C in soils ~50-80 cm. There was a significant effect of size class on total aggregate C ($P<0.0001$; Table S2.10B), whereby the total aggregate C of silt+clays was significantly greater compared to small macroaggregates at all five transect locations ($P=0.001$; Fig 2.4C; Table S2.11B). Additionally, the total microaggregate C (g) was significantly greater compared to small macroaggregates C (g) at the bare, field edge, and ditch bank zones ($P=0.02$). Total aggregate C in silt+clay size class comprised 50% of the total aggregate C found in crop, crop edge, bare, field edge, and ditch bank soils at ~50-80 cm (Fig S2.1C).

In the deepest soils (~80+ cm), there was no significant interaction between the location on the transect and aggregate size class or transect location alone on aggregate size distribution, but there was a significant effect of size class ($P<0.0001$; Table S2.12A). The aggregate distribution of microaggregates and silt+clays was significantly greater compared to the large macroaggregates and small macroaggregates at all five transect locations (Fig 2.3D; Table S2.13A). There was no significant interaction between the location on the transect and aggregate size class or location alone on total aggregate C, but there was a significant effect of size class on total aggregate C ($P<0.0001$). The total aggregate C of silt+clays was significantly greater compared to large and small macroaggregates at all five transect locations ($P=0.001$; Fig 2.4D; Table S2.12B; Table S2.13B). Total aggregate C of silt+clays was also significantly greater compared to

microaggregates at all transect locations except crop edge ($P=0.001$). Silt+clay total aggregate C comprised over 50% of the total aggregate C found in the crop, crop edge, bare, field edge, and ditch bank soils in the deepest soils (Fig S2.1D).

Discussion

This study is the first to explore the effects of SWI on soil C in agricultural soils by (1) quantifying the size of C pools along a SWI transect and (2) understanding how C is protected within aggregate size classes. Overall, we found larger soil C pools (and higher bulk C concentrations) in the ditch banks. We also observed higher total aggregate C in large macroaggregates at field edge and ditch bank soils in the top 50 cm of the soil profile. We suggest five main drivers of these patterns: wetting events; organo-metal complexation; increased salinity; vegetation type, structure, and management; and soil management activities (Fig 2.5).

Largest soil C pool in ditch bank

It is well-established that salt marshes have high rates of soil C storage compared to agricultural soils because microbial decomposition is slower in anaerobic soils than aerobic soils (Bridgham et al. 2006, Mitsch and Gosselink 2015). Therefore, repeated wetting events of field edges and ditch banks may lead to increased C storage as a function of suppressed microbial decomposition (Fig 2.2A & B). In addition, wetting events can dissolve crystalline Fe oxides into poorly-crystalline structures under anoxic conditions (Wahid and Kamalam 1993). Tully et al. (2019b) showed the structure of Fe changed from crystalline to poorly-crystalline along a SWI transect on coastal agricultural fields, and others have shown that poorly-crystalline Fe forms organo-metal

complexes under fluctuating redox conditions (Wahid and Kamalam 1993, Sodano et al. 2017). Amorphous or poorly-crystalline metal oxides form complexes with organic matter, thus stabilizing soil C (Torn et al. 1997, Mikutta et al. 2006, Lalonde et al. 2012, Huang et al. 2016), and likely contributing to high levels of organic matter in the field edges and ditch banks (Fig 2.5).

We have previously shown soil salinity in the crop zone to be around 3 ppt (5.6 dS m⁻¹; Tully et al. 2019b). Comparatively, soil salinity at the ditch bank is around 7 ppt (12 dS m⁻¹; Tully et al. 2019b), which is about a quarter the strength of ocean water. Although such a dramatic change in salinity will impact biogeochemical cycling (Tully et al. 2019a), the effect of salinity on soil C storage remains unclear. Research reports contrasting results on the relationships between salinity levels and C decomposition. For instance, Ardón et al. (2018) and Herbert et al. (2018) both showed suppressed CO₂ emissions following SWI (suggesting C storage), yet other studies showed increased microbial mineralization and decomposition with increased salinity (suggesting C loss; Weston et al. 2006, Craft 2007, Weston et al. 2011, Wang et al. 2019). Additionally, a study on tidal marshes indicated no relationship between salinity and decomposition rates (no change in C storage; Mendelsohn et al. 1999). Although greenhouse gas emissions (e.g. CO₂) and decomposition rates were outside the scope of our research, we found larger C pools on the edges of farm fields and ditches, suggesting that C storage may be facilitated by the influx of saline water in our system. Thus, several abiotic drivers (e.g. wetting events, poorly-crystalline Fe oxides, and salinity) interact synergistically to facilitate the formation of large C pools in field edges and ditch banks (Fig 2.2A & 2.5).

In addition to abiotic drivers, the patterns in C pools can also be explained by biotic factors such as changes in vegetation type, structure, and management. The SWI transect is characterized by a dramatic change in vegetation over a short distance (30-80 m). The center of the farm field is dominated by a monoculture agricultural crop (e.g. corn, soybean, wheat), the crop edge is characterized by a patchy, poorly performing crop, and the bare area has no vegetation (Fig 2.5). Although the field edge is still actively managed (e.g. planted, sprayed with herbicides, mowed), crops (i.e. corn, soybean, and wheat) are unable to grow. Instead, perennial wetland plants and native forbs dominate the field edge (Gedan and Fernández-Pascual 2019). Farmers battling SWI will mow and spray the field edge and ditch bank in order to manage the growth and invasion of wetland species. However, the vegetation is too dense for herbicide application to be effective (Larry Fykes, *personal communication*), and mowing the vegetation does not remove the belowground biomass. Compared to annual crops (which must be replanted every year), perennial wetland plants will provide a greater source of organic C to soils in the form of residues. As SWI continues to advance inland, perennial wetland species will likely outcompete annual crop species as repeated wetting events and soil salinity have indirectly selected for plant species that can tolerate water and salt stress. Wetland perennial species have a deeper rooting system (15-51 cm; USDA NRCS 2017) than standard annual crops (10-20 cm; Fan et al. 2016), which may trap sediments and their associated organic C, thereby increasing soil C pools (McLeod et al. 2011, Kell 2012). Therefore, the type of vegetation at the field edge and ditch banks may facilitate the accumulation of C (Fig 2.5). Soil salinity levels on intruded fields are far above the salinity tolerance of standard crops grown in the region (mean of 4 dS m⁻¹; Tanji and

Kielen 2002), but within the range of wetland plant species (32-72 dS m⁻¹; Hester et al. 1996, Lissner and Schierup 1997, Mauchamp and Mésleard 2001, Konisky and Burdick 2004, Achenbach et al. 2013). Therefore, the type, structure, and management of marsh vegetation at the field edges and ditch banks may facilitate the accumulation of soil C (Fig 2.5).

Finally, soil management activities (e.g. no-till, animal manure application) may affect soil C pools on salt-intruded fields. Maryland farmers have practiced no-till farming for the last four decades, but for centuries, conventional mechanized tillage was common in the region (Huggins and Reganold 2008). Conventional tillage breaks the soil surface in order to increase soil aeration, incorporate plant residues into the soil, and accelerate decomposition (Mikha and Rice 2004). No-till farming allows plant residues to remain on the soil surface resulting in slower SOM turnover and decomposition, therefore building soil C (Beare et al. 1994b, Six et al. 1998, West and Post 2002, Grandy and Robertson 2007). Studies show the conversion from conventional-till to no-till results in an increase in soil C within ten years (Angers et al. 1992, Beare et al. 1994b, West and Post 2002, Grandy and Robertson 2006). We reported C concentrations in the crop, crop edge, and bare zones to 50 cm (mean 15.8 mg C g⁻¹) that were similar to that of conventional-till soils (mean 16 mg C g⁻¹; Fig 2.2B; Martens et al. 2004) despite years of no-till. In contrast, C concentrations in the top 50 cm at the field edge and ditch bank (mean 65 mg C g⁻¹) were 4 times higher than in the center of the field, but still lower than in tidal wetland soils (mean 180 mg C g⁻¹ to 50 cm; Morris et al. 2016). Finally, the Eastern Shore, MD is a major producer of poultry, and local agricultural fields use poultry manure as a fertilizer (Kleinman et al. 2007, 2012). Despite large inputs of

poultry manure annually, soil C concentrations were not higher compared to other studies (Aoyama et al. 1999b, Watts et al. 2010). Therefore, we suggest the legacy of soil tillage was a more important driver of soil C across the transect than manure application.

Aggregate soil C across a SWI transect

In the soil aggregate hierarchy, silt+clay particles are considered the building blocks of microaggregates, which comprise small macroaggregates and, finally, large macroaggregates (Tisdall and Oades 1982). Thus, it is unsurprising that silt+clays comprised the greatest proportion of aggregate mass across the intrusion transect at each depth category (Fig 2.3). Further, soil C is considered to be more physically protected from microbial degradation as you move up the soil aggregate hierarchy, with the greatest physical protection conferred by macroaggregates (Six et al. 2002, 2004). We observed large amounts of aggregate-associated C in large and small macroaggregates in the ditch bank soils, suggesting that C in these soils is physically protected from microbial degradation. We believe that high amounts of large macroaggregate-associated C in the ditch bank zone compared to other size classes was likely due to wetting events, organo-metal complexes, vegetation, and to a lesser extent, soil management activities.

Wetting events associated with SWI can both support and suppress soil aggregation depending on the clay mineralogy (Singer et al. 1992, Attou et al. 1998, Bronick and Lal 2005). For instance, SWI can lead to sodium-induced clay dispersion, which could reduce aggregate stability if soils do not flocculate when dispersed (Mehner and Jennings 1985, Rengasamy et al. 1984, Rengasamy and Olsson 1991). Aggregation may be further suppressed if the soil has predominantly swelling clays (e.g. smectite),

which naturally disperse and disassociate from one another under wet conditions (Singer et al. 1992). In soils containing non-swelling clays (e.g. kaolinite), clay particles will disperse when wet but form clay bridges and coatings among silt particles as they dry, thus supporting flocculation and aggregation (Attou et al. 1998). Focal fields contain primarily kaolinitic clays (Wilson 1999), suggesting the soils tend to disperse when wet but aggregate when they dry (Weil and Brady 2016). Therefore, the aggregation in the ditch bank soils were likely a result of the positive effect of clay dispersion and flocculation following repeated wetting events (Fig 2.3).

As previously mentioned, the structure of Fe changes from crystalline to poorly-crystalline along a SWI transect and under fluctuating redox conditions (Tully et al. 2019b, Wahid and Kamalam 1993, Sodano et al. 2017), thus forming complexes with organic matter and stabilizing soil C (Torn et al. 1997, Mikutta et al. 2006, Lalonde et al. 2012, Huang et al. 2016). Higher concentrations of poorly-crystalline Fe can contribute to the physical protection of aggregate-associated C as it binds organic matter to clay particles via cation bridging to form microaggregates (Huang et al. 2016). As larger aggregates form, the C associated with each size class becomes progressively more protected because smaller size classes are encapsulated inside larger aggregate size classes. Organo-metal complexation may confer additional stabilizing mechanisms because they aid in binding aggregates together.

The field edges and ditch banks are dominated by wetland perennial grasses and the invasive reed, *Phragmites australis*, all of which have deep fibrous rooting systems (Hoagland et al. 2001, Scholz and Lee 2005, Dhote and Dixit 2009). Previous work has shown that a high density of roots and hyphae enmesh particles and release organic

compounds that hold microaggregates together, thus forming highly stable macroaggregates that store more C than smaller size classes (Tisdall and Oades 1982, Six et al. 2000b, Grandy and Robertson 2007, Perfect et al. 1990a, Drury et al. 1991, Bronick and Lal 2005). Further, macroaggregate C is often derived from plant material residues (Tisdall and Oades 1982, von Lützow et al. 2006). Therefore, the high distribution and amount of C associated with large macroaggregates in the field edge and ditch bank soils were likely a result of the positive effect of high density, perennial wetland vegetation on aggregate formation.

Finally, the focal farms are not tilled and receive heavy poultry manure additions, two soil management activities that are likely to support macroaggregate formation in cultivated soils. For example, many studies indicate that no-till management increases the distribution and physical protection of C within macroaggregates (Beare et al. 1994a, Grandy and Robertson 2006, 2007). As the focal farms have been in no-till for over four decades (Larry Fykes, *personal communication*), we expected to a higher distribution of large and small macroaggregates in the crop, crop edge, and bare soils compared to conventionally tilled soils. However, this was not the case as we observed macroaggregate distributions under 0.2 g per g bulk soil, which is more comparable to conventional-till fields (0.3 g macroaggregate per g bulk soil), than no-till fields (0.5 g macroaggregate per g bulk soil; Beare et al. 1994b, Six et al. 2000b, Grandy and Robertson 2007). In addition, we expected that the application of poultry manure would enhance macroaggregate formation in the focal farm soils overall (Angers and N'Dayegamiye 1991, Aoyama et al. 1999a). Poultry manure additions may facilitate the formation and stabilization of macroaggregates through the decomposition of particulate

organic matter from manure, which leads to the production of hyphae, a binding agent for macroaggregates (Tisdall 1994, Aoyama et al. 1999a). Despite poultry manure applications to the crop, crop edge, and bare regions of the farms, we observed the lowest amount of C associated with large macroaggregates in these soil zones. We propose that repeated passes of heavy machinery across the farms disrupted the formation of macroaggregates in these parts of the field. For instance, farmers battling SWI often must plant fields several times due to poor crop germination (de la Reguera et al. *in prep*). Therefore, any positive effects of no-till and manure additions may have been muted by farmer management in the face of SWI: and higher levels of aggregation at the field edge and ditch banks were due to the positive influence of wetting events with saltwater intrusion, organo-metal complexation, and vegetation type, structure, and management on aggregate formation (Fig 2.5).

Farmland to wetland?

As SWI continues to move inland and onto agricultural fields, promoting the physical protection of C will be critical to soil long-term C storage (Jastrow et al. 2007). The focal farm fields have been experiencing SWI for at least a century, but the effects have worsened within the last five decades (Larry Fykes, *personal communication*). Understanding and quantifying the change in soil C pools and how C is protected in soils is imperative in fields experiencing SWI as they have the potential to become C sinks and, ultimately, “blue carbon” ecosystems (Fig S2.3). Blue C ecosystems (e.g. mangroves, tidal wetlands, seagrass meadows) are highly efficient C sinks because the soil does not become saturated with C due to vertical accretion and dense vegetation with complex rooting systems (Chmura et al. 2003, Mcleod et al. 2011). The change in

vegetation type and structure and the larger C pools in the ditch bank soils have the potential to sequester and store C at the same scale as blue C ecosystems. Farmers can enroll in the Conservation Reserve Enhancement Program (CREP) to take their farmland out of production for at least a decade and establish wetlands, thus changing the vegetation type and structure with the potential to store more C. It is important to start managing salt-intruded farm fields now so they can continue to sequester C in the future.

Conclusion

The purpose of this study was to (1) quantify how C pools changed along a SWI transect and (2) understand the degree to which soil C was physically protected via soil aggregates in coastal farm fields. Overall, we found the largest soil C pools in the ditch bank soils compared to all other locations on the SWI transect. Additionally, most of the C was stored in the top 50 cm and in the large macroaggregate size class in the ditch bank soils. The patterns we observed in soil C were explained by five main drivers: wetting events; organo-metal complexation; increased salinity; vegetation type, structure, and management; and soil management activities. Farmlands experiencing SWI are at the forefront of climate change and rising sea levels. The management of these lands is crucial if we want to preserve soil C now and sequester more C in the future.

Tables and Figures

Table 2.1. Characteristics of the six no-till focal farms on the Eastern Shore of Maryland.

	Farm 1	Farm 2	Farm 3	Farm 4	Farm 5	Farm 6	
County	Somerset	Somerset	Somerset	Somerset	Somerset	Dorchester	
Previous crop rotation (2017)	corn-soy	soy-winter rye cover crop	sorghum	fallow	fallow	sorghum	
Texture class	silt loam	silt loam	sandy loam	silt loam	silt loam	silt loam	
Soil type	mesic Typic Hapludults	mesic Typic Hapludults	mesic Typic Endoaquults	mesic Typic Endoaquults	mesic Typic Endoaquults	mesic Typic Endoaquults	
Soil series	Queponco	Queponco	Othello-Fallsington complex	Quindocqua	Quindocqua	Elkton	
Length of transect (m)	56	78	71	34	26	27	
Transect points and depths per core	Crop	9	7	8	7	8	6
	Crop edge	7	7	7	8	8	6
	Bare	6	7	7	8	8	6
	Field edge	7	5	6	8	9	5
	Ditch bank			4	8	8	

Table 2.2. Carbon calculations and metrics used in analysis.

Name	Units	Description	Calculation	Equation no.
Bulk C pool	Mg C ha ⁻¹	Total pool of C (g) to 100 cm depth scaled to ha	$\sum(\text{C concentration (mg C g}^{-1}\text{ bulk soil) * bulk density (g cm}^{-3}\text{) * soil depth chunk (cm) * 100)$	1
Total aggregate mass (aggregate fraction mass)	g	Weight of aggregates after air drying without rocks (contains sand)	oven dried agg wt (g) - tin wt (g) - rock wt (g)	2
Sand mass	g	Weight of sand in each aggregate class	proportion of sand * total aggregate mass (g)	3
Sand-free aggregate mass	g	Weight of aggregates without sand	Total aggregate mass (g) - sand mass (g)	4
Aggregate distribution	g aggregate g ⁻¹ soil	Proportion of sand-free aggregate mass normalized to the total sand-free soil mass	Sand-free aggregate mass (g) ÷ $\sum(\text{sand-free aggregate mass of large macroaggregate, small macroaggregate, microaggregate, silt+clay of the given sample})$	5
Total aggregate C	g C in sand-free aggregate	Amount of C in each aggregate normalized by sand-free aggregate mass	(C concentration * sand-free aggregate mass) ÷ 1000	6

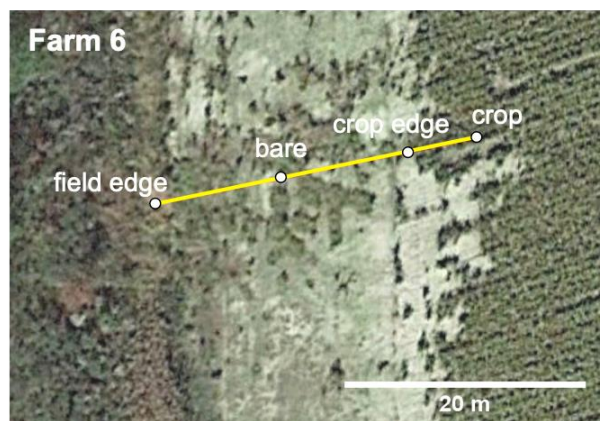
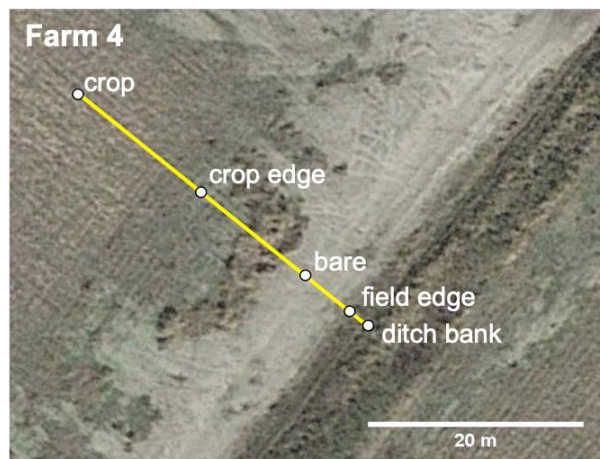
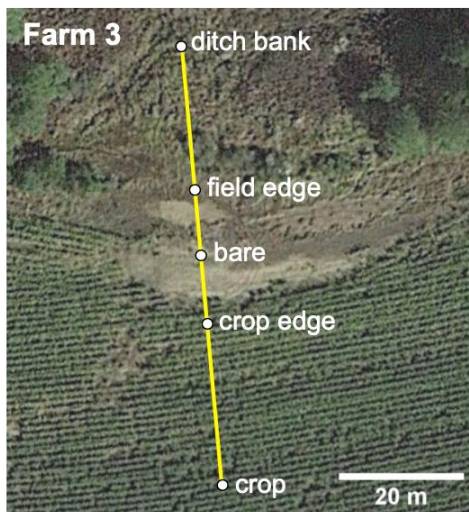
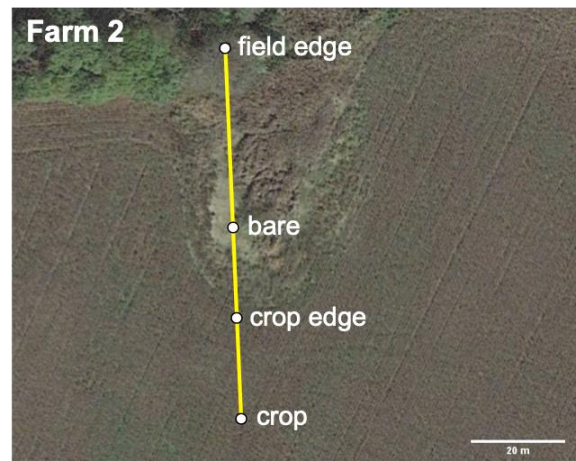
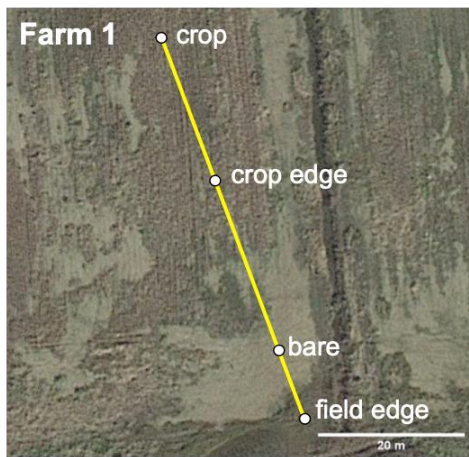
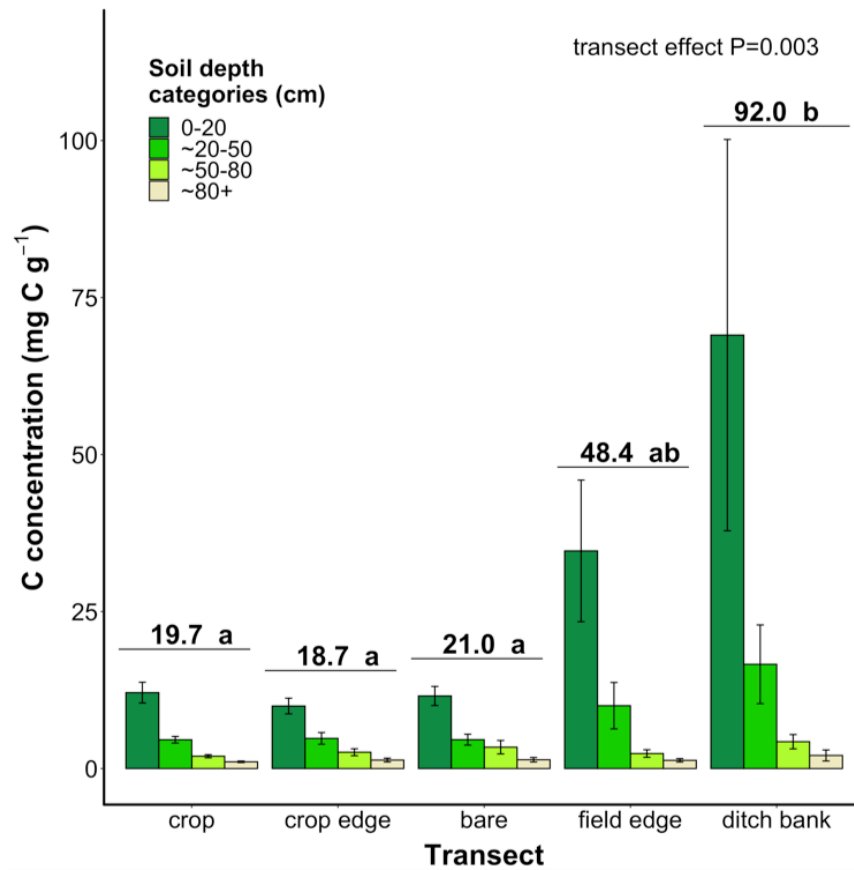


Figure 2.1. Aerial view of SWI in Farm 1-6 and locations of transition zones along the transect.

(A) Bulk soil C concentration



(B) Bulk soil C pool

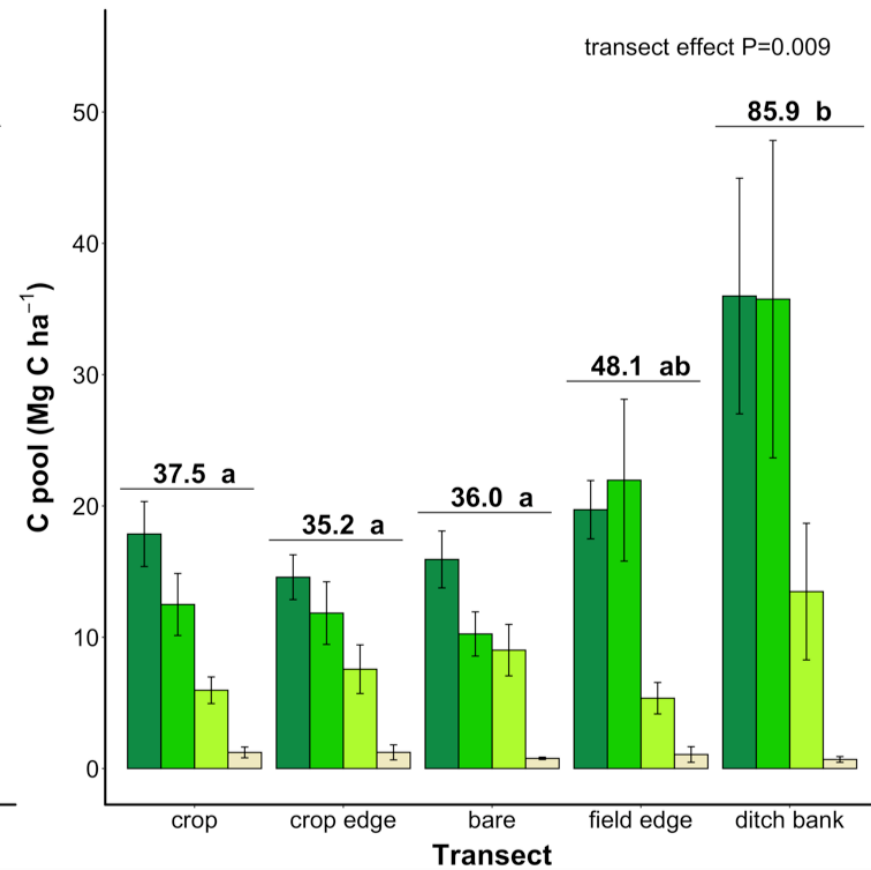


Figure 2.2. Bulk soil C (A) concentration (mg C g^{-1}) and (B) pool (Mg C ha^{-1}) in bulk soils (not fractionated by size class) along the SWI transect at 0-20 cm, ~20-50 cm, ~50-80 cm, and ~80+ cm. Error bars are the standard error of the mean. Values above horizontal bars indicate the size of the total bulk soil C (A) concentration for each transect location and (B) C pool for each transect location. Different letters are statistically significant at $P < 0.05$ in Tukey *post hoc* pairwise comparison.

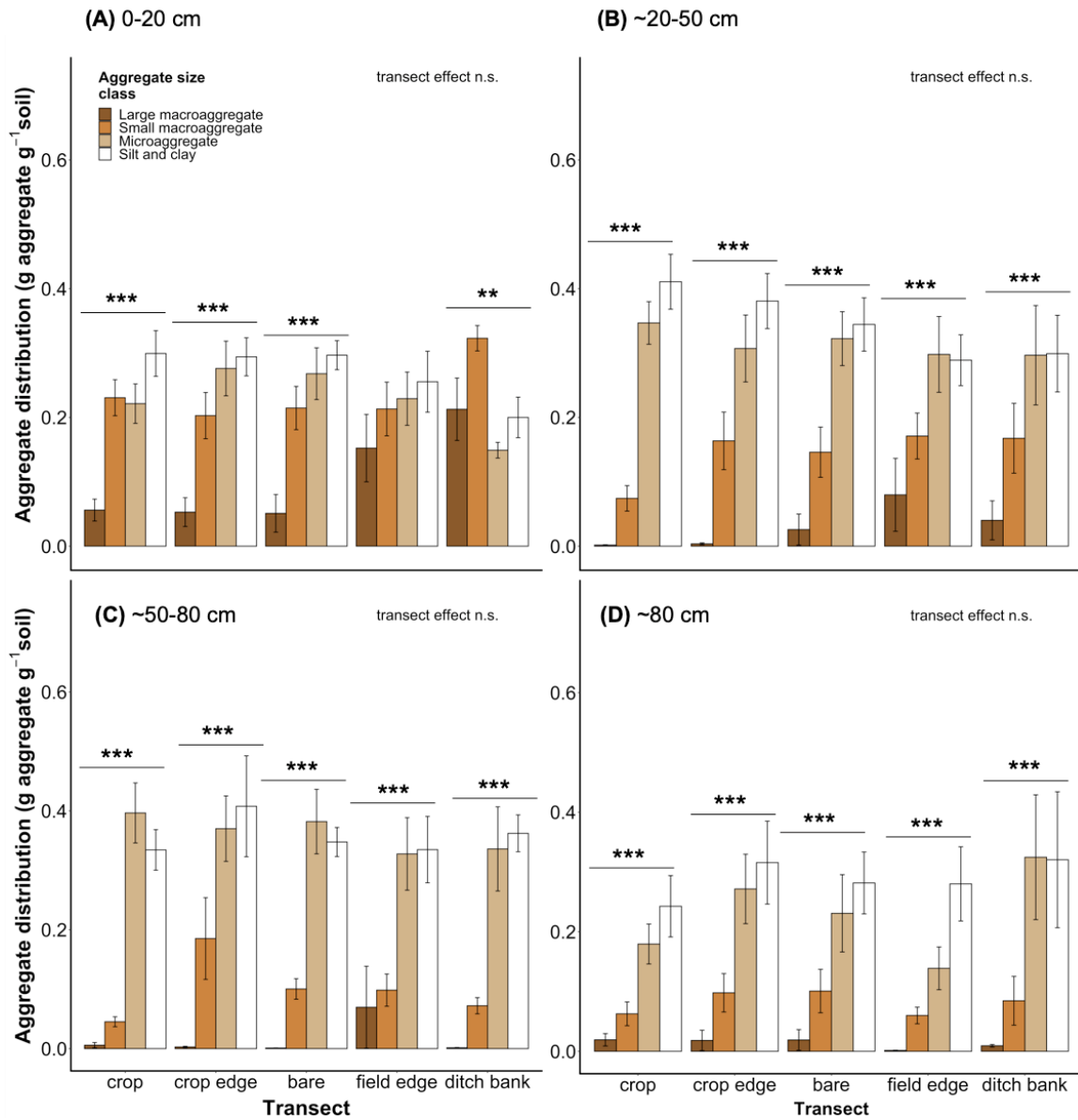


Figure 2.3. Aggregate distribution (g sand-free aggregate g⁻¹ soil) in (A) 0-20 cm, (B) ~20-50 cm, (C) ~50-80 cm, and (D) ~80+ cm along the SWI transect. Error bars are the standard error of the mean. Transect location within depth categories are statistically significant at P<0.05 in Tukey *post hoc* pairwise comparisons. Asterisk (*) indicates significance by class within a transect point at *P<0.05, **P<0.01, ***P<0.005 in Tukey *post hoc* pairwise comparisons.

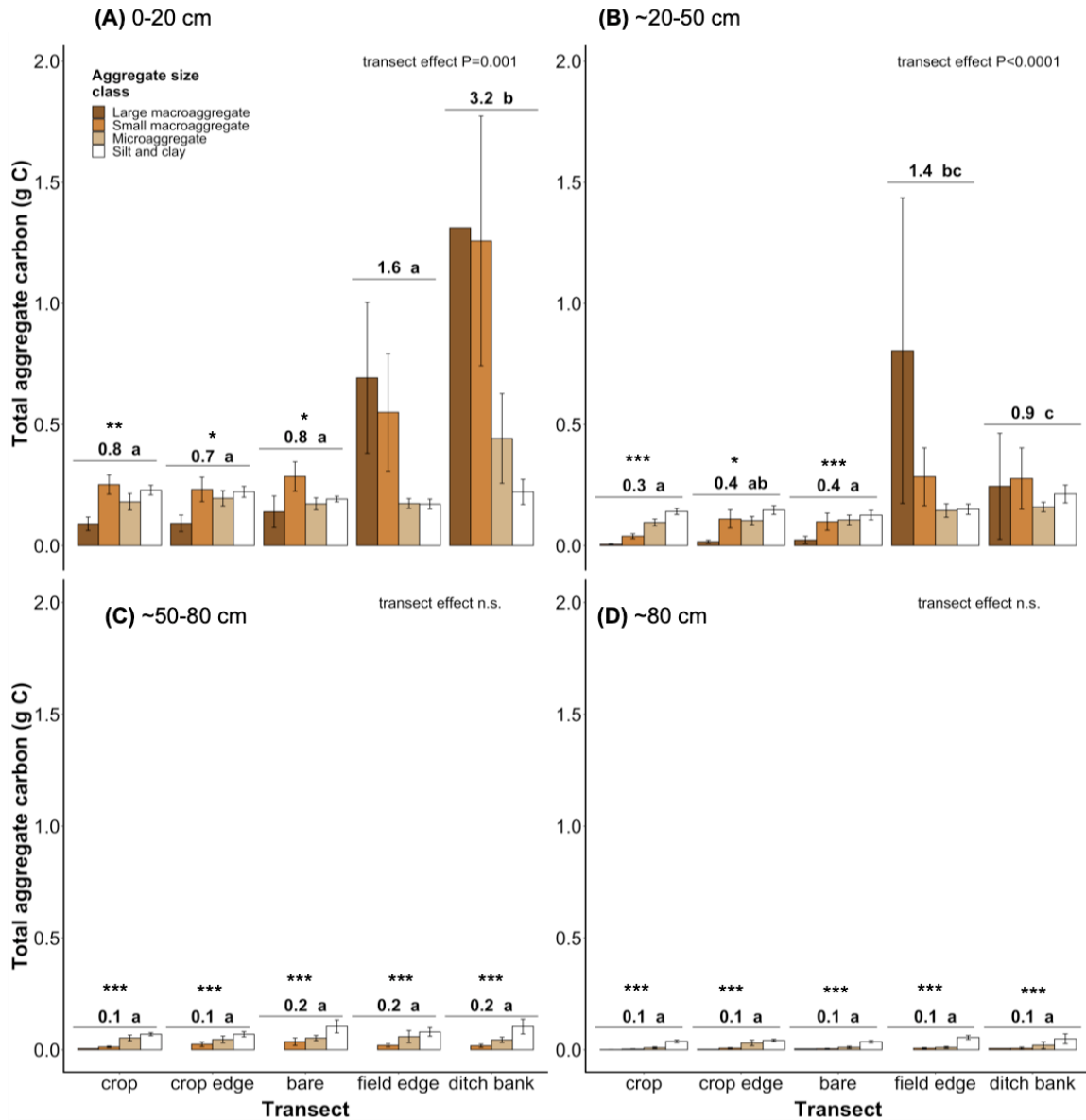


Figure 2.4. Total aggregate C (g C sand-free aggregate) in (A) 0-20 cm, (B) ~20-50 cm, (C) ~50-80 cm, and (D) ~80+ cm along the SWI transect. Error bars are the standard error of the mean. Values above horizontal bars indicate the total aggregate C for each transect location. Different letters are statistically significant at $P < 0.05$ in Tukey *post hoc* pairwise comparisons. Asterisk (*) indicates significance by class within a transect point at * $P < 0.05$, ** $P < 0.01$, *** $P < 0.005$ in Tukey *post hoc* pairwise comparisons.

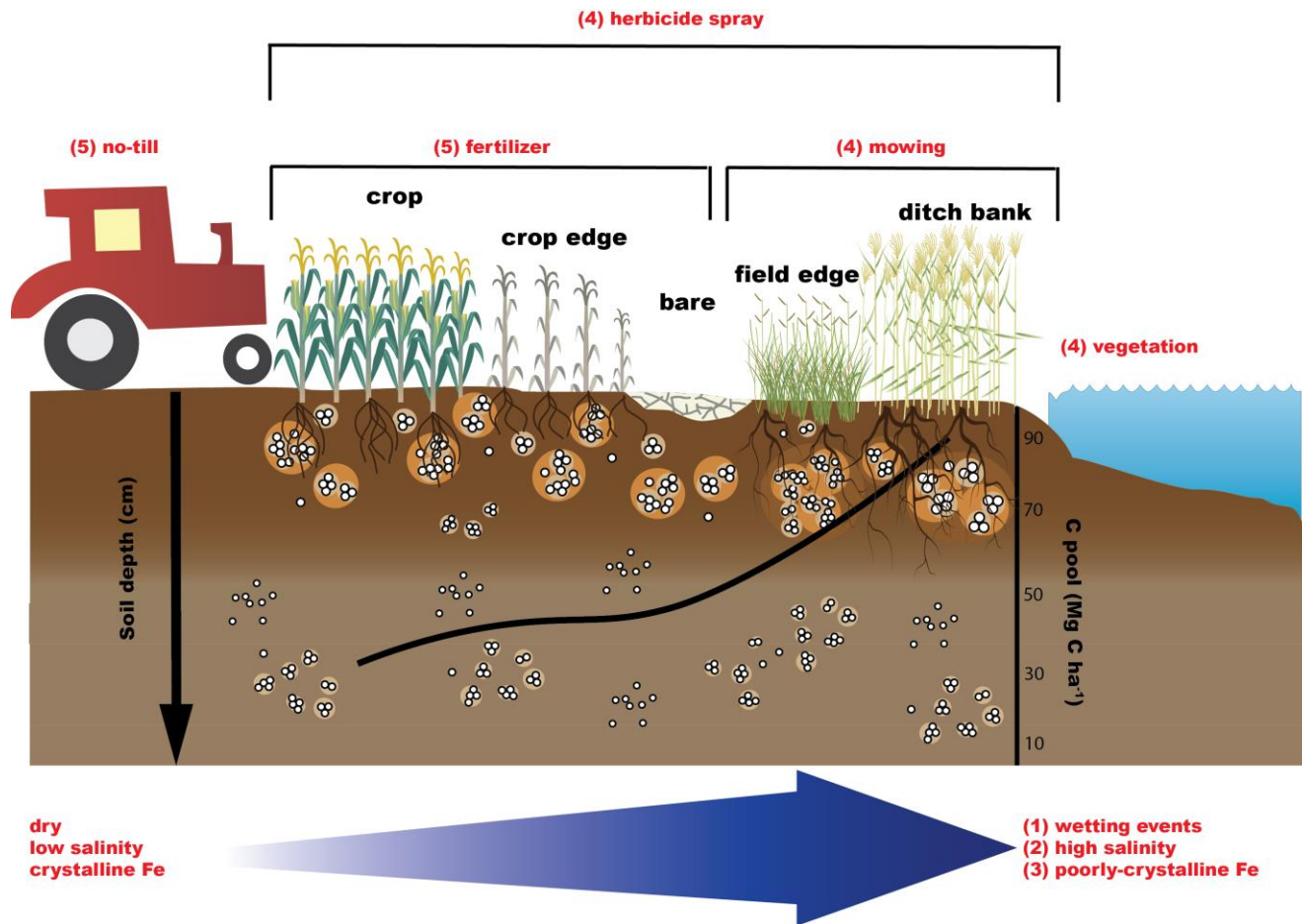


Figure 2.5. Drivers of soil C pools and physically protected soil C. Red text indicates drivers (wetting events, increased salinity, organo-metal complexation, changes in vegetation type, and soil management activities). Crop, crop edge, bare, field edge, and ditch bank are zones along the SWI transect. White circles in soil are silt+clays and light brown circles surrounding silt+clays are microaggregates. The orange circles surrounding microaggregates are small macroaggregates and dark brown circles surrounding small macroaggregates are large macroaggregates.

Supplemental Material

Table S2.1. Summary statistics of global linear mixed-effect (LME) model for bulk soil C concentration. Summary statistics of reduced LME model (no interaction effect between location on the transect and depth category) for bulk soil C concentration. Fixed effects are location on the transect, depth category, and the interaction between location on the transect and depth category.

(A)	LME model on bulk soil C concentration					
	Global model			Reduced model		
	df (df _{num} , df _{den})	F-statistic	P	df (df _{num} , df _{den})	F-statistic	P
Fixed effects						
Transect	(4, 155.45)	8.16	5.31e-06	(4, 170.98)	4.28	0.003
Depth category	(3, 155.22)	118.75	<2.2e-16	(3, 171.49)	111.41	<2.2e-16
Transect * depth category	(12, 154.93)	1.02	0.43			

(B)	LME model on bulk soil C pool					
	Global model			Reduced model		
	df (df _{num} , df _{den})	F-statistic	P	df (df _{num} , df _{den})	F-statistic	P
Fixed effects						
Transect	(4, 145.98)	3.12	0.017	(4, 161.41)	3.48	0.009
Depth category	(3, 146.06)	96.05	<2e-16	(3, 163.97)	16.60	1.83e-09
Transect * depth category	(12, 144.86)	1.13	0.34			

Table S2.2. Summary statistics of linear mixed-effect (LME) model to examine the effect of SWI on total bulk soil C concentration and pool (to 100 cm). Degrees of freedom numerator and denominator and P-value for each transect point and for model reported.

	Crop	Crop edge	Bare	Field edge	Ditch bank	ANOVA, Tukey's HSD
C concentration	(3, 34.50) 2.17e-14	(3, 30.89) 1.07e-07	(3, 33.083) 4.94e-11	(3, 26.23) 1.24e-08	(3, 14.00) 2.37e-05	F(4, 170.98)=4.28, P=0.003
C pool	(3, 36) 5.41e-09	(3, 27.231) 2.08e-06	(3, 31.352) 0.0007	(3, 25.45) 1.04e-07	(3, 14.089) 4.75e-06	F(4, 161.41)=3.48, P=0.009

Table S2.3. Summary statistics of linear mixed-effect (LME) model to examine the size of the bulk C concentration and pool at the four depth categories. Degrees of freedom numerator and denominator and P-value for each depth category and for model reported.

	0-20	~20-50	~50-80	~80+	ANOVA, Tukey's HSD
C concentration	(4, 197) 7.59e-05	(4, 159.11) 5.52e-05	(4, 129.03) 0.51	(4, 83.73) 0.33	(3, 171.49)=111.41, P<0.001
C pool	(4, 47) 0.006	(4, 41.198) 0.008	(4, 38.659) 0.22	(4, 10.625) 0.99	(3, 163.97)=16.595, P<0.001

Table S2.4. Total bulk soil C concentration (mg C g⁻¹) for each transect location (crop, crop edge, bare, field edge, and ditch bank) at four depth categories (0-20 cm, ~20-50 cm, ~50-80 cm, and ~80+ cm; mean ± SE). Different uppercase letters signify statistically significant differences at P<0.05 among transect location within depth category. Lower case letters signify statistically significant differences at P<0.05 among depth category within transect location.

	Crop	Crop edge	Bare	Field edge	Ditch bank
0-20 cm	12.09 ± 1.65 ^{ABa}	9.95 ± 1.25 ^{Aa}	11.56 ± 1.52 ^{Aa}	34.65 ± 11.28 ^{BCa}	69.02 ± 31.15 ^{Ca}
~20-50 cm	4.58 ± 0.53 ^{Ab}	4.80 ± 0.93 ^{Ab}	4.60 ± 0.87 ^{Ab}	10.01 ± 3.70 ^{ABb}	16.60 ± 6.27 ^{Bb}
~50-80 cm	1.96 ± 0.25 ^{Ac}	2.60 ± 0.55 ^{Abc}	3.40 ± 1.07 ^{Ac}	2.39 ± 0.60 ^{Ac}	4.37 ± 1.14 ^{Ac}
~80+	1.07 ± 0.13 ^{Ad}	1.35 ± 0.31 ^{Ac}	1.40 ± 0.36 ^{Ac}	1.31 ± 0.27 ^{Ac}	1.08 ± 0.88 ^{Ac}

Table S2.5. Total bulk soil C pool (Mg C ha⁻¹) for each transect location (crop, crop edge, bare, field edge, and ditch bank) at four depth categories (0-20 cm, ~20-50 cm, ~50-80 cm, and ~80+ cm; mean ± SE). Different uppercase letters signify statistically significant differences at P<0.05 among transect location within depth category. Lower case letters signify statistically significant differences at P<0.05 among depth category within transect location.

	Crop	Crop edge	Bare	Field edge	Ditch bank
0-20 cm	17.86 ± 2.47 ^{Aa}	14.57 ± 1.70 ^{Aa}	15.92 ± 2.17 ^{Aa}	19.71 ± 2.22 ^{ABa}	35.98 ± 8.97 ^{Bab}
~20-50 cm	12.49 ± 2.36 ^{Ab}	11.84 ± 2.39 ^{Aa}	10.25 ± 1.68 ^{Aab}	21.96 ± 6.16 ^{ABa}	35.75 ± 12.09 ^{Ba}
~50-80 cm	5.96 ± 1.01 ^{Ab}	7.56 ± 1.85 ^{Aa}	9.02 ± 1.95 ^{Abc}	5.35 ± 1.20 ^{Ab}	13.47 ± 5.20 ^{Ab}
~80+	1.23 ± 0.41 ^{Ac}	1.23 ± 0.57 ^{Ab}	0.77 ± 0.09 ^{Ac}	1.07 ± 0.59 ^{Ac}	0.69 ± 0.22 ^{Ab}

Table S2.6. Summary statistics of linear mixed-effect (LME) model of depth category 0-20 cm of (A) aggregate distribution (g aggregate per g bulk soil) and (B) total aggregate C (g C).

(A)	LME model at 0-20 cm			(B)	LME model at 0-20 cm		
	Aggregate distribution				Total aggregate C		
Fixed effects	df (df _{num} , df _{den})	F- statistic	P	Fixed effects	df (df _{num} , df _{den})	F-statistic	P
Transect	(4, 196.87)	0.49	0.74	Transect	(4, 177.19)	7.48	1.38e-05
Aggregate size	(3, 195.36)	31.65	<2.2e-16	Aggregate size	(3, 177.19)	6.11	0.0006
Transect * aggregate size	(12, 195.36)	2.71	0.002	Transect * aggregate size	(12, 177.27)	2.44	0.006

Table S2.7. (A) Aggregate distribution (g aggregate per g bulk soil) and (B) total aggregate C (g C) at depth category 0-20 cm for each transect location (crop, crop edge, bare, field edge, and ditch bank) at four aggregate size classes (large macroaggregate, small macroaggregate, microaggregate, silt+clay; mean \pm SE). Different uppercase letters signify statistically significant differences at $P < 0.05$ among aggregate size class within transect location.

(A)	Crop	Crop edge	Bare	Field edge	Ditch bank
Large macroaggregates	0.06 \pm 0.02 ^A	0.05 \pm 0.02 ^A	0.05 \pm 0.03 ^A	0.15 \pm 0.05 ^A	0.21 \pm 0.05 ^{AB}
Small macroaggregates	0.23 \pm 0.03 ^B	0.20 \pm 0.04 ^B	0.22 \pm 0.03 ^B	0.21 \pm 0.04 ^{AB}	0.32 \pm 0.02 ^B
Microaggregates	0.22 \pm 0.04 ^B	0.28 \pm 0.04 ^B	0.27 \pm 0.04 ^B	0.23 \pm 0.04 ^A	0.15 \pm 0.01 ^A
Silt+clay	0.30 \pm 0.04 ^B	0.29 \pm 0.03 ^B	0.30 \pm 0.02 ^B	0.26 \pm 0.05 ^A	0.20 \pm 0.03 ^A
(B)	Crop	Crop edge	Bare	Field edge	Ditch bank
Large macroaggregates	0.09 \pm 0.03 ^A	0.09 \pm 0.03 ^A	0.14 \pm 0.07 ^A	0.69 \pm 0.31 ^A	1.31 \pm 0.69 ^{AB}
Small macroaggregates	0.25 \pm 0.04 ^B	0.23 \pm 0.05 ^B	0.29 \pm 0.06 ^B	0.55 \pm 0.24 ^A	1.26 \pm 0.52 ^A
Microaggregates	0.18 \pm 0.03 ^B	0.20 \pm 0.03 ^B	0.17 \pm 0.03 ^{AB}	0.17 \pm 0.02 ^A	0.44 \pm 0.19 ^{AB}
Silt+clay	0.23 \pm 0.02 ^B	0.22 \pm 0.02 ^B	0.19 \pm 0.01 ^B	0.17 \pm 0.02 ^A	0.22 \pm 0.52 ^B

Table S2.8. Summary statistics of linear mixed-effect (LME) model of depth category ~20-50 cm of (A) aggregate distribution (g aggregate per g bulk soil) and (B) total aggregate C (g C).

(A)	LME model at ~20-50 cm			(B)	LME model at ~20-50 cm		
	Aggregate distribution				Total aggregate C		
Fixed effects	df (df _{num} , df _{den})	F- statistic	P	Fixed effects	df (df _{num} , df _{den})	F-statistic	P
Transect	(4, 192.52)	0.64	0.64	Transect	(4, 143.80)	12.99	4.68e-09
Aggregate size	(3, 190.91)	158.06	<2.2e-16	Aggregate size	(3, 143.26)	13.48	8.50e-08
Transect * aggregate size	(12, 190.91)	1.40	0.17	Transect * aggregate size	(12, 143.15)	1.89	0.04

Table S2.9. (A) Aggregate distribution (g aggregate per g bulk soil) and (B) total aggregate C (g C) at depth category ~20-50 cm for each transect location (crop, crop edge, bare, field edge, and ditch bank) at four aggregate size classes (large macroaggregate, small macroaggregate, microaggregate, silt+clay; mean \pm SE). Different uppercase letters signify statistically significant differences at $P < 0.05$ among aggregate size class within transect location.

(A)	Crop	Crop edge	Bare	Field edge	Ditch bank
Large macroaggregates	0.00 \pm 0.00 ^A	0.00 \pm 0.00 ^A	0.03 \pm 0.02 ^A	0.08 \pm 0.05 ^A	0.04 \pm 0.03 ^A
Small macroaggregates	0.07 \pm 0.02 ^B	0.16 \pm 0.05 ^B	0.15 \pm 0.04 ^B	0.17 \pm 0.04 ^B	0.17 \pm 0.05 ^B
Microaggregates	0.35 \pm 0.03 ^C	0.31 \pm 0.05 ^C	0.32 \pm 0.04 ^C	0.30 \pm 0.06 ^B	0.30 \pm 0.08 ^B
Silt+clay	0.41 \pm 0.04 ^C	0.38 \pm 0.04 ^C	0.34 \pm 0.04 ^C	0.29 \pm 0.04 ^B	0.30 \pm 0.06 ^B
(B)	Crop	Crop edge	Bare	Field edge	Ditch bank
Large macroaggregates	0.01 \pm 0.00 ^A	0.02 \pm 0.01 ^A	0.02 \pm 0.02 ^A	0.81 \pm 0.63 ^A	0.25 \pm 0.22 ^A
Small macroaggregates	0.04 \pm 0.01 ^A	0.11 \pm 0.04 ^{AB}	0.10 \pm 0.04 ^B	0.29 \pm 0.13 ^A	0.28 \pm 0.13 ^A
Microaggregates	0.09 \pm 0.01 ^B	0.10 \pm 0.02 ^B	0.11 \pm 0.02 ^{BC}	0.15 \pm 0.03 ^A	0.16 \pm 0.02 ^A
Silt+clay	0.13 \pm 0.01 ^C	0.15 \pm 0.02 ^B	0.13 \pm 0.02 ^C	0.15 \pm 0.02 ^A	0.21 \pm 0.04 ^A

Table S2.10. Summary statistics of linear mixed-effect (LME) model of depth category ~50-80 cm of (A) aggregate distribution (g aggregate per g bulk soil) and (B) total aggregate C (g C).

(A)	LME model at ~50-80 cm			(B)	LME model at ~50-80 cm		
	Aggregate distribution				Total aggregate C		
Fixed effects	df (df _{num} , df _{den})	F- statistic	P	Fixed effects	df (df _{num} , df _{den})	F-statistic	P
Transect	(4, 177.51)	0.78	0.54	Transect	(4, 117.59)	1.22	0.30
Aggregate size	(3, 174.63)	270.47	<2e-16	Aggregate size	(3, 116.88)	32.77	1.92e-15
Transect * aggregate size	(12, 174.63)	1.24	0.26	Transect * aggregate size	(8, 116.83)	0.78	0.63

Table S2.11. (A) Aggregate distribution (g aggregate per g bulk soil) and (B) total aggregate C (g C) at depth category ~50-80 cm for each transect location (crop, crop edge, bare, field edge, and ditch bank) at four aggregate size classes (large macroaggregate, small macroaggregate, microaggregate, silt+clay; mean \pm SE). Different uppercase letters signify statistically significant differences at $P < 0.05$ among aggregate size class within transect location.

(A)	Crop	Crop edge	Bare	Field edge	Ditch bank
Large macroaggregates	0.00 \pm 0.00 ^A	0.00 \pm 0.00 ^A	0.00 \pm 0.00 ^A	0.06 \pm 0.06 ^A	0.00 \pm 0.00 ^A
Small macroaggregates	0.04 \pm 0.01 ^B	0.19 \pm 0.07 ^B	0.10 \pm 0.02 ^B	0.10 \pm 0.03 ^B	0.07 \pm 0.01 ^B
Microaggregates	0.40 \pm 0.05 ^C	0.37 \pm 0.06 ^C	0.38 \pm 0.05 ^C	0.33 \pm 0.06 ^B	0.34 \pm 0.07 ^C
Silt+clay	0.33 \pm 0.03 ^C	0.41 \pm 0.09 ^C	0.35 \pm 0.03 ^C	0.34 \pm 0.06 ^B	0.36 \pm 0.03 ^C
(B)	Crop	Crop edge	Bare	Field edge	Ditch bank
Large macroaggregates	0.01 ^A				
Small macroaggregates	0.01 \pm 0.00 ^A	0.02 \pm 0.01 ^A	0.04 \pm 0.02 ^A	0.02 \pm 0.01 ^A	0.02 \pm 0.01 ^A
Microaggregates	0.05 \pm 0.01 ^B	0.05 \pm 0.02 ^A	0.05 \pm 0.01 ^B	0.16 \pm 0.03 ^B	0.04 \pm 0.01 ^B
Silt+clay	0.07 \pm 0.01 ^B	0.07 \pm 0.01 ^B	0.10 \pm 0.03 ^B	0.28 \pm 0.02 ^B	0.10 \pm 0.03 ^C

Table S2.12. Summary statistics of linear mixed-effect (LME) model of depth category ~80+ cm of (A) aggregate distribution (g aggregate per g bulk soil) and (B) total aggregate C (g C).

(A)	LME model at ~80+ cm			(B)	LME model at ~80+ cm		
	Aggregate distribution				Total aggregate C		
Fixed effects	df (df _{num} , df _{den})	F- statistic	P	Fixed effects	df (df _{num} , df _{den})	F-statistic	P
Transect	(4, 104.73)	2.11	0.08	Transect	(4, 67.73)	2.35	0.06
Aggregate size	(3, 102.97)	102.45	<2e-16	Aggregate size	(3, 65.17)	38.26	2.22e-14
Transect * aggregate size	(12, 102.97)	0.46	0.93	Transect * aggregate size	(11, 64.92)	0.55	0.86

Table S2.13. (A) Aggregate distribution (g aggregate per g bulk soil) and (B) total aggregate C (g C) at depth category ~80+ cm for each transect location (crop, crop edge, bare, field edge, and ditch bank) at four aggregate size classes (large macroaggregate, small macroaggregate, microaggregate, silt+clay; mean \pm SE). Different uppercase letters signify statistically significant differences at $P < 0.05$ among aggregate size class within transect location.

(A)	Crop	Crop edge	Bare	Field edge	Ditch bank
Large macroaggregates	0.02 \pm 0.01 ^A	0.02 \pm 0.02 ^A	0.02 \pm 0.02 ^A	0.00 \pm 0.00 ^A	0.01 \pm 0.00 ^A
Small macroaggregates	0.06 \pm 0.02 ^B	0.10 \pm 0.03 ^B	0.10 \pm 0.04 ^B	0.06 \pm 0.01 ^B	0.09 \pm 0.04 ^B
Microaggregates	0.18 \pm 0.03 ^C	0.27 \pm 0.06 ^C	0.23 \pm 0.07 ^C	0.14 \pm 0.04 ^C	0.33 \pm 0.10 ^C
Silt+clay	0.24 \pm 0.05 ^C	0.32 \pm 0.07 ^C	0.28 \pm 0.05 ^C	0.28 \pm 0.06 ^C	0.32 \pm 0.11 ^C
(B)	Crop	Crop edge	Bare	Field edge	Ditch bank
Large macroaggregates	0.00 \pm 0.00 ^A	0.00 ^{AB}	0.00 ^A		0.01 ^A
Small macroaggregates	0.00 \pm 0.00 ^A	0.01 \pm 0.00 ^A	0.00 \pm 0.00 ^A	0.01 \pm 0.00 ^A	0.01 \pm 0.01 ^A
Microaggregates	0.01 \pm 0.00 ^A	0.03 \pm 0.01 ^{BC}	0.01 \pm 0.00 ^A	0.01 \pm 0.00 ^A	0.02 \pm 0.02 ^B
Silt+clay	0.01 \pm 0.01 ^B	0.04 \pm 0.01 ^C	0.04 \pm 0.01 ^B	0.06 \pm 0.01 ^B	0.05 \pm 0.02 ^C

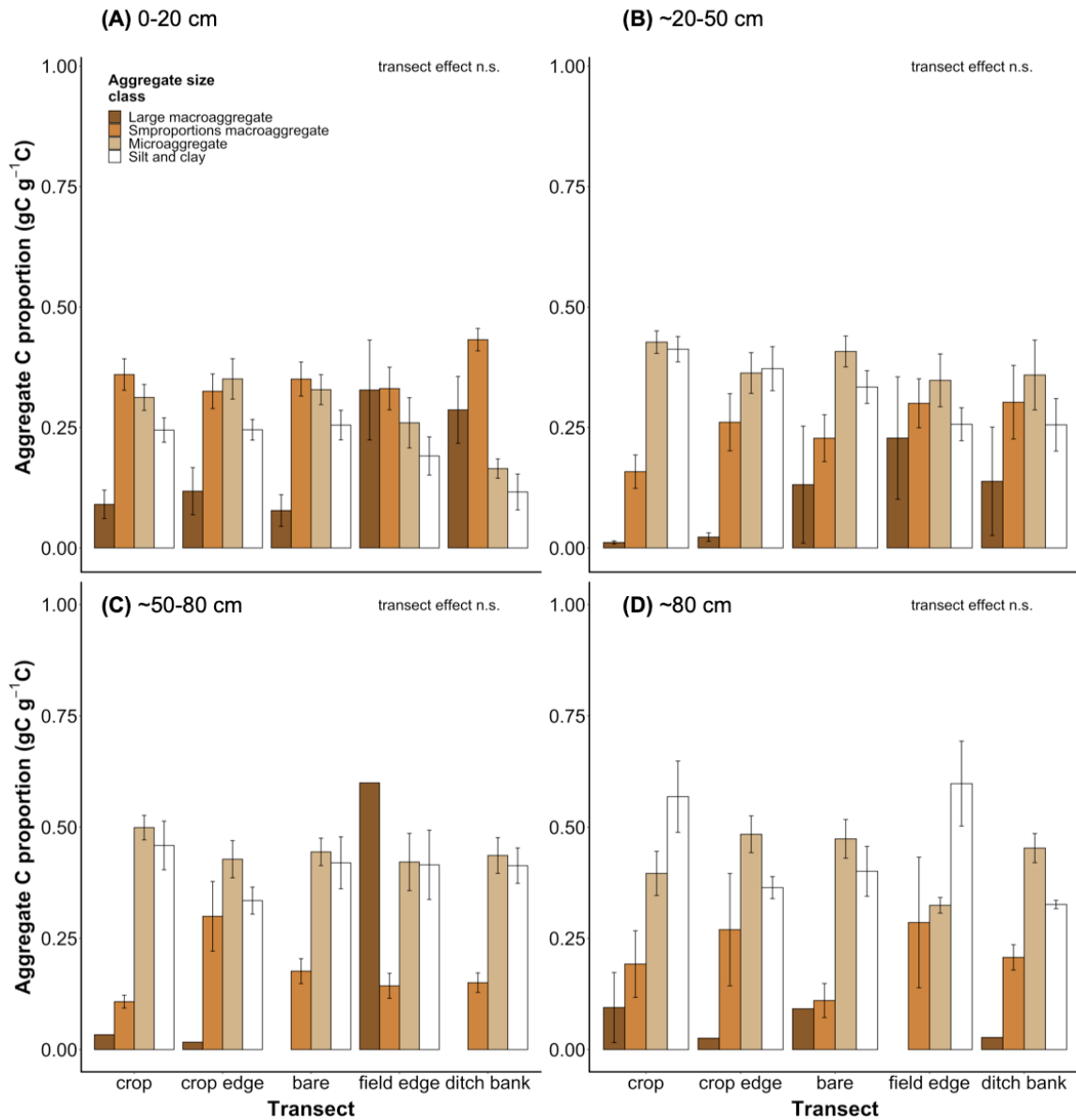


Figure S2.1. Normalized total aggregate C (g C g⁻¹ C) in (A) 0-20 cm, (B) ~20-50 cm, (C) ~50-80 cm, and (D) ~80+ cm along the SWI transect. Error bars are the standard error of the mean. Transect locations within depth categories are statistically significant at P<0.05 in Tukey post-hoc pairwise comparisons.

The calculation for normalized total aggregate C is as follows:

$$\frac{\text{Total aggregate C}}{\Sigma(\text{total aggregate C of LM, sM, m, sc in a given sample})}$$

LM, large macroaggregate; sM, small macroaggregate; m, microaggregate; sc, silt+clay.

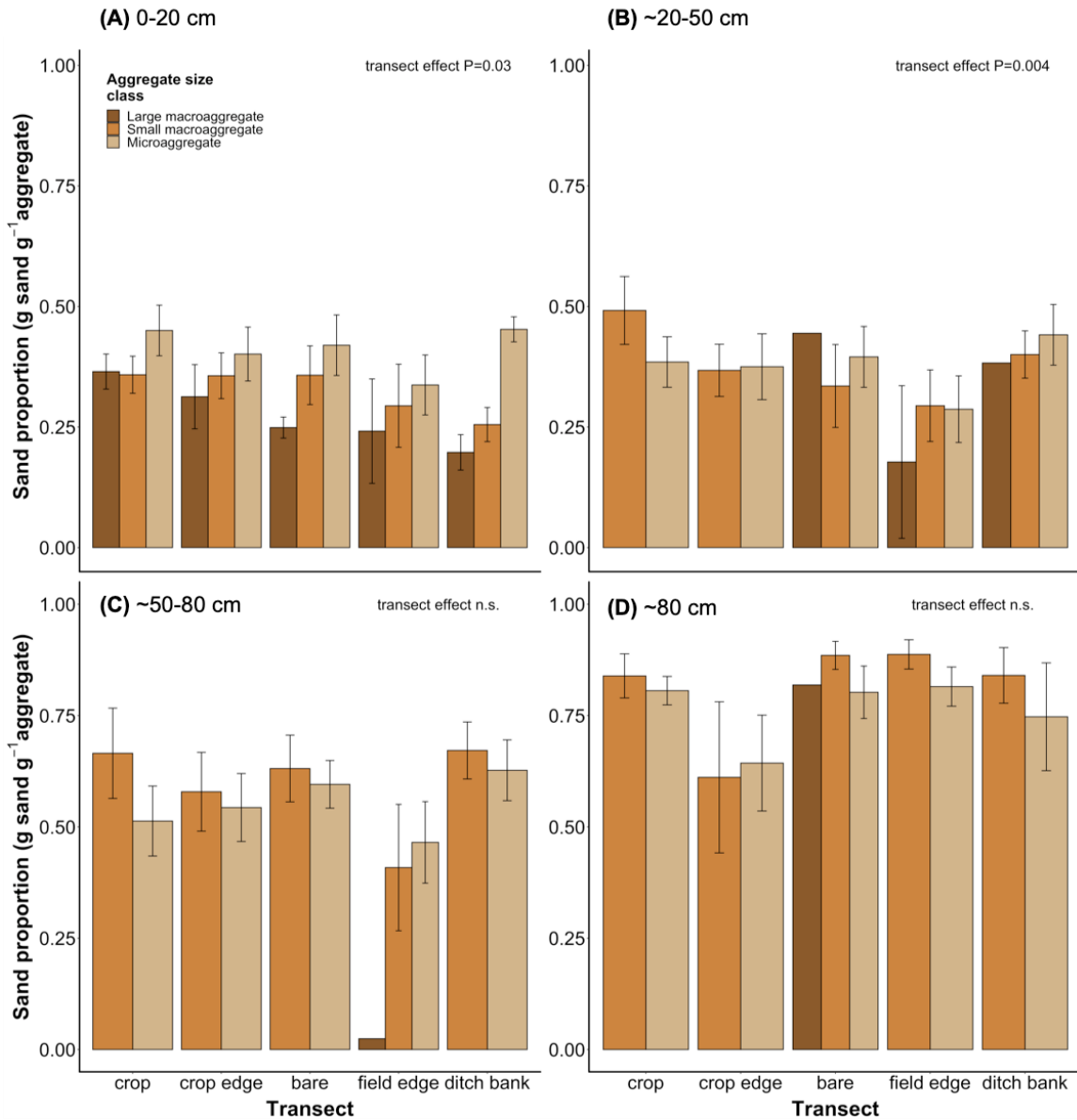


Figure S2.2. Sand proportion (g sand g⁻¹ aggregate) in (A) 0-20 cm, (B) ~20-50 cm, (C) ~50-80 cm, and (D) ~80+ cm along the SWI transect. Error bars are the standard error of the mean. Transect locations within depth categories are statistically significant at P<0.05 in Tukey post-hoc pairwise comparisons.

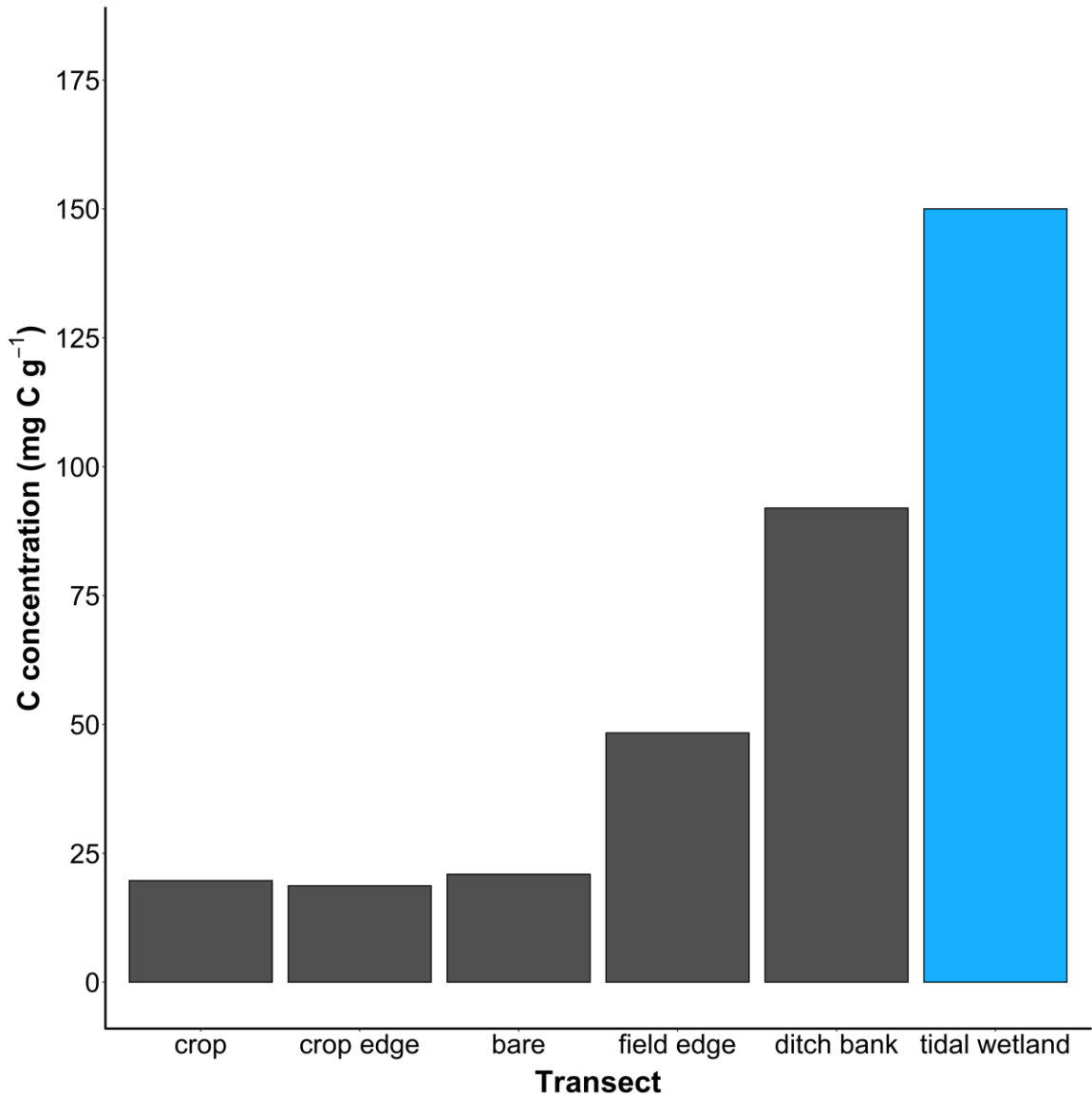


Figure S2.3. Soil C concentration (mg C g⁻¹) in the top 50 cm along the SWI transect and an average tidal wetland (Morris et al. 2016).

References

- Achenbach, L., F. Eller, L. X. Nguyen, and H. Brix. 2013. Differences in salinity tolerance of genetically distinct *Phragmites australis* clones. *AoB PLANTS* 5.
- Adolf, V. I., S. Shabala, M. N. Andersen, F. Razzaghi, and S.-E. Jacobsen. 2012. Varietal differences of quinoa's tolerance to saline conditions. *Plant and Soil* 357:117–129.
- Adolf, V. I., S.-E. Jacobsen, and S. Shabala. 2013. Salt tolerance mechanisms in quinoa (*Chenopodium quinoa* Willd.). *Environmental and Experimental Botany* 92:43–54.
- Ågren, G. I., and E. Bosatta. 2002. Reconciling differences in predictions of temperature response of soil organic matter. *Soil Biology and Biochemistry* 34:129–132.
- Almansouri, M. 2001. Effect of salt and osmotic stresses on germination in durum wheat (*Triticum durum* Desf.). *Plant and Soil* 231:243–254.
- Angers, D. A., and G. R. Mehuys. 1988. Effects of cropping on macro-aggregation of a marine clay soil. *Canadian Journal of Soil Science* 68:723–732.
- Angers, D. A., and A. N'Dayegamiye. 1991. Effects of manure application on carbon, nitrogen, and carbohydrate contents of a silt loam and its particle-size fractions. *Biology and Fertility of Soils* 11:79–82.
- Angers, D. A., A. Pesant, and J. Vigneux. 1992. Early Cropping-Induced Changes in Soil Aggregation, Organic Matter, and Microbial Biomass. *Soil Science Society of America Journal* 56:115.
- Aoyama, M., D. A. Angers, and A. N'Dayegamiye. 1999a. Particulate and mineral associated organic matter in water-stable aggregates as affected by mineral fertilizer and manure applications. *Canadian Journal of Soil Science* 79:295–302.
- Aoyama, M., D. A. Angers, A. N'Dayegamiye, and N. Bissonnette. 1999b. Protected organic matter in water-stable aggregates as affected by mineral fertilizer and manure applications. *Canadian Journal of Soil Science* 79:419–425.
- Ardón, M., J. L. Morse, B. P. Colman, and E. S. Bernhardt. 2013. Drought-induced saltwater incursion leads to increased wetland nitrogen export. *Global Change Biology* 19:2976–2985.
- Ardón, M., A. M. Helton, and E. S. Bernhardt. 2016. Drought and saltwater incursion synergistically reduce dissolved organic carbon export from coastal freshwater wetlands. *Biogeochemistry* 127:411–426.
- Ardón, M., A. M. Helton, and E. S. Bernhardt. 2018. Salinity effects on greenhouse gas emissions from wetland soils are contingent upon hydrologic setting: a microcosm experiment. *Biogeochemistry* 140:217–232.
- Ashraf, M., and N. A. Akram. 2009. Improving salinity tolerance of plants through conventional breeding and genetic engineering: An analytical comparison. *Biotechnology Advances* 27:744–752.
- Attou, F., A. Bruand, and Y. Le Bissonnais. 1998. Effect of clay content and silt-clay fabric on stability of artificial aggregates. *European Journal of Soil Science* 49:569–577.
- Barica, J. 1972. Salinization of groundwater in arid zones. *Water Research* 6:925–933.

- Bates D, M. Maechler, B. Bolker, and S. Walker. 2013. lme4: linear mixed-effects models using Eigen and S4. <https://cran.r-project.org/web/packages/lme4/lme4.pdf>
- Beare, M. H., P. F. Hendrix, M. L. Cabrera, and D. C. Coleman. 1994a. Aggregate Protected and Unprotected Organic Matter Pools in Conventional- and No-Tillage Soils. *Soil Science Society of America Journal* 58:787.
- Beare, M. H., P. F. Hendrix, and D. C. Coleman. 1994b. Water-Stable Aggregates and Organic Matter Fractions in Conventional- and No-Tillage Soils. *Soil Science Society of America Journal* 58:777–786.
- Ben-Hur, M., G. Yolcu, H. Uysal, M. Lado, and A. Paz. 2009. Soil structure changes: aggregate size and soil texture effects on hydraulic conductivity under different saline and sodic conditions. *Soil Research* 47:688.
- Bhattachan, A., R. E. Emanuel, M. Ardon, E. S. Bernhardt, S. M. Anderson, M. G. Stillwagon, E. A. Ury, T. K. Bendor, and J. P. Wright. 2018. Evaluating the effects of land-use change and future climate change on vulnerability of coastal landscapes to saltwater intrusion. *Elem Sci Anth* 6:62.
- Bibi, A., H. A. Sadaqat, M. H. N. Tahir, and H. M. Akram. 2012. Screening of sorghum (*Sorghum bicolor* Var Moench) for drought. *J. Anim. Plant Sci.* 23:671–678.
- Box, G., and D. Cox. 1964. An Analysis of Transformations. *Journal of the Royal Statistical Society* 26:211–252.
- Bridgham, S. D., J. Patrick Megonigal, J. K. Keller, N. B. Bliss, and C. Trettin. 2006. The carbon balance of North American wetlands. *Wetlands* 26:889–916.
- Bronick, C. J., and R. Lal. 2005. Soil structure and management: a review. *Geoderma* 124:3–22.
- Carpita, N., D. Sabularse, D. Montezinos, and D. P. Delmer. 1979. Determination of the Pore Size of Cell Walls of Living Plant Cells. *Science* 205:1144–1147.
- Carpıcı, E. B., N. Celik, and G. Bayram. 2009. Effects of salt stress on germination of some maize (*Zea mays* L.) cultivars. *African Journal of Biotechnology* 8:4918–4922.
- Chambers, L. G., T. Z. Osborne, and K. R. Reddy. 2013. Effect of salinity-altering pulsing events on soil organic carbon loss along an intertidal wetland gradient: a laboratory experiment. *Biogeochemistry* 115:363–383.
- Chandra Babu, R., J. Zhang, A. Blum, T.-H. David Ho, R. Wu, and H. T. Nguyen. 2004. HVA1, a LEA gene from barley confers dehydration tolerance in transgenic rice (*Oryza sativa* L.) via cell membrane protection. *Plant Science* 166:855–862.
- Chen, Y., C. Li, B. Zhang, J. Yi, Y. Yang, C. Kong, C. Lei, and M. Gong. 2019. The Role of the Late Embryogenesis-Abundant (LEA) Protein Family in Development and the Abiotic Stress Response: A Comprehensive Expression Analysis of Potato (*Solanum Tuberosum*). *Genes* 10:148.
- Chmura, G. L., S. C. Anisfeld, D. R. Cahoon, and J. C. Lynch. 2003. Global carbon sequestration in tidal, saline wetland soils. *Global Biogeochemical Cycles* 17:1–12.
- Colmer, T. D., and T. J. Flowers. 2008. Flooding tolerance in halophytes. *New Phytologist* 179:964–974.

- Coote, D. R., C. A. Malcolm-McGovern, G. J. Wall, W. T. Dickinson, and R. P. Rudra. 1988. Seasonal variation of erodibility indices based on shear strength and aggregate stability in some Ontario soils. *Canadian Journal of Soil Science* 68:405–416.
- Craft, C. 2007. Freshwater input structures soil properties, vertical accretion, and nutrient accumulation of Georgia and U.S tidal marshes. *Limnology and Oceanography* 52:1220–1230.
- Debez, A., K. Ben Hamed, C. Grignon, and C. Abdelly. 2004. Salinity effects on germination, growth, and seed production of the halophyte *Cakile maritima*. *Plant and Soil* 262:179–189.
- Denef, K., J. Six, K. Paustian, and R. Merckx. 2001. Importance of macroaggregate dynamics in controlling soil carbon stabilization: short-term effects of physical disturbance induced by dry–wet cycles. *Soil Biology and Biochemistry* 33:2145–2153.
- Dhote, S., and S. Dixit. 2009. Water quality improvement through macrophytes—a review. *Environmental Monitoring and Assessment* 152:149–153.
- Dornbos, D. L., R. E. Mullen, and R. E. Shibles. 1989. Drought Stress Effects During Seed Fill on Soybean Seed Germination and Vigor. *Crop Science* 29:476.
- Drury, C. F., J. A. Stone, and W. I. Findlay. 1991. Microbial Biomass and Soil Structure Associated with Corn, Grasses, and Legumes. *Soil Science Society of America Journal* 55:805.
- Dungait, J. A. J., D. W. Hopkins, A. S. Gregory, and A. P. Whitmore. 2012. Soil organic matter turnover is governed by accessibility not recalcitrance. *Global Change Biology* 18:1781–1796.
- Ejeta, G., and J. E. Knoll. 2007. Marker-Assisted Selection in Sorghum. Page *in* R. K. Varshney and R. Tuberosa, editors. *Genomics-assisted crop improvement*. Vol. 2 Vol. 2. Springer Verlag, Dordrecht.
- El Naim, A. M., K. E. Mohammed, E. A. Ibrahim, and N. N. Suleiman. 2012. Impact of Salinity on Seed Germination and Early Seedling Growth of Three Sorghum (*Sorghum biolor* L. Moench) Cultivars. *Science and Technology* 2:16–20.
- Erdei, L., and E. Taleisnik. 1993. Changes in water relation parameters under osmotic and salt stresses in maize and sorghum. *Physiologia Plantarum* 89:381–387.
- Faijunnahar, M., A. Baque, and A. Habib. 2017. Polyethylene Glycol (PEG) Induced Changes in Germination, Seedling Growth and Water Relation Behavior of Wheat (*Triticum aestivum* L.) Genotypes. *Universal Journal of Plant Science* 5:49–57.
- Fan, J., B. McConkey, H. Wang, and H. Janzen. 2016. Root distribution by depth for temperate agricultural crops. *Field Crops Research* 189:68–74.
- Farooq, M., S. M. A. Basra, N. Ahmad, and K. Hafeez. 2005. Thermal Hardening: A New Seed Vigor Enhancement Tool in Rice. *Journal of Integrative Plant Biology* 47:187–193.
- Flowers, T. J. 2004. Improving crop salt tolerance. *Journal of Experimental Botany* 55:307–319.
- Flowers, T. J., and T. D. Colmer. 2008. Salinity tolerance in halophytes. *New Phytologist* 179:945–963.

- Flowers, T. J., and T. D. Colmer. 2015. Plant salt tolerance: adaptations in halophytes. *Annals of Botany* 115:327–331.
- Flowers, T. J., H. K. Galal, and L. Bromham. 2010. Evolution of halophytes: multiple origins of salt tolerance in land plants. *Functional Plant Biology* 37:604.
- Foster, S., A. Pulido-Bosch, Á. Vallejos, L. Molina, A. Llop, and A. M. MacDonald. 2018. Impact of irrigated agriculture on groundwater-recharge salinity: a major sustainability concern in semi-arid regions. *Hydrogeology Journal* 26:2781–2791.
- Francois, L. E., T. Donovan, and E. V. Maas. 1984a. Salinity Effects on Seed Yield, Growth, and Germination of Grain Sorghum1. *Agronomy Journal* 76:741.
- Francois, L. E., T. Donovan, and E. V. Maas. 1984b. Salinity Effects on Seed Yield, Growth, and Germination of Grain Sorghum1. *Agronomy Journal* 76:741.
- Gedan, K. B., and E. Fernández-Pascual. 2019. Salt marsh migration into salinized agricultural fields: A novel assembly of plant communities. *Journal of Vegetation Science*.
- Geressu, K., and M. Gezaghegne. 2008. Response of some lowland growing sorghum (*Sorghum bicolor* L. Moench) accessions to salt stress during germination and seedling growth. *African Journal of Agricultural Research* 3:044–048.
- Ghassemi, F., A. Jakeman, and H. Nix. 1995. *Salinisation of Land and Water Resources: Human Causes, Extent, Management and Case Studies*. CAB International.
- Ghassemi-Golezani, K., and M. Taifeh-Noori. 2011. Soybean performance under salinity stress. *Soybean-Biochemistry, Chemistry and Physiology*. InTech.
- Grandy, A. S., and G. P. Robertson. 2006. Aggregation and Organic Matter Protection Following Tillage of a Previously Uncultivated Soil. *Soil Science Society of America Journal* 70:1398.
- Grandy, A. S., and G. P. Robertson. 2007. Land-Use Intensity Effects on Soil Organic Carbon Accumulation Rates and Mechanisms. *Ecosystems* 10:59–74.
- Gürel, F., Z. N. Öztürk, C. Uçarlı, and D. Rosellini. 2016. Barley Genes as Tools to Confer Abiotic Stress Tolerance in Crops. *Frontiers in Plant Science* 7.
- Hanks, R. J., and F. C. Thorp. 1957. Seedling Emergence of Wheat, Grain Sorghum, and Soybeans as Influenced by Soil Crust Strength and Moisture Content. *Soil Science Society Proceedings*:357–359.
- Hardegree, S. P., and W. E. Emmerich. 1990. Effect of Polyethylene Glycol Exclusion on the Water Potential of Solution-Saturated Filter Paper. *PLANT PHYSIOLOGY* 92:462–466.
- Hennessee L., M. J. Valentino, and A. M. Lesh. 2003. *Updating Shore Erosion Rates in Maryland*. Maryland Geological Survey. Coastal and Estuarine Geology File Report No. 03-05. Baltimore, Maryland, USA.
- Herbert, E. R., J. Schubauer-Berigan, and C. B. Craft. 2018. Differential effects of chronic and acute simulated seawater intrusion on tidal freshwater marsh carbon cycling. *Biogeochemistry* 138:137–154.
- Hester, M. W., I. A. Mendelssohn, and K. L. McKee. 1996. Intraspecific variation in salt tolerance and morphology in the coastal grass *spartina patens* (poaceae). *American Journal of Botany* 83:1521–1527.

- Hoagland, C. R., L. E. Gentry, M. B. David, and D. A. Kovacic. 2001. Plant Nutrient Uptake and Biomass Accumulation in a Constructed Wetland. *Journal of Freshwater Ecology* 16:527–540.
- van Hoorn, J. W. 1991. Development of soil salinity during germination and early seedling growth and its effect on several crops. *Agricultural Water Management* 20:17–28.
- Hosseini, M. K., A. A. Powell, and I. J. Bingham. 2002. Comparison of the seed germination and early seedling growth of soybean in saline conditions. *Seed Science Research* 12:165–172.
- Hothorn, T., F. Bretz, and P. Westfall. 2008. Simultaneous Inference in General Parametric Models. *Biometrical Journal* 50:346–363.
- Houghton, R. A., and J. L. Hackler. 2008. Carbon Flux to the Atmosphere from Land Use Changes 1850-2005.
- Huang, J., and R. E. Redmann. 1995. Salt tolerance of *Hordeum* and *Brassica* species during germination and early seedling growth. *Canadian Journal of Plant Science* 75:815–819.
- Huang, X., H. Jiang, Y. Li, Y. Ma, H. Tang, W. Ran, and Q. Shen. 2016. The role of poorly crystalline iron oxides in the stability of soil aggregate-associated organic carbon in a rice–wheat cropping system. *Geoderma* 279:1–10.
- Huggins, D. R., and J. P. Reganold. 2008. No-Till: The Quiet Revolution. *Scientific American* 299:70–77.
- Igartua, E., M. P. Gracia, and J. M. Lasa. 1995. Field responses of grain sorghum to a salinity gradient. *Field Crops Research* 42:15–25.
- Jacobsen, S.-E., A. Mujica, and C. R. Jensen. 2003. The Resistance of Quinoa (*Chenopodium quinoa* Willd.) to Adverse Abiotic Factors. *Food Reviews International* 19:99–109.
- Jacobsen, S.-E., C. Monteros, J. L. Christiansen, L. A. Bravo, L. J. Corcuera, and A. Mujica. 2005. Plant responses of quinoa (*Chenopodium quinoa* Willd.) to frost at various phenological stages. *European Journal of Agronomy* 22:131–139.
- Jacobsen, S.-E., C. Monteros, L. J. Corcuera, L. A. Bravo, J. L. Christiansen, and A. Mujica. 2007. Frost resistance mechanisms in quinoa (*Chenopodium quinoa* Willd.). *European Journal of Agronomy* 26:471–475.
- Jastrow, J. D., J. E. Amonette, and V. L. Bailey. 2007. Mechanisms controlling soil carbon turnover and their potential application for enhancing carbon sequestration. *Climatic Change* 80:5–23.
- Kell, D. B. 2012. Large-scale sequestration of atmospheric carbon via plant roots in natural and agricultural ecosystems: why and how. *Philosophical Transactions of the Royal Society B: Biological Sciences* 367:1589–1597.
- Khan, M. A., and D. J. Weber, editors. 2008. *Ecophysiology of high salinity tolerant plants*. Springer, Dordrecht.
- Khayatnezhad, M., R. Gholamin, S. Jamaati-e-Somarin, and R. Zabihi-e-Mahmoodabad. 2010. Effects of Peg Stress on Corn Cultivars (*Zea mays* L.) At Germination Stage:3.
- Kırmızı, S., and R. W. Bell. 2012. Responses of barley to hypoxia and salinity during seed germination, nutrient uptake, and early plant growth in solution culture. *Journal of Plant Nutrition and Soil Science* 175:630–640.

- Kleinman, P., A. Allen, B. Needelman, A. Sharpley, P. Vadas, L. Saporito, G. Folmer, and R. Bryant. 2007. Dynamics of phosphorus transfers from heavily manured Coastal Plain soils to drainage ditches. *Journal of Soil and Water Conservation* 62:225–235.
- Kleinman, P., K. S. Blunk, R. Bryant, L. Saporito, D. Beegle, K. Czymmek, Q. Ketterings, T. Sims, J. Shortle, J. McGrath, F. Coale, M. Dubin, D. Dostie, R. Maguire, R. Meinen, A. Allen, K. O'Neill, L. Garber, M. Davis, B. Clark, K. Sellner, and M. Smith. 2012. Managing manure for sustainable livestock production in the Chesapeake Bay Watershed. *Journal of Soil and Water Conservation* 67:54A-61A.
- Konisky, R. A., and D. M. Burdick. 2004. Effects of stressors on invasive and halophytic plants of New England salt marshes: A framework for predicting response to tidal restoration. *Wetlands* 24:434–447.
- Koyro, H.-W. 1997. Ultrastructural and physiological changes in root cells of Sorghum plants [*Sorghum bicolor* x *S. sudanensis* cv. Sweet Sioux) induced by NaCl. *Journal of Experimental Botany* 48:693–706.
- Lalonde, K., A. Mucci, A. Ouellet, and Y. G elinas. 2012. Preservation of organic matter in sediments promoted by iron. *Nature* 483:198–200.
- Lang, A. 1967. Osmotic coefficients and water potentials of sodium chloride solutions from 0 to 40°C. *Australian Journal of Chemistry* 20:2017.
- Lehmann, J., and M. Kleber. 2015. The contentious nature of soil organic matter. *Nature* 528:60–68.
- Li, W.-T., C. Liu, Y.-X. Liu, Z.-E. Pu, S.-F. Dai, J.-R. Wang, X.-J. Lan, Y.-L. Zheng, and Y.-M. Wei. 2013. Meta-analysis of QTL associated with tolerance to abiotic stresses in barley. *Euphytica* 189:31–49.
- Lissner, J., and H.-H. Schierup. 1997. Effects of salinity on the growth of *Phragmites australis*. *Aquatic Botany* 55:247–260.
- von L utzow, M., I. K ogel-Knabner, K. Ekschmitt, H. Flessa, G. Guggenberger, E. Matzner, and B. Marschner. 2007. SOM fractionation methods: Relevance to functional pools and to stabilization mechanisms. *Soil Biology and Biochemistry* 39:2183–2207.
- von L utzow, M., I. Kogel-Knabner, K. Ekschmitt, E. Matzner, G. Guggenberger, B. Marschner, and H. Flessa. 2006. Stabilization of organic matter in temperate soils: mechanisms and their relevance under different soil conditions - a review. *European Journal of Soil Science* 57:426–445.
- Maas, E. V., G. J. Hoffman, G. D. Chaba, J. A. Poss, and M. C. Shannon. 1983. Salt sensitivity of corn at various growth stages. *Irrigation Science* 4:45–57.
- Maas, E. V., J. A. Poss, and G. J. Hoffman. 1986. Salinity sensitivity of sorghum at three growth stages. *Irrigation Science* 7.
- Malcolm, C. V., V. A. Lindley, J. W. O'Leary, H. V. Runciman, and E. G. Barrett Lennard. 2003. Halophyte and glycophyte salt tolerance at germination and the establishment of halophyte shrubs in saline environments. *Plant and Soil* 253:171–185.
- Martens, D. A., T. E. Reedy, and D. T. Lewis. 2004. Soil organic carbon content and composition of 130-year crop, pasture and forest land-use managements. *Global Change Biology* 10:65–78.

- Mauchamp, A., and F. Mésleard. 2001. Salt tolerance in *Phragmites australis* populations from coastal Mediterranean marshes. *Aquatic Botany* 70:39–52.
- McLeod, E., G. L. Chmura, S. Bouillon, R. Salm, M. Björk, C. M. Duarte, C. E. Lovelock, W. H. Schlesinger, and B. R. Silliman. 2011. A blueprint for blue carbon: toward an improved understanding of the role of vegetated coastal habitats in sequestering CO₂. *Frontiers in Ecology and the Environment* 9:552–560.
- Mehnert, E., and A. A. Jennings. 1985. The effect of salinity-dependent hydraulic conductivity on saltwater intrusion episodes. *Journal of Hydrology* 80:283–297.
- Mendelssohn, I. A., B. K. Sorrell, H. Brix, H.-H. Schierup, B. Lorenzen, and E. Maltby. 1999. Controls on soil cellulose decomposition along a salinity gradient in a *Phragmites australis* wetland in Denmark. *Aquatic Botany* 64:381–398.
- Metternicht, G. I., and J. A. Zinck. 2003. Remote sensing of soil salinity: potentials and constraints. *Remote Sensing of Environment* 85:1–20.
- Mikha, M. M., and C. W. Rice. 2004. Tillage and Manure Effects on Soil and Aggregate Associated Carbon and Nitrogen. *Soil Science Society of America Journal* 68:809.
- Mikutta, R., M. Kleber, M. S. Torn, and R. Jahn. 2006. Stabilization of Soil Organic Matter: Association with Minerals or Chemical Recalcitrance? *Biogeochemistry* 77:25–56.
- Mitsch, W. J., and J. G. Gosselink. 2015. *Wetlands* (5th Edition). John Wiley & Sons, Inc., Hoboken, NJ, USA.
- Morris, J. T., D. C. Barber, J. C. Callaway, R. Chambers, S. C. Hagen, C. S. Hopkinson, B. J. Johnson, P. Megonigal, S. C. Neubauer, T. Troxler, and C. Wigand. 2016. Contributions of organic and inorganic matter to sediment volume and accretion in tidal wetlands at steady state: Sediment bulk density and ignition loss. *Earth's Future* 4:110–121.
- Munns, R., R. A. James, and A. Läuchli. 2006. Approaches to increasing the salt tolerance of wheat and other cereals. *Journal of Experimental Botany* 57:1025–1043.
- Munns, R., and M. Tester. 2008. Mechanisms of Salinity Tolerance. *Annual Review of Plant Biology* 59:651–681.
- National Oceanic and Atmospheric Administration, National Centers for Environmental Information. 2018. Climate Data Online. <https://www.ncdc.noaa.gov/cdo-web/>
- Netondo, G. W., J. C. Onyango, and E. Beck. 2004. Sorghum and Salinity: I. Response of Growth and Water Relations, and Ion Accumulation to NaCl salinity. *Crop Physiology and Metabolism* 44:797–805.
- Oades, J. M. 1984. Soil organic matter and structural stability: mechanisms and implications for management. *Plant and Soil* 76:319–337.
- Orchard, P. W., and R. S. Jessop. 1984. The response of sorghum and sunflower to short term waterlogging. *Plant and Soil* 81:119–132.
- Panuccio, M. R., S. E. Jacobsen, S. S. Akhtar, and A. Muscolo. 2014. Effect of saline water on seed germination and early seedling growth of the halophyte quinoa. *AoB PLANTS* 6:plu047–plu047.
- Parida, A. K., and A. B. Das. 2005. Salt tolerance and salinity effects on plants: a review. *Ecotoxicology and Environmental Safety* 60:324–349.

- Parihar, P., S. Singh, R. Singh, V. P. Singh, and S. M. Prasad. 2015. Effect of salinity stress on plants and its tolerance strategies: a review. *Environmental Science and Pollution Research* 22:4056–4075.
- Patanè, C., A. Saita, and O. Sortino. 2013. Comparative Effects of Salt and Water Stress on Seed Germination and Early Embryo Growth in Two Cultivars of Sweet Sorghum. *Journal of Agronomy and Crop Science* 199:30–37.
- Paul, E. A., A. Kravchenko, A. S. Grandy, and S. Morris. 2015. Soil Organic Matter Dynamics: Controls and management for sustainable ecosystem functioning. Pages 104–134 *The Ecology of Agricultural Landscapes: Long-Term Research on the Path to Sustainability*. Oxford University Press, New York, New York, USA.
- Perfect, E., B. D. Kay, W. K. P. van Loon, R. W. Sheard, and T. Pojasok. 1990a. Rates of Change in Soil Structural Stability under Forages and Corn. *Soil Science Society of America Journal* 54:179.
- Perfect, E., B. D. Kay, W. K. P. van Loon, R. W. Sheard, and T. Pojasok. 1990b. Factors Influencing Soil Structural Stability within a Growing Season. *Soil Science Society of America Journal* 54:173.
- Peterson, A., and K. Murphy. 2015. Tolerance of Lowland Quinoa Cultivars to Sodium Chloride and Sodium Sulfate Salinity. *Crop Science* 55:331.
- Plante, A. F., and W. B. McGill. 2002. Intraseasonal Soil Macroaggregate Dynamics in Two Contrasting Field Soils Using Labeled Tracer Spheres. *Soil Science Society of America Journal* 66:1285.
- Prado, F. E., C. Boero, M. Gallardo, and J. A. González. 2000. Effect of NaCl on germination, growth, and soluble sugar content in *Chenopodium quinoa* Willd. seeds. *Botanical Bulletin of Academia Sinica* 41:8.
- Promkhambut, A., A. Polthanee, C. Akkasaeng, and A. Younger. 2011. Growth, yield and aerenchyma formation of sweet and multipurpose sorghum (*Sorghum bicolor* L. Moench) as affected by flooding at different growth stages. *Australian Journal of Crop Science* 5:954–965.
- Qadir, M., E. Quillérou, V. Nangia, G. Murtaza, M. Singh, R. J. Thomas, P. Drechsel, and A. D. Noble. 2014. Economics of salt-induced land degradation and restoration. *Natural Resources Forum* 38:282–295.
- R Development Core Team. 2019. R: a language and environment for statistical computing. R Foundation for Statistical Computing, Vienna, Austria. <https://www.R-project.org/>
- Radic, V., D. Beatovic, and J. Mrdja. 2007. Salt tolerance of corn genotypes (*Zea mays* L.) during germination and later growth. *Journal of Agricultural Sciences, Belgrade* 52:115–120.
- Ranal, M. A., and D. G. de Santana. 2006. How and why to measure the germination process? *Revista Brasileira de Botânica* 29:1–11.
- Rani, C. R., C. Reema, and S. Alka. 2012. Salt Tolerance of *Sorghum bicolor* Cultivars during Germination and Seedling Growth 1:10.
- de la Reguera, E., M. Palmer, K. Gedam, and K. Tully. *in prep*. The effect of salinity on species survival and carbon storage on the lower eastern shore of Maryland due to saltwater intrusion. MS, University of Maryland, College Park, College Park, Maryland.

- Rengasamy, P., R. Greene, G. Ford, and A. Mehanni. 1984. Identification of dispersive behaviour and the management of red-brown earths. *Soil Research* 22:413.
- Rengasamy, P., and K. A. Olsson. 1991. Sodicity and soil structure. *Australian Journal of Soil Research* 29:935–952.
- Roy, S. J., S. Negrão, and M. Tester. 2014. Salt resistant crop plants. *Current Opinion in Biotechnology* 26:115–124.
- Roychoudhury, A., and M. Chakraborty. 2013. Biochemical and Molecular Basis of Varietal Difference in Plant Salt Tolerance:33.
- Ruiz-Carrasco, K., F. Antognoni, A. K. Coulibaly, S. Lizardi, A. Covarrubias, E. A. Martínez, M. A. Molina-Montenegro, S. Biondi, and A. Zurita-Silva. 2011. Variation in salinity tolerance of four lowland genotypes of quinoa (*Chenopodium quinoa* Willd.) as assessed by growth, physiological traits, and sodium transporter gene expression. *Plant Physiology and Biochemistry* 49:1333–1341.
- Sallenger, A. H., K. S. Doran, and P. A. Howd. 2012. Hotspot of accelerated sea-level rise on the Atlantic coast of North America. *Nature Climate Change* 2:884–888.
- Sarkar, B., M. Singh, S. Mandal, G. J. Churchman, and N. S. Bolan. 2018. Clay Minerals—Organic Matter Interactions in Relation to Carbon Stabilization in Soils. Pages 71–86 *The Future of Soil Carbon*. Elsevier.
- Schmidt, M. W. I., M. S. Torn, S. Abiven, T. Dittmar, G. Guggenberger, I. A. Janssens, M. Kleber, I. Kögel-Knabner, J. Lehmann, D. A. C. Manning, P. Nannipieri, D. P. Rasse, S. Weiner, and S. E. Trumbore. 2011. Persistence of soil organic matter as an ecosystem property. *Nature* 478:49–56.
- Scholz, M., and B. Lee. 2005. Constructed wetlands: a review. *International Journal of Environmental Studies* 62:421–447.
- Scott, S. J., R. A. Jones, and W. A. Williams. 1984. Review of Data Analysis Methods for Seed Germination. *Crop Science* 24:1192.
- Sedgwick, P. 2012. Multiple significance tests: the Bonferroni correction. *BMJ* 344:e509–e509.
- Shabala, L., A. Mackay, Y. Tian, S.-E. Jacobsen, D. Zhou, and S. Shabala. 2012. Oxidative stress protection and stomatal patterning as components of salinity tolerance mechanism in quinoa (*Chenopodium quinoa*). *Physiologia Plantarum* 146:26–38.
- Shani, U., and L. M. Dudley. 2001. Field Studies of Crop Response to Water and Salt Stress. *Soil Science Society of America Journal* 65:1522.
- Singer, M. J., R. J. Southard, D. N. Warrington, and P. Janitzky. 1992. Stability of Synthetic Sand-Clay Aggregates after Wetting and Drying Cycles. *Soil Science Society of America Journal* 56:1843.
- Six, J., H. Bossuyt, S. Degryze, and K. Denef. 2004. A history of research on the link between (micro)aggregates, soil biota, and soil organic matter dynamics. *Soil and Tillage Research* 79:7–31.
- Six, J., R. T. Conant, E. A. Paul, and K. Paustian. 2002. Stabilization mechanisms of soil organic matter: Implications for C-saturation of soils 241:155–176.
- Six, J., E. T. Elliott, and K. Paustian. 2000a. Soil macroaggregate turnover and microaggregate formation: a mechanism for C sequestration under no-tillage agriculture. *Soil Biology and Biochemistry* 32:2099–2103.

- Six, J., E. T. Elliott, K. Paustian, and J. W. Doran. 1998. Aggregation and Soil Organic Matter Accumulation in Cultivated and Native Grassland Soils. *Soil Science Society of America Journal* 62:1367.
- Six, J., K. Paustian, E. T. Elliott, and C. Combrink. 2000b. Soil structure and organic matter I. Distribution of aggregate-size classes and aggregate-associated carbon. *Soil Science Society of America Journal* 64:681–689.
- Sodano, M., C. Lerda, R. Nisticò, M. Martin, G. Magnacca, L. Celi, and D. Said Pullicino. 2017. Dissolved organic carbon retention by coprecipitation during the oxidation of ferrous iron. *Geoderma* 307:19–29.
- Sollins, P., P. Homann, and B. A. Caldwell. 1996. Stabilization and destabilization of soil organic matter: mechanisms and controls. *Geoderma* 74:65–105.
- Southeastern Regional Climate Center. 2018. Historical Climate Summaries for Maryland. https://sercc.com/climateinfo/historical/historical_md.html
- Sun, Y., F. Liu, M. Bendevis, S. Shabala, and S.-E. Jacobsen. 2014. Sensitivity of Two Quinoa (*Chenopodium quinoa* Willd.) Varieties to Progressive Drought Stress. *Journal of Agronomy and Crop Science* 200:12–23.
- Syswerda, S. P., A. T. Corbin, D. L. Mokma, A. N. Kravchenko, and G. P. Robertson. 2011. Agricultural Management and Soil Carbon Storage in Surface vs. Deep Layers. *Soil Science Society of America Journal* 75:92.
- Tanji, K. K., and N. C. Kielen. 2002. Agricultural drainage water management in arid and semi-arid areas. Food and Agriculture Organization of the United Nations, Rome.
- Tari, I., G. Laskay, Z. Takács, and P. Poór. 2013. Response of Sorghum to Abiotic Stresses: A Review. *Journal of Agronomy and Crop Science* 199:264–274.
- Tisdall, J. M. 1994. Possible role of soil microorganisms in aggregation in soils. *Plant and Soil* 159:115–121.
- Tisdall, J. M., and J. M. Oades. 1982. Organic matter and water-stable aggregates in soils. *Journal of Soil Science* 33:141–163.
- Torn, M. S., S. E. Trumbore, O. A. Chadwick, P. M. Vitousek, and D. M. Hendricks. 1997. Mineral control of soil organic carbon storage and turnover. *Nature* 389:170–173.
- Tully, K., K. Gedan, R. Epanchin-Niell, A. Strong, E. S. Bernhardt, T. BenDor, M. Mitchell, J. Kominoski, T. E. Jordan, S. C. Neubauer, and N. B. Weston. 2019a. The Invisible Flood: The Chemistry, Ecology, and Social Implications of Coastal Saltwater Intrusion. *BioScience* 69:368–378.
- Tully, K. L., D. Weissman, W. J. Wyner, J. Miller, and T. Jordan. 2019b. Soils in transition: saltwater intrusion alters soil chemistry in agricultural fields. *Biogeochemistry* 142:339–356.
- U.S. Department of Agriculture. 2017. Census of Agriculture County Profile – Somerset and Dorchester County, Maryland. https://www.nass.usda.gov/Publications/AgCensus/2017/Online_Resources/County_Profiles/Maryland/index.php
- U.S. Department of Agriculture, Natural Resources Conservation Service. 2017. The PLANTS Database. <https://plants.sc.egov.usda.gov/java/>
- U.S. Department of Agriculture, Natural Resources Conservation Service. 2019. Web Soil Survey. <https://websoilsurvey.sc.egov.usda.gov/>

- U.S. Salinity Laboratory Staff. 1954. Diagnosis and improvement of saline and alkali soils. USDA Agriculture Handbook 60. U.S. Gov. Print. Office, Washington, DC.
- Venables, W. N., and B. D. Topley. 2002. *Modern Applied Statistics with S*. Fourth Edition. Springer, New York, New York, USA.
- Ventura, Y., A. Eshel, D. Pasternak, and M. Sagi. 2015. The development of halophyte based agriculture: past and present. *Annals of Botany* 115:529–540.
- Verslues, P. E., E. S. Ober, and R. E. Sharp. 1998. Root Growth and Oxygen Relations at Low Water Potentials. Impact of Oxygen Availability in Polyethylene Glycol Solutions. *Plant Physiology* 116:1403–1412.
- Wahid, P. A., and N. V. Kamalam. 1993. Reductive dissolution of crystalline and amorphous Fe (III) oxides by microorganisms in submerged soil. *Biology and fertility of soils* 15:144–148.
- Wang, F., K. D. Kroeger, M. E. Gonness, J. W. Pohlman, and J. Tang. 2019. Water salinity and inundation control soil carbon decomposition during salt marsh restoration: An incubation experiment. *Ecology and Evolution* 9:1911–1921.
- Watts, D. B., H. A. Torbert, S. A. Prior, and G. Huluka. 2010. Long-Term Tillage and Poultry Litter Impacts Soil Carbon and Nitrogen Mineralization and Fertility. *Soil Science Society of America Journal* 74:1239.
- Weil, R. R., and N. C. Brady. 2016. *The Nature and Properties of Soil*. 15th edition. Pearson, Columbus, OH.
- Welbaum, G. E., T. Tissaoui, and K. J. Bradford. 1990. Water Relations of Seed Development and Germination in Muskmelon (*Cucumis melo* L.):9.
- West, T. O., and W. M. Post. 2002. Soil organic carbon sequestration rates by tillage and crop rotation. *Soil Science Society of America Journal* 66:1930–1946.
- Weston, N. B., R. E. Dixon, and S. B. Joye. 2006. Ramifications of increased salinity in tidal freshwater sediments: Geochemistry and microbial pathways of organic matter mineralization. *Journal of Geophysical Research* 111.
- Weston, N. B., M. A. Vile, S. C. Neubauer, and D. J. Velinsky. 2011. Accelerated microbial organic matter mineralization following salt-water intrusion into tidal freshwater marsh soils. *Biogeochemistry* 102:135–151.
- Wichelns, D., and M. Qadir. 2015. Achieving sustainable irrigation requires effective management of salts, soil salinity, and shallow groundwater. *Agricultural Water Management* 157:31–38.
- Williams, W. 1986. Conductivity and salinity of Australian salt lakes. *Marine and Freshwater Research* 37:177.
- Wilson, M. J. 1999. The origin and formation of clay minerals in soils: past, present and future perspectives. *Clay Minerals* 34:7–25.
- Woodstock, L. W. 1988. Seed imbibition: a critical period for successful germination. *Journal of Seed Technology* 12:1–15.
- Wuebker, E. F., R. E. Mullen, and K. Koehler. 2001. Flooding and Temperature Effects on Soybean Germination. *Crop Science* 41:1857.
- Zaman, M., S. A. Shahid, and L. Heng. 2018. *Guideline for Salinity Assessment, Mitigation and Adaptation Using Nuclear and Related Techniques*. Springer International Publishing, Cham.

- Zhang, H., L. J. Irving, C. McGill, C. Matthew, D. Zhou, and P. Kemp. 2010. The effects of salinity and osmotic stress on barley germination rate: sodium as an osmotic regulator. *Annals of Botany* 106:1027–1035.
- Zhao, K.-F., J. Song, H. Fan, S. Zhou, and M. Zhao. 2010. Growth Response to Ionic and Osmotic Stress of NaCl in Salt-tolerant and Salt-sensitive Maize. *Journal of Integrative Plant Biology* 52:468–475.
- Zheng, Y., Z. Wang, X. Sun, A. Jia, G. Jiang, and Z. Li. 2008. Higher salinity tolerance cultivars of winter wheat relieved senescence at reproductive stage. *Environmental and Experimental Botany* 62:129–138.
- Zhu, J.-K. 2001. Plant salt tolerance. *Trends in Plant Science* 6:66–71.
- Zörb, C., C. M. Geilfus, and K. J. Dietz. 2019. Salinity and crop yield. *Plant Biology* 21:31–38.